Distribution Agreement

In presenting this thesis or dissertation as a partial fulfillment of the requirements for an advanced degree from Emory University, I hereby grant to Emory University and its agents the non-exclusive license to archive, make accessible, and display my thesis or dissertation in whole or in part in all forms of media, now or hereafter known, including display on the world wide web. I understand that I may select some access restrictions as part of the online submission of this thesis or dissertation. I retain all ownership rights to the copyright of the thesis or dissertation. I also retain the right to use in future works (such as articles or books) all or part of this thesis or dissertation.

Signature:

_____ _____

Darcie A. Cook Date

LRRK2 Function in Immune Cells and Contribution to Parkinson's Disease

By

Darcie A. Cook
Doctor of Philosophy

Graduate Division of Biological and Biomedical Sciences
Immunology and Molecular Pathogenesis

_____

Malú G. Tansey, Ph.D.
Advisor

_____

Jeremy M. Boss, Ph.D.
Committee Member

_____

W. Michael Caudle, Ph.D.
Committee Member

_____

Jacob Kohlmeier, Ph.D.
Committee Member

_____

Thomas Kukar, Ph.D.
Committee Member

Accepted:

_____

Lisa A. Tedesco, Ph.D.
Dean of the James T. Laney School of Graduate Studies

_____

Date

LRRK2 Function in Immune Cells and Contribution to Parkinson's Disease

By

Darcie A. Cook
B.S., Rensselaer Polytechnic Institute, 2011

Advisor: Malú G. Tansey, Ph.D.

An abstract of
A dissertation submitted to the Faculty of the
James T. Laney School of Graduate Studies of Emory University
in partial fulfillment of the requirements for the degree of
Doctor of Philosophy in Immunology and Molecular Pathogenesis
2017

ABSTRACT

LRRK2 Function in Immune Cells and Contribution to Parkinson's Disease

By Darcie A. Cook

Leucine rich repeat kinase 2 (LRRK2) is a large protein with a GTPase and kinase domain and several protein-interacting domains. Mutations in the *lrrk2* gene, specifically the enzymatic domains, are one of the most common causes of autosomal dominant Parkinson's disease (PD). LRRK2 has been reported as a regulator of many cellular pathways, including inflammatory signaling, cytoskeletal maintenance, and autophagy. LRRK2 expression is enriched in cells of the immune system (CD4+ and CD8+ T cells, CD14+ monocytes, and CD19+ B cells), but its function in the immune system and its effects on age-related immunosenescence are as yet unknown. Its regulatory function of nuclear factor of activated T cells (NFAT) and nuclear factor kappa B (NF-κB) implicates LRRK2 in the development of the inflammatory environment characteristic of PD. Mutations or polymorphisms in the *lrrk2* gene are also associated with several other immunological diseases, including Crohn's disease and increased risk for leprosy infection, indicating that LRRK2 plays an important role in proper immune function. The aim of this study was to determine the expression pattern of LRRK2 in immune cell subsets and correlate it with the immunophenotype of cells from PD and healthy subjects. In this study, it was shown that LRRK2 expression was increased in B cells, T cells, and CD16+ monocytes of PD patients compared to healthy controls (HC). LRRK2 induction was also increased in monocytes and dividing T cells in PD patients compared to HCs. In addition, PD patient monocytes secreted more inflammatory cytokines compared to HC, and cytokine expression positively correlated with LRRK2 expression in T cells from PD

but not HCs. Finally, the regulatory surface protein that limits T cell activation signals, CTLA-4 (cytotoxic T-lymphocyte-associated protein 4), was decreased in PD compared to HC in T cells. Studies involving G2019S-LRRK2 overexpressing and wild type LRRK2 overexpressing mice were performed to assess contribution of mutant LRRK2 to dysregulation of inflammatory pathways. While data are still preliminary, results implicate gain-of-function kinase mutations in dysregulation of both NFAT and NF-κB signaling. In sum, these findings suggest that LRRK2 has a regulatory role in immune cells and PD. Functionally, the positive correlations between LRRK2 expression levels in T cell subsets, cytokine expression and secretion, and T cell activation states strongly suggest that targeting LRRK2 with therapeutic interventions is likely to have direct effects on immune cell function.

LRRK2 Function in Immune Cells and Contribution to Parkinson's Disease

By

Darcie A. Cook
B.S., Rensselaer Polytechnic Institute, 2011

Advisor: Malú G. Tansey, Ph.D.

A dissertation submitted to the Faculty of the
James T. Laney School of Graduate Studies of Emory University
in partial fulfillment of the requirements for the degree of
Doctor of Philosophy in Immunology and Molecular Pathogenesis
2017

ACKNOWLEDGMENTS

I'd like to thank my advisor Malú Tansey for all of her support through the years of graduate school. Thank you for giving me the flexibility to pursue interests outside of the standard academic bench route. Thank you Dr. Mike Caudle for your scientific input, helpful career advice, and being a second mentor throughout the grad school process. Thank you to the rest of my committee members Dr. Tom Kukar, Dr. Jerry Boss, and Dr. Jake Kohlmeier for your scientific guidance and training provided.

Thank you Tami Hutto and Dr. Nael McCarty for mentoring me through the BEST program and opening up my world to new and exciting possibilities. Thank you to my Atlanta Science Festival family, Dr. Sarah Peterson, Dr. Meisa Salaita, and Jordan Rose. You three took a chance on me and ushered me into the exciting realm of science education. To my museum colleagues, Trudi Ellerman, Mary Hilpertshauser, Judy Gantt, and Virginia Howell, thank you for welcoming me into your world and showing me the ropes.

Dr. George Kannarkat and Dr. Katie MacPherson were with me from the very beginning as the first group of graduate students to join the lab. I'll never forget all of the late nights/early mornings together in the lab and weekends spent relaxing, crafting, and decorating cakes. To my co-dependent labmate, Elizabeth Kline: I would have lost my mind without your enthusiastic tube labeling and love of doing the tasks that I hated. Thank you for being there even when I didn't deserve the help. Laura Butkovich, thank you for still wanting to be my friend after I chased you down a hallway, my life would have less love in it without you. Valerie Joers, thanks for always being on call with emotionally supportive cheese and beer! A huge thanks to Dr. Brandi Wynn, honorary

Tansey lab member. I cannot thank you enough for your scientific guidance and emotional support. I'd also like to thank the rest of the members of the Tansey lab. The collaborative environment, warmth, and support I've received from everyone throughout the years from members past and present was essential to my success.

Thank you Josh Kessler for always putting a smile on my face with your crazy antics. Thank you Dr. Mark Lucera for being my scientific cheerleader especially in the dark times. Lindsay Miller, I definitely wouldn't have made it through grad school without our wine nights. Thank you Amy Torczynski, my best and oldest friend, for the hours upon hours of phone calls and the years of hijinx we've found ourselves in. Thanks to my fellow IMP cohort, college friends, and high school friends who were always there when I needed it. Kylie Ainslie, thanks for being such a wonderful roommate, making sure I was always fed, and for being stressed for me throughout the thesis writing process.

And finally, thank you to my family. To my brother, Trent, for being a voice of reason and saying the right thing even if you didn't know it. To my dad and step-mom for enthusiastically supporting whatever path I chose to take. To my grandparents, for all the meals and the wonderful family time that allowed me to recharge at the holidays. Last but not least, thank you to my mom and step-dad. Mom, you encouraged me to always strive to be my best. You never gave up on me, even if I already had. Your limitless love and passionate support gave me the strength to get to where I am today. I love you forever and always.

TABLE OF CONTENTS:

FIGURES AND TABLES:

Chapter 1: Introduction

Incorporates previously published work[1].

1.1 The Aging Immune System, Neuroinflammation, and Neurodegeneration

1.1a Immunosenescence and Inflammaging

It is well established that as an individual ages, so does the immune system. Immune aging is paradoxically characterized by both immunosenescence, a loss of effector function, and inflammaging, a chronic low level of inflammation that persists with age. Both the innate and adaptive arms of the immune system experience immunosenescence making it more difficult to fight off infection and maintain homeostatic conditions in the body. In addition to immune cells becoming less effective in mounting a proper response, as cells age, they can enter into a Senescence-Associated Secretory Phenotype (SASP) wherein they continuously secrete low levels of the pro-inflammatory cytokines IL-6, TNF, IL-1β, and C-reactive protein (CRP)[2]. In fact, reports indicate increased mononuclear secretion of IL-6, TNF, and IL-1β in aged adults compared to healthy young controls[3] and increased circulating levels of IL-6, IL-8, MCP-1, and TNF in older individuals[4-6].

IL-6 is considered to be the main cytokine associated with aging[7]. IL-6 production is modulated by the immune transcription factor nuclear factor kappa B (NF-κB) and induced by inflammatory stimuli (cytokines, infections, toxins) that activate the degradation of inhibitory proteins that control the NF-κB pathway[8]. The normal function of IL-6 is to activate the adaptive immune response by promoting expansion of T cells and differentiation of B cells, induce fever to assist fighting infection, and modulate

production of other acute phase reactant proteins. Chronically elevated levels of IL-6 are the primary contributor to the inflammaging phenotype associated with age.

In addition to increased cytokine secretion, SASP is associated with decreases in proliferative responses, upregulation of senescence markers, and telomere shortening. NF-κB activation and signaling[9,10], latent viral infection, and autoreactive T cells[11] all contribute to SASP. A number of studies have reported that astrocytes and microglia also experience age-related senescence[12,13]. A detailed description of immunosenescent phenotypes in innate and adaptive cells can be found below.

1.1b Innate Immune Aging and Dysfunction

The innate immune system is the first arm to respond to infection or physical injury. Each cell type has a very specific function, but all cells are capable of secreting cytokines and chemokines to mount a targeted immune response. Monocytes, macrophages, and dendritic cells primarily phagocytose and present antigens to the adaptive arm while natural killer (NK) cells, neutrophils, mast cells, basophils, and eosinophils have a more targeted capture and lysis function.

All cells of the innate system become dysregulated over time as an individual ages. In mice and humans, aged hematopoietic stem cells (HSC) preferentially differentiate into myeloid cells to the detriment of the lymphoid population[14-16]. Despite this skewing, innate population frequencies appear to remain stable, or by some reports, decrease with age. While the overall frequency of monocytes doesn't change, there is evidence to suggest that the pro-inflammatory non-classical subset of $CD14^{+}CD16^{+}$ monocytes is increased while the classical $CD14^{+}CD16^{-}$ population is decreased[17-19].

Numbers of neutrophils remain unchanged in elderly populations while frequencies of plasmacytoid dendritic cells (pDCs) and myeloid dendritic cells (mDCs) have been reported either as decreased or unchanged[20-22]. Little is known about population and functional changes in mast cells, basophils, and eosinophils as very few aging studies have been performed on these cell types[23].

Circulating monocytes, the precursor cells to both macrophages and dendritic cells, have many age-related defects in their effector functions. Aged monocytes experience dysregulated cytokine production following activation through Toll-like receptors (TLR). TLR surface expression is changed with age as evidenced by TLR1 expression decreasing while TLR2 remains constant[19,24]. This altered expression leads to decreased activation of downstream signaling and reduced production of TNF and IL-6 following stimulus[24]. Both protein and mRNA expression of TLR5 are increased in human adherent monocytes from elderly subjects, resulting in increased IL-8 and IL-6 production[25]. Because non-adherent monocytes did not display this increase, it is likely a phenotype of activated cells. Basal levels of TNF production and LPS-induced TNF by the $CD14^{+}CD16^{+}$ pro-inflammatory subset also increase with age in humans[18]. While there are variations in the expression levels of TLR proteins and cytokine expression, the overall trend with aging is towards a chronic pro-inflammatory environment.

Expression of co-stimulatory molecules on innate cells is essential for engagement of the adaptive immune system and upregulation is dependent upon engagement of TLRs on the cell surface. *In vitro*, human monocytes show a decreased expression of the co-stimulatory molecules CD80 and CD86 following TLR stimulation which strongly correlated with antibody responses to the trivalent inactivated influenza

vaccine[26]. Phagocytosis of foreign bacteria and apoptotic cells has also been reportedly altered in aging cells although results are mixed. Several studies in aged mice report normal phagocytosis of bacteria by macrophages[27,28] whereas studies of human monocytes report age-associated defects[18,22]. Both mice and human macrophages have impaired phagocytosis of apoptotic cells[22,29]. The variations in reports are likely due to the fact that most of the experiments are done on isolated monocytes in culture under various conditions and time points, but the overall trend is one of defective activation and phagocytosis.

Dendritic cells are considered to be the bridge between innate and adaptive immunity because their primary function is to scan the periphery for foreign invaders and activate the adaptive immune system by presenting antigen. While multiple studies have been performed to assess age-related functional changes in mDCs, results have been contradictory. Some studies show an increase in pro-inflammatory cytokine secretion while others show decreases or no change[22,30]. The story is a bit clearer for pDCs as studies are in agreement that pDCs from elderly subjects are deficient at releasing pro-inflammatory cytokines (TNF, IL-6, IL-12, IFN-γ, IFN-β, and IFN-α) following stimulation[20,31]. Data in both mouse DCs and human Langerhans cells, a DC subset specific to the skin, show defects in response to chemotactic signals[32,33]. Taken together, these data indicate that monocytes, macrophages, and DC subsets are dysregulated in such a way that contributes to the immunosenescent phenotype associated with aging.

Neutrophils also have a reduced migratory response towards a chemotactic signal in elderly subjects compared to young controls[34]. In addition to the cells taking longer to get to inflamed tissue, studies in mice suggest that there is prolonged inflammation at the

site of injury or infection because the capacity for neutrophils to leave the tissue is also inhibited[35]. Neutrophils have two primary effector functions: phagocytosis and the production of neutrophil extracellular traps (NETs). As an individual ages, neutrophils lose their ability to effectively phagocytose opsonized pathogens while maintaining efficient phagocytosis of non-opsonized particles[36,37]. While NET function hasn't been assessed in humans, NET formation is decreased in an aged mouse model of MRSA infection[38].

Finally, the inflammasome is a cellular cascade that begins following detection of foreign pathogens within the cell. It contributes to the activation of the inflammatory response by regulating caspases that produce pro-inflammatory cytokines such as IL-1β and IL-18, and pyroptosis, a form of programmed cell death[39]. In aged C57BL/6 mice, compared to younger mice, there is reduced production of IL-1β and IL-18 following stimulation of the NLRP3 (NOD-, LRR-, and pyrin domain-containing 3) inflammasome with influenza[40]. Interestingly, aged NLRP3 knockout mice showed improvements on learning and memory tests[41]. It is likely that despite the diminished ability of the inflammasome to induce cytokine secretion, in a chronic inflammatory environment it will remain activated and contribute to the inflammation. Taken together, these data suggest that there is a balance that must be struck between inflammasome activation and regulation.

The innate arm of the immune system is the first responder to a foreign invader. A properly initiated immune response is essential to the control of infection, but if the response is not dampened following resolution of the infection, tissue damage will occur. The above illustrates that aging cells become less responsive to inflammatory stimulus

while simultaneously secreting pro-inflammatory cytokines that contribute to the senescence associated secretory phenotype that is characteristic of aging.

1.1c Adaptive Immune Aging and Dysfunction

The lymphocytes of the adaptive immune system are highly specialized to fight specific infections. T cells mature in the thymus where they differentiate into cells that assist in maturation or specifically kill virus-infected cells. B cells mature in the bone marrow and primarily function to secrete antibodies and assist in maturation. The hallmarks of adaptive immunosenescence are a decreased naïve T cell population, an increased memory T cell population, decreased T cell receptor (TCR) diversity, and decreased T cell proliferation *in vitro*[42,43]. While most of the age-related defects reported have been in T cells, there are also alterations in B cell memory populations and antibody production[44-46].

Normal T cell development and maturation occurs when lymphoid progenitor cells migrate from the bone marrow to the thymus. In the thymus, T cells undergo selection and differentiation before export into the periphery as mature T cells. At adolescence, a process called thymic involution occurs, where the structure of the thymus changes and the stroma is replaced by adipose tissue[43]. Individuals over 50 have about 15% of thymic tissue remaining as about 3% of the thymus atrophies per year[47]. This involution leads to an overall decrease in the output of new T cells resulting in a decreased naïve cell compartment and increased memory T cell compartment. In addition, there is evidence to suggest that not only are there fewer naïve T cells being produced, but there is a greater output of potentially harmful self-reactive T cells as they

are not properly negatively selected in the involuted thymus[11,48]. Studies performed on individuals thymectomized in early childhood recapitulate these aging-associated T cell phenotypes indicating that thymic involution is the primary culprit[49].

Not only are T cell compartments altered, but there are defects in effector functions with age as well. Both $CD4^+$ and $CD8^+$ naïve T cells have altered TCR signaling cascades with diminished activation and ERK phosphorylation following TCR engagement[50,51]. TCR repertoire diversity is diminished due to thymic involution, decreased naïve cell output, and chronic viral antigen stimulation[52]. Naïve $CD4^+$ T cells from aged mice show defects in trafficking to the lymph node prior to encountering their cognate antigen[53]. In adults older than 65, 50% of their $CD4^+$ T cells are without expression of the co-stimulatory molecule CD28[54].

$CD4^+$ T regulatory (Treg) cells are responsible for controlling an active immune response by suppressing effector T cells. Tregs are generally characterized by high expression of CD25, the transcription factor FoxP3, and the secretion of anti-inflammatory cytokines such as IL-4, IL-10, and TGF-β. Older adults have a higher number of Tregs with an increased immunosuppressive capacity that contributes to the immunosenescent environment in the elderly[55-57]. While Tregs serve an essential function for controlling inflammation, too many of them can be harmful as they will suppress the normal and necessary function of the immune system. Balance between anti- and pro-inflammatory cells is essential.

$CD8^+$ T cells from aging adults have increased expression of PD-1, an immunosuppressive surface molecule that leads to T cell anergy. Telomere shortening has been implicated in the reduced clonal expansion of T cells with age[58]. Like $CD4^+$ T

cells, they also have diminished CD28 expression and proliferative capacity[59,60]. In addition, aged $CD8^+$ T cells have increased expression of the senescence marker CD57 and decreased levels of the cytotoxic molecules perforin and granzyme[61,62]. With all of these defects in subset populations and effector functions, both $CD4^+$ and $CD8^+$ aged T cells have a reduced capacity to proliferate and respond appropriately to an inflammatory stimulus.

1.1d Inflammation in the Brain and Neurodegeneration

Up until recently, the brain was considered to be an immune-privileged site because of the tightly sealed blood brain barrier (BBB). As new research comes to light, it is clear that there is substantial communication between the immune system and the central nervous system (CNS), and in fact, the immune system is necessary for normal learning and memory processes[63,64]. IL-4 secreted by $CD4^+$ T cells induces microglia to produce brain-derived neurotrophic factor (BDNF), insulin-growth factor (IGF)-1, and transforming growth factor (TGF)-β, proteins that are essential for neuronal growth and function[65,66].

In 2015, Louveau et al, described an extensive network of lymphatic vessels in the meningeal compartment of the brain that drains into the deep cervical lymph nodes[67]. Prior to this discovery, it was thought that immune cells only infiltrated into the brain during injury, infection, or with disease. Learning about this system has led to a reassessment of tolerance in the brain and its status as an immune-privileged site. These meningeal lymphatic vessels allow for immune cell monitoring and trafficking into the brain, if necessary. Importantly, the deep cervical lymph nodes can also be used to

analyze the immune cell traffic and activation within the brain. Further study of dysregulation of this lymphatic system could provide insight into neuroinflammation and neurodegeneration.

There are also resident immune cells in the brain that serve vital homeostatic functions. Microglia are the primary resident innate immune cells that serve to clear debris from the brain. While they are considered to be the "macrophages" of the brain, they are a distinct cell subset derived from the yolk sac during fetal development and are maintained through local proliferation[68,69]. Microglia are commonly described as being polarized into one of two major phenotypes—M1, a pro-inflammatory, phagocytic subset, and M2, a homeostatic, maintenance subset; however, this dichotomy vastly oversimplifies the plasticity of microglia and their phenotypes *in vivo*[70].

Under homeostatic conditions, microglia are primarily in a resting state where they clear debris such as apoptotic cells, promote wound healing, and secrete neurotransmitters and neurotrophic factors necessary for proper brain development and neuronal maintenance[71]. When microglia become activated, they secrete pro-inflammatory cytokines that recruit other immune cells to the area. Studies in both humans and animal models show age-related defects in the inflammatory profile of microglia. Microglia from aged rats have shortened telomeres and diminished telomerase activity compared to young controls likely contributing to decreased proliferative capacity[72]. Older humans have increased IL-1α expression compared to younger controls[73] while microglia from aged nonhuman primates show increased MHC-II expression compared to young[74]. When microglia are chronically activated, they

contribute to a pro-inflammatory environment that can recruit more immune cells to the site and is cytotoxic to neurons.

The blood brain barrier (BBB) is the first line of defense to keeping the brain healthy and intact. If the BBB breaks down, this can lead to infiltration of bacteria/viruses, increased trafficking of potentially harmful immune cells, and accumulation of other neurotoxic blood-derived products that can contribute to neuroinflammation and degeneration[75]. As an individual ages, the BBB loses integrity, likely due to the chronic low-level inflammatory environment associated with age, allowing increased immune cell infiltration into the brain[76,77]. Inflammatory mediators such as chemokines, cytokines, and cell adhesion molecules increase the permeability of the BBB and allow for immune cell entry into the brain[77].

Immune trafficking is important for the normal response to brain injury or infection; however, there is a pattern to these responses wherein pro-inflammatory cells initiate a response that is subsequently followed by an influx of wound-healing/anti-inflammatory cells to resolve the response. Th1 cells are primarily drivers of inflammation and secrete the pro-inflammatory cytokines IFN-γ and TNF. These cytokines then serve to activate macrophages/microglia and $CD8^+$ T cells. Th2 and Treg cells are considered to be more "neuroprotective" as they secrete cytokines with an anti-inflammatory profile (IL-4, IL-5, IL-10, and IL-13). Dysregulation of immune cell trafficking under homeostatic conditions can cause upregulation of inflammatory cytokines within the brain that subsequently activates microglia initiating a cascade of pro-inflammatory signaling that ultimately results in neurotoxicity[78]. During normal aging in humans, the BBB begins to breakdown specifically in the hippocampus, a region

essential for learning and memory. Montagne and colleagues found that the breakdown is more severe in individuals with mild cognitive impairment (MCI) suggesting the BBB integrity is a crucial factor in preventing neurodegeneration[79].

The balance between pro-inflammatory and anti-inflammatory immune cell types in the brain is essential to normal function and response to injury and infection. The chronic low-level inflammation associated with aging can cause this balance to become dysregulated and lead to increased immune cell infiltration into the brain. Infiltration increases the inflammatory milieu of surrounding cells leading to their activation which ultimately leads to an environment conducive to neurodegeneration.

1.1e Parkinson's Disease: Etiology, Pathogenesis, and Inflammation

Parkinson's disease (PD) is a progressive age-related movement disorder characterized pathologically by degeneration of dopaminergic (DA) neurons in the substantia nigra (SN) and formation of neuronal inclusions of aggregated α-synuclein (α-syn) called Lewy bodies. In the past few years, it has become clear that non-motor symptoms such as REM-sleep behavior disorder, constipation, and anosmia begin decades prior to motor symptoms; however, clinical diagnosis generally occurs much later in life following presentation of motor symptoms. To determine severity of disease and rate of progression, a physical examination is given where symptoms such as muscle rigidity, bradykinesia, and resting tremor are ranked on a clinical scale[80,81]. The ability to identify individuals "at-risk" for development of PD through the use of a biomarker or early screening for non-motor symptoms will be an important step towards understanding the pathological progression of disease.

Although the disease has been extensively studied for decades, the etiology still remains unclear. By the time a clinical diagnosis is made, there is already ~70% loss of DA neurons in the SN[80]. Genetic mutations account for between 5-10% of PD cases caused by mutations in the *SNCA*, *LRRK2*, *PARK2, DJ-1, PINK1,* or vacuolar protein sorting-associated protein 35 *(VPS35)* genes[82]. With the exception of LRRK2, these mutations generally lead to the development of PD at an earlier age of onset. In addition to mutation, commonly occurring genetic polymorphisms identified in genome-wide association studies (GWAS) have also been associated with increased risk for development of idiopathic PD. Given that the number of polymorphisms associated with PD is increasing, it is likely that the combination of genes and environmental exposures throughout life plays a crucial role in the development of disease[81]. Exposure to the toxin MPTP (1-methyl-4-fenyl-1,2,3,6-tetrahydropyridine)[83] and pesticides such as rotenone and paraquat[84,85] are known to cause PD. In fact, MPTP has become one of the primary methods to induce DA neuronal cell loss in animal models of PD. Use of non-steroidal anti-inflammatory drugs (NSAIDs), drinking caffeine, and smoking have all been shown to be protective against the development of PD[86,87]. While the complex interplay of these exposures with an individuals' genetics is not yet known, parsing out these interactions will be another step towards identifying "at-risk" individuals and preventing development of disease.

The Braak hypothesis (**Fig 1.1**) proposes that PD progresses in a predictable pattern that begins in the periphery (both the neurons in the nasal cavity and the gut) and subsequently progresses to the CNS[88-90]. The hypothesis suggests that α-syn aggregates in the gut and nasal passages and this leads to the formation of pathogenic Lewy bodies.

These Lewy bodies than traverse up the vagus or olfactory nerve toward the brain where degeneration occurs. There is ample clinical and experimental evidence to support the idea that PD pathology begins in the periphery. Both constipation and anosmia are pre-motor symptoms of the disease, and Lewy body pathology is evident in nasal and gastrointestinal compartments[91]. Experimental evidence also suggests that α-syn can be transported between neurons and potentially perpetuate formation of new aggregates in a prion-like fashion supporting the idea that Lewy pathology progresses from the periphery to the CNS[92]. While critics maintain that not every case of PD displays this pattern of development and progression[90], this hypothesis has ample clinical and scientific support as a useful model to study disease pathology.

One of the pathological hallmarks of PD is inflammation. The normal response of the immune system to a foreign antigen is to initiate a pro-inflammatory response, fight off the infection, and then, importantly, go back to a steady-state, non-inflammatory environment following resolution. As the immune system becomes dysregulated with age, this steady-state becomes pro-inflammatory and neurotoxic. Elevated levels of the pro-inflammatory cytokines IFN-γ, IL-1β, and IL-6 were found post-mortem in the CSF and nigrostriatal regions of PD subjects compared to age-matched healthy controls [93-96]. Given that DA neurons in the midbrain are particularly susceptible to death when exposed to pro-inflammatory cytokines like TNF and IFN-γ [93,97-99], chronic inflammation in the CSF is a likely culprit in this neurotoxicity.

Innate antigen presenting cells become activated through binding of a pattern recognition receptor (PRR) such as a Toll-like receptor (TLR). When they encounter an antigen such as lipopolysaccharide (LPS), they upregulate Major Histocompatibility

Complex-II (MHC-II). MHC-II proteins have a binding pocket for peptide fragments that presents antigen to $CD4^+$ T cells. When a $CD4^+$ T cell recognizes the combination of peptide and MHC-II, it will become activated and initiate a response. Humans have three types of MHC-II: HLA-DR, HLA-DP, and HLA-DQ. In subjects with PD compared to healthy controls, PD patients have increased levels of HLA-DR positive microglia in the substantia nigra indicating that microglia in the PD brain are chronically activated[100]. In nonhuman primate models of PD induced with MPTP, microglia activation is upregulated and appears to be chronic given that it is seen years after MPTP dosing[101]. Because microglia densely populate the substantia nigra, dysregulation of these cells could be leading to the enhanced cell death seen in this region with PD[102].

In addition to immune activation in the brain, there is substantial evidence supporting the role of the peripheral immune system in PD. T cell infiltration into the SN has been shown in both animal models and post-mortem brains of PD[103]. In a mouse model of PD induced by MPTP, mice lacking $CD4^+$ T cells have decreased DA neuron degeneration compared to wild type suggesting that infiltration of $CD4^+$ T cells is contributing to neurodegeneration[103]. Another study showed that following viral overexpression of α-syn in the nigra, MHC-II knockout mice exhibited less DA degeneration compared to wild type controls[104]. While this finding is interesting, a global knockout of MHC-II results in mice that lack both antigen presentation and $CD4^+$ T cells so it will be important to determine if this phenotype holds in a model that lacks antigen presentation, but still has a full complement of $CD4^+$ T cells. PD subjects have a decreased frequency of T cells circulating in the blood compared to healthy controls and this decrease appears to be strictly due to decreases in $CD4^+$ T cell frequency[105]. Because

it is difficult to determine T cell subset frequencies from human brains, it is not known whether this decrease is a result of cells infiltrating into the brain or just a general decrease in the $CD4^+$ T cell compartment. Barring the logistics of obtaining human brain samples, it would be intriguing to investigate potential differences in the PD brain compared to age-matched healthy controls.

In the past few years, multiple studies have reported evidence to suggest that PD is an autoimmune disease. In support of the Braak hypothesis, these studies indicate that autoimmune pathology begins in the periphery and then progresses to the CNS. T cells isolated from PD patients were exposed to MHC-II proteins loaded with α-syn peptides. These cells recognized and responded to these α-syn peptide:MHC-II complexes by producing IL-4 and IFN-γ[106]. Another study found that PD $CD8^+$ T cells exposed to α-syn produced significantly more TNF and IFN-γ while PD $CD4^+$ T cells produced more TNF[107]. Microglia also become pro-inflammatory in response to α-syn. Erythrocytes have been reported to secrete extracellular vesicles (ECV) containing high amounts of α-syn that can cross the BBB[108]. Translocation of ECV across the BBB was significantly increased when mice were treated with LPS, making the BBB leaky. These ECV were then taken up by microglia in the brain causing the microglia to initiate an inflammatory response after exposure to α-syn.

1.1f Conclusion

Dysregulation and dysfunction of the immune system is a normal process that occurs with age. Cells of both the innate and adaptive arms become senescent and pro-inflammatory. They lose their ability to respond appropriately to a foreign antigen due to

defects in proliferation, trafficking, and effector function. Despite these defects, immune cells also enter into SASP and secrete a chronic low-level of pro-inflammatory cytokines that can ultimately lead to leakiness in the BBB and leave individuals primed towards development of a neurodegenerative disease. Finding ways to reverse immune cell senescence and control low-level inflammation are two crucial pathways towards protecting against disease.

1.2 Leucine Rich Repeat Kinase 2, Parkinson's Disease, and Immune Function

Mutations in the leucine-rich repeat kinase 2 (LRRK2) protein were identified in 2004 as a potential marker for PD[109,110]. The identification of the link between LRRK2 mutations and PD led to an exciting new pathway for researchers to pursue. Because clinical presentation of LRRK2-associated PD and idiopathic PD is very similar[111-114], the study of LRRK2 function is likely to give insight into idiopathic PD etiology. Up to this point, studies involving LRRK2 and its associated mutations have focused on their effects on neuronal function. Within the past few years, it has become clear that increased inflammation, both in the brain and the periphery, is associated with the pathology of the disease[100,115-118]. The enriched expression of LRRK2 in both innate and adaptive immune cells and its designation as a member of the immune-regulating receptor-interacting protein kinase (RIPK) family[119,120] places LRRK2 in a unique position as a potential regulator of inflammatory and immune responses that influences risk for age-related degeneration.

1.2a LRRK2 Structure and Function

In 2002, the *PARK8* locus on chromosome 12 was identified in a study involving a large Japanese family with many generations affected with PD[121]. Two years later, two labs independently cloned and identified mutations in the *PARK8* gene encoding LRRK2, as causes for dominantly inherited PD[109,110]. LRRK2, also known as dardarin (from the Basque word 'dardara', for tremor), is a large protein, containing 51 exons and 2527 amino acids (~286kDa), with several different functional and protein-interacting domains[121,122]. Enzymatic domains include a ROC (Ras of complex) GTPase domain[123] and a serine/threonine kinase domain[124]. Several protein-interacting domains including a leucine-rich repeat (LRR) domain, a C-terminal WD40 repeat domain, and armadillo and ankyrin repeat domains also comprise the LRRK2 protein (**Fig 1.2**).

The kinase domain is a serine/threonine kinase whose physiological substrate had not been definitively established until very recently. A number of studies have identified a subset of Rab GTPases, proteins necessary for proper vesicular trafficking, as a physiologic substrate for LRRK2 kinase activity[125-128]. Pathogenic LRRK2 mutations cause increased phosphorylation of Rabs[125]. Interestingly, overexpression of Rab proteins attenuates α-syn-induced pathology and neurodegeneration in both animal and cellular models of PD[129]. It is likely that the functional regulation of Rab proteins by LRRK2 alters vesicular trafficking and contributes to disease progression. Other potential substrates include autophosphorylation sites, ERM (ezrin/radixin/moesin) proteins, mitogen activated protein kinase (MAPK), eukaryotic initiation factor 4E (eIF4E)-binding protein (4E-BP), and 14-3-3 proteins[130]. There have been over 20 autophosphorylation sites found on LRRK2 including both serine and threonine residues[131-135]. There is currently much debate over which sites are "bona fide"

autophosphorylation sites, however, the primary candidate sites cluster to the GTPase domain binding pocket (pSer1292 being the most likely) as opposed to the kinase domain[133-135]. Most kinases have a conserved DFG (aspartic acid, phenylalanine, glycine) motif at the hinge region of the kinase activation loop, but LRRK2 has a DYG (aspartic acid, tyrosine, glycine) motif. Although the significance of this alteration has not been determined, it could contribute to unique structural differences in the kinase domain. The most common LRRK2 mutation, G2019S, occurs in the glycine of this loop, giving mutant LRRK2 a DFS (aspartic acid, phenylalanine, serine) loop potentially altering protein dynamics and flexibility[130].

LRRK2 is part of the Roco family of GTPases with a ROC-COR domain: a ROC domain with a C-terminal of Roc (COR) domain directly following it[136]. LRRK2 GTPase function has been confirmed and GTP binding is essential for the regulation of LRRK2 kinase activity[137]. There are currently two theories about the GTPase function and its regulatory role. The first involves the GTP-dependent formation of LRRK2 dimers composing the active state. Consistent with this idea, the G2019S mutation appears to increase the amount of LRRK2 in dimer form[138]. The second theory proposes that LRRK2 acts as a Ras-GTPase with an "on-off" switch where GTP binding activates the protein, and hydrolysis to GDP inactivates terminating signaling. This model requires tight regulation via GEFs (guanine nucleotide exchange factor) to promote GDP release and new GTP binding thereby activating the protein and GAPs (GTPase activating protein) to promote GTP hydrolysis to GDP turning the protein off. In support of this model, a putative GEF[139] and GAP[140,141] have been proposed although they may not be

specific to LRRK2[142]. Further studies are needed to parse out the activating mechanism of the GTPase.

LRRK2, but not LRRK1 (a LRRK2 paralogue similar to, but distinctly different from LRRK2) can interact with 14-3-3 proteins[143]. This interaction is mediated by phosphorylation at the Ser^{910} and Ser^{935} sites[144]. Pathogenic LRRK2 mutations display reduced phosphorylation at these sites, disrupting 14-3-3 protein binding and leading to accumulation of LRRK2 in the cytoplasm in pools that resemble inclusion bodies[144]. It is worth noting that phosphorylation at these two serine sites does not control kinase activity. Inhibiting LRRK2 kinase activity via H-1152 and sunitinib in HEK-293 cells recapitulates the mutant phenotype by decreasing phosphorylation at Ser^{910} and Ser^{935} and disrupting 14-3-3 binding resulting in LRRK2 inclusion bodies[145]. Results from these studies indicate that LRRK2 does not directly autophosphorylate at these sites, but somehow indirectly regulates phosphorylation of these serine residues either by activating a nearby kinase or inhibiting phosphatase activity[145].

LRRK2 has been linked to regulation of autophagy, neurite outgrowth, vesicular trafficking and cytoskeletal components[146-149]. An interesting new model proposes that LRRK2 regulates clearance of vesicles derived from the trans-Golgi network in an autophagy-dependent manner[150]. This function is regulated by the phosphorylation of LRRK2 by casein kinase 1α, which promotes recruitment of LRRK2 to the trans-Golgi membrane[151]. Interaction with the GEF, ARHGEF7, mediates these effects, which is consistent with the ideas stated above, where GEFs mediate GTPase activity, which in turn regulate kinase activity. LRRK2 has also been implicated in autophagic function although the evidence is mixed as to whether mutations increase or decrease autophagy.

DA neurons derived from iPSC from idiopathic PD or LRRK2-associated PD show accumulations of autophagic vacuoles[152]; however, fibroblasts from G2019S subjects showed increased autophagic flux compared to control fibroblasts in a MEK/ERK dependent fashion[153]. The contradictions between these studies lend more support to the idea that LRRK2 function is very specific to the cell type in which it is acting.

Studies involving co-localization and ultra-structural analysis show that PD-associated LRRK2 mutations enhance oligomer formation and interact with the microtubule network. Kinase function and the WD40 domain are essential to this microtubule interaction[154]. Phosphorylation of cytoskeletal components stabilizes their formation and prevents remodeling of the network. Recombinant human LRRK2 phosphorylates β-tubulin and G2019S LRRK2 enhances this phosphorylation three-fold[155]. In addition, phosphorylated ERM proteins are significantly decreased in neuronal cultures from LRRK2 knockout mice and significantly increased in neuronal cultures from both wild type LRRK2 and G2019S transgenic mice[156]. These data suggest that normal function of LRRK2 stabilizes the cytoskeletal network. Because a dynamic cytoskeleton is essential to neurite formation and cellular remodeling, increased stabilization associated with mutant LRRK2 could be a factor contributing to neurodegeneration[157].

Given the multiple and highly diverse protein interacting domains, it is not surprising that LRRK2 has also been identified to be involved in the Wnt signaling pathway[158,159]. The Wnt signaling pathway has many cell regulatory functions, both in immune cells discussed further below and in neuronal cells[160]. LRRK2 interacts with the disheveled family of proteins that are essential to the Wnt signaling cascade via the ROC-

Cor domain. Experiments also showed that this interaction stabilizes LRRK2 protein expression[161]. In addition, LRRK2 interacts with WNT/PCP proteins and potentially regulates the balance between WNT/PCP and WNT/β-catenin signaling[162]. In support of this, over-expression of LRRK2 repressed β-catenin signaling while loss of LRRK2 enhances canonical Wnt signaling[163]. LRRK2 has also been associated with MAPK signaling[164,165] and the transcription factors nuclear factor kappa B (NF-κB)[166,167] and nuclear factor of activated T cells (NFAT)[168], detailed below. With multiple enzymatic and protein interacting domains, it has been difficult to determine the specific physiologic function of LRRK2 and its relation to PD etiology.

1.2b LRRK2 Expression

LRRK2 expression is ubiquitous. It is expressed throughout brain tissue, including human cortex cerebri, hippocampus, and striatum[169]. Cell specific expression in the brain includes astrocytes, microglia[170], and neurons[171]. Expression in peripheral tissues such as lung, heart, kidney, and immune organs such as thymus, spleen, and lymph nodes has also been reported[109,110,169,170]. Full length LRRK2 has been detected via western blot in monocytes, dendritic cells, microglia, B cells, and T cells[166,172]. Reports of expression in $CD4^+$ and $CD8^+$ T cells have been inconsistent and contradictory depending on the assay (western blot, real time PCR, flow cytometry) and reagents used (antibodies, primers). Although it has been reported that LRRK2 mRNA is close to undetectable in $CD4^+$ and $CD8^+$ T cells[173], the work reported here has reproducibly shown protein expression via flow cytometric analysis and can say with confidence that LRRK2 is expressed in both circulating $CD4^+$ and $CD8^+$ T cells[105]. Protein expression is highest in

$CD14^+$ monocytes, with an intermediate level in $CD19^+$ B cells and the lowest expression in $CD4^+$ and $CD8^+$ T cells. Most recently, expression has been shown in endothelial cells[167].

In neurons, endothelial cells, and immune cells, LRRK2 localizes mostly to the cytoplasm, with some enrichment at mitochondrial membranes, and presence at cellular and lysosomal membranes following stimulation[174-176]. Recruitment of LRRK2 to the membrane results in the formation of LRRK2 dimers that have increased kinase activity compared to the monomeric form[176]. Consistent with previous reports, this increased kinase activity is associated with increased GTP binding[123,176]. Membrane-associated LRRK2 also has decreased levels of phosphorylation compared to cytosolic LRRK2[176]. More recently, Schapansky et al. provided evidence suggesting that membrane recruitment of LRRK2 in macrophages is an essential step necessary for the regulatory role of LRRK2 in autophagy[175].

Although the focus of this chapter is on immune cells, the reader is directed to reviews that highlight the role of LRRK2 in neuronal cells and its function in the brain. Gomez-Suaga et al. writes an in depth review of the neurobiology of LRRK2 and its role in autophagy and synaptic alterations[142], Blesa et al. discusses dopaminergic cell vulnerability in the context of LRRK2 animal models of PD[177], Martin et al. provides an overview of LRRK2 pathobiology and neuronal dysfunction[178], and Rudenko et al. details the direct toxic effect LRRK2 can have on neurons in addition to the shortening of neurite outgrowths associated with mutations[179].

1.2c LRRK2 Mutations, Polymorphisms, and Disease

There are multiple mutations and normal genetic variations in the LRRK2 locus that have been identified and associated with disease[180]; however, six of these are known to be the most common pathogenic mutations in PD[179]. Four of these, R1441G, R1441C, R1441H, and Y1699C, are located in the ROC-COR GTPase domain, and two, G2019S and I2020T are in the kinase domain (**Fig 1.2**)[181,182]. Mutations in LRRK2 account for 1-2% of all PD cases, but are particularly prevalent in the Ashkenazi Jewish population (40%) and North African Arab population (39%)[112]. The mutation penetrance ranges from 28% at 54 years of age to 74% at 79 years of age. In terms of clinical presentation and pathology, LRRK2-associated PD most closely resembles idiopathic PD, making it an important model to study the underlying cause of idiopathic PD[111-114]. Because LRRK2 mutations generally cause late-onset PD, LRRK2 is thought to be a susceptibility gene that increases an individual's risk with age.

The R1441G and R1441C mutations, located in the ROC GTPase domain, result in decreased GTPase activity[123,183]. These mutations also exhibit neuronal toxicity. In an R1441C knock-in mouse model, although there was no dopaminergic neuron loss, the mice had impaired dopaminergic neurotransmission and D2 dopamine receptor dysfunction[184]. Another mutation, Y1699C is in the COR domain and also results in a decrease in GTPase activity[185]. This mutation also disrupts Wnt signaling by weakening interactions between LRRK2 and disheveled (DVL) proteins while the R1441G and R1441C mutations strengthen the interaction[161]. Interestingly, the R1398H variant, which enhances GTPase activity, is protective against PD and results in enhanced Wnt signaling[186].

The most abundant mutation, G2019S, is located in the kinase domain and results in enhanced kinase activity[174,187] due to stabilization of the kinase activation loop[188]. Neuronal cell death induced by mutations in LRRK2 has been shown to be kinase dependent[187,189]. The kinase domain has homology with mitogen activated protein kinase kinase kinases (MAPKKK), a series of proteins essential to the MAPK signaling pathway. MAPK signaling is a pathway that begins at the membrane and ultimately results in activation of transcription factors that affect gene expression[164]. Studies addressing signal transduction of the MAPK pathway in leukocytes found decreased phosphorylation of Src, HSP27, and JNK in both patients with G2019S PD and idiopathic PD compared to healthy controls[165]. Although not directly correlated with LRRK2 kinase activity, this indicates a potential dysregulation of MAPK signaling that could contribute to the development of disease regardless of mutation. The similar pathology seen in both G2019S PD and idiopathic PD is consistent with the clinical features of G2019S PD closely resembling those of idiopathic PD[111-114], reinforcing the notion that elucidation of the molecular mechanism underlying the dominantly inherited LRRK2 mutations will shed light on the causes of idiopathic PD.

In a study evaluating both protein and mRNA expression patterns in idiopathic PD and G2019S patients, it was found that there are no differences in neuronal mRNA distribution (using in situ hybridization) between idiopathic PD and G2019S subjects, with widespread neuronal LRRK2 mRNA expression seen in the neocortical regions, brainstem, locus coeruleus, hippocampus, and dopaminergic neurons of the substantia nigra. Consistent expression was also seen in vascular smooth muscle cells. Using qRT-PCR, Sharma et al discovered that total mRNA expression was decreased in idiopathic

PD cases in the parietal cortex, cerebellum, amygdala, frontal cortex, and cingulate gyrus; however, there were no alterations in protein levels (by western blot analyses) between subjects[190].

The I2020T mutation in LRRK2 is also located in the kinase domain, but its effect on kinase activity remains controversial. There are multiple studies reporting increased kinase activity[134,191,192], one decreased activity[193], and several reports of no change[182,194,195]. It has also been reported that I2020T does increase kinase activity via stabilization of the kinase activation loop, similar to the mechanism of the G2019S mutation[196]. Most recently, a phosphoproteomic study has identified Rab proteins as a physiologic substrate for LRRK2 kinase activity and, by this measure, indicates that all pathogenic LRRK2 mutants increase kinase activity[125]. If Rab truly is a physiologic substrate for LRRK2, future studies can employ phosphorylation state of Rab to fully parse out how these mutations alter enzymatic activity.

In addition to mutations, single nucleotide polymorphisms (SNPs) in LRRK2 have also been associated with disease risk. In 2008, SNPs in LRRK2 were identified as a susceptibility factor for the chronic inflammatory condition Crohn's Disease by a meta-genome wide association study (GWAS)[197]. Liu et al identified a potential mechanism for LRRK2 in Crohn's disease via negative regulation of NFAT[168]. Mice deficient in LRRK2 show increased translocation of NFAT into the nucleus resulting in enhanced NFAT activity. This regulation of NFAT appears to be dependent upon the non-coding RNA repressor of NFAT (NRON). The exact mechanism of regulation and how LRRK2 specifically interacts with NRON remains to be elucidated. LRRK2 knock-out mice also had exacerbated colitis consistent with a role for LRRK2 as a negative regulator

important in controlling inflammatory bowel disease[168]. LRRK2 SNPs have also been associated with susceptibility to leprosy in the Han Chinese population[198,199].

There are also three protective variants of LRRK2, M2397T and R1398L/H. M2397T is a variant that protects against leprosy[199]. It appears to increase NFAT activity in HEK293 cells following LPS stimulation, indicating that increasing the immune response is a necessary mechanism to control *M. Leprae* infection. Interestingly, M2397T is also a risk allele for Crohn's disease, suggesting that immune balance is essential to protecting against disease and autoimmune dysfunction[168]. R1398L/H is a polymorphism found in the ROC domain that is associated with decreased risk for PD. This particular polymorphism leads to increased GTP hydrolysis and decreased GTP binding, the exact opposite activity of what is reported for pathogenic mutations[186]. Through the study of myriad mutations and SNPs, LRRK2 has been identified as a regulator of MAPK signaling, a negative regulator of NFAT, and thus, we have gained insight into the kinase domain and its activity. With this new and exciting information, the link between LRRK2 and immune regulation becomes stronger.

1.2d LRRK2 Regulation of the Immune System

The immune system is a highly complex and tightly regulated system responsible for protecting the body against infection, cancer, and other cellular damage. When an immune cell recognizes a foreign antigen the cell enters an activated state; a series of signaling cascades (NFAT, NFκB, Wnt, etc) begins that results in the upregulation of pro-inflammatory cytokines, adhesion molecules, and further activation and differentiation of innate and adaptive immune cells. This pro-inflammatory state results

in altered cell trafficking, differentiation, and mRNA and protein expression, all of which are part of an orchestrated response aimed at elimination or neutralization of the invading pathogen.

LRRK2 is a member of the receptor interacting protein (RIP) kinase family, which are a group of proteins that detect and respond to cellular stress by regulating cell death and activation of the immune system[119,120]. In various cell types, LRRK2 expression has been reported to increase in response to the pro-inflammatory signals IFN-γ[166,173,200], LPS[172,201], and IL-1β[167]. Increases after IFN-γ stimulation have been observed in $CD14^+$ macrophages, $CD3^+$ T cells, and $CD19^+$ B cells[105,166,173,200]. Also, IFN-γ stimulation was shown to increase LRRK2 mRNA and protein expression specifically in the non-classical $CD14^+CD16^+$ monocyte population[173]. Inhibition of LRRK2 with multiple inhibitors results in decreased CD14, CD16, and MHC-II expression indicating that LRRK2 is playing a significant role in the activation of monocytes via IFN-γ[173]. Recently, it was reported that increased expression of LRRK2 in monocytes following IFN-γ stimulation is via extracellular signal-related kinase 5 (ERK5) signaling[200].

G2019S LRRK2 has also been linked to increased phosphorylation of ERK1/2 and dysregulation of basal autophagy through this pathway[153,202]. LRRK2 mRNA levels increased following LPS stimulation of mouse bone marrow derived macrophages (BMDMs)[172]. In addition, LRRK2 protein levels in these BMDMs increased following transduction of lentiviral particles[172]. Following cranial injection of LPS, microglia also display increased expression of LRRK2 and increased kinase activity[201]. Interestingly, despite strong up-regulation of LRRK2 protein with LPS stimulation, no changes in LRRK2 mRNA levels were seen[201]. LRRK2 is also increased in the gut lamina propria

macrophages, B cells, and dendritic cells of patients with Crohn's disease who experience chronic inflammation in the gut[166]. Increased LRRK2 expression after inflammatory stimulus dependent on ERK signaling implicates LRRK2 as key player in regulation of inflammatory signaling pathways.

In human umbilical vein endothelial cells (HUVECs), LRRK2 expression is increased following stimulation with IL-1β[167]. In addition, IL-1β also leads to increased induction of VCAM-1, an adhesion molecule important for immune cell trafficking, in HUVECs overexpressing both WT and G2019S LRRK2. This increased VCAM-1 induction appears to be kinase dependent, as the kinase dead LRRK2 mutant, K1347A, does not recapitulate this phenotype[167]. Multiple studies have linked LRRK2 to regulation of the NF-κB signaling pathway. Overexpression of WT LRRK2 and expression of the G2019S mutant in HUVECs led to increased phosphorylation of IκBα allowing for increased translocation of NF-κB into the nucleus[167]. LRRK2 silencing via shRNA resulted in decreased COX-2 production in fibroblasts from PD patients[203]. LRRK2 is also capable of phosphorylating RCAN1—a protein that positively regulates inflammatory signaling via inhibition of phosphatases— to increase transcriptional activity of NF-κB and production of IL-8[204]. Another study showed that in cultured microglia, LRRK2 can also positively regulate NF-κB through downregulation of the inhibitory p50 subunit[205]. NF-κB is the transcription factor that controls expression of pro-inflammatory cytokines, chemokines, and adhesion molecules. In this way, LRRK2 levels or activity may be critical in modulating NF-κB-dependent responses in immune cells.

In support of this, the LRRK2 knockout rat was reported to be protected from LPS and α-synuclein induced neurodegeneration. There are also fewer pro-inflammatory myeloid cells in the brains of these rats indicating that inhibition of LRRK2 could decrease the neuroinflammation and cell loss seen in PD[206]. Furthermore, there are altered immune cell frequencies detected in the spleen of these LRRK2 knockout rats[207]. Under normal resting conditions, LRRK2 knockout rat spleens have higher percentages of CD4, CD3, and CD11b positive cells, but significantly lower B cells[207]. When infected with a rat-adapted influenza virus, LRRK2 knockout rats showed a decreased percentage of $CD11b^+$ cells, but an increase in the percentage of $CD3^+$, $CD4^+$, and $CD8^+$ cells compared to their wild type counterparts[207]. Although these LRRK2 knockout animals have little-to-no PD-like pathology, they do exhibit significant pathology in the kidneys with accumulation of α-synuclein and ubiquitinated proteins, severe dysfunction in the autophagic-lysosomal pathways, and increased inflammatory and oxidative stress damage[207,208].

In addition to kidney pathology, LRRK2 knockout rats and mice also have lung pathology with enlarged lysosome-related storage organelles called lamellar bodies (LB) in type II alveolar lung epithelial cells[209-211]. LBs are important for storage of surfactant, a compound necessary to maintain proper surface tension and equilibrium in the lung. After ATP treatment, LRRK2 knockout rats showed increased calcium-dependent exocytosis of LBs indicating that LRRK2 plays a modulatory role in calcium signaling and exocytic pathways[211]. With the lung being a barrier site in the immune system, the apparent homeostatic role of LRRK2 in lung function is another indication that LRRK2 is necessary for proper immune function and control.

In a study using mice overexpressing LRRK2 with the R1441G mutation, microglia stimulated with LPS had increased expression and secretion of pro-inflammatory cytokines compared to wild type LRRK2 microglia[212]. Expression of LRRK2 protein was also significantly increased in both wild type and R1441G microglia following stimulation with LPS or IFN-γ[212]. Conditioned media from the LRRK2 R1441G mutant stimulated microglia was then added to primary neuronal cultures and resulted in an increase in neuronal death compared to the conditioned media from wild type LRRK2 stimulated microglia[212]. In an *in vitro* kinase assay, R1441C mutations led to increased kinase activity and a decreased rate of GTP hydrolysis[123]. Additionally, there is evidence supporting the idea that GTP binding stimulates LRRK2 kinase activity, indicating the potential role of LRRK2 in integrating cellular signaling pathways[123].

In a human dermal fibroblast model, a LRRK2 dependent increase in COX-2 RNA, but not protein levels, was observed in subjects with G2019S PD, R1441G PD and idiopathic PD compared to age-matched controls[203]. Knockdown of LRRK2 also led to blunted COX-2 responses after LPS stimulation[203]. Following stimulation with LPS, fibroblasts from subjects with idiopathic PD and subjects with LRRK2 R1441G mutations showed blunted responses as evidenced by diminished IL-6 and TNF RNA levels[203]. Consistent with previous reports, in these fibroblasts LRRK2 RNA levels increased following IFN-γ stimulation, but were shown to decrease with LPS stimulation[203]. Following LPS stimulation, in R1441G and iPD fibroblasts, NF-κB transcriptional activity was attenuated, consistent with a modulatory role of LRRK2 in NF-κB activation[203]. Taken together, these studies implicate LRRK2 as a key regulatory protein in inflammation. These types of studies remain unreplicated in immune cells, but

future investigations will shed light on the physiological role of LRRK2 in immune cells should the regulation turn out to be similar in nature.

1.2e LRRK2 Kinase/Small Molecule Inhibitors and Antisense Oligonucleotides (ASO)

Because many pathogenic LRRK2 mutations result in enhanced kinase activity, a proposed logical next step in PD therapeutics has been to develop inhibitors to dampen this increased activity. Because the sequence similarities between kinases are high, it is difficult to develop an inhibitor specific to the LRRK2 kinase domain; however, there are a few significant amino acid differences in LRRK2 that can be exploited. The DFG hinge motif in the activation loop of most kinases is DYG in LRRK2 and DYS in the G2019S mutation[213,214]. Despite this unique sequence, highly selective LRRK2 inhibitors remained elusive. In the past few years, there has been an uptick in the production of selective inhibitors and antisense oligonucleotides to actually knockdown whole LRRK2 protein. What follows is a brief summary of important experiments using inhibitors and modifiers to investigate LRRK2 function. The reader is directed to a review of LRRK2 inhibitors, their efficacy and specificity by Kramer et al.[215] and a review of patents by Kethiri et al.[216] for additional detail.

LRRK2-IN-1 was considered to be the first specific small molecule inhibitor of LRRK2 and was widely used until better inhibitors were designed, however its use has significant caveats. It does not cross the blood brain barrier limiting its utility as a therapy for neurodegeneration. It also potently inhibits ERK5, another ubiquitous kinase that regulates cell signaling, limiting its use both in research and the clinic[217]. In a mouse microglial culture, treatment with LRRK2 inhibitors LRRK2-IN-1 and sunitinib

decreased p38 MAPK phosphorylation and iNOS induction, two molecules important for the TNF release pathway[201]. Although, these data suggest that inhibition of LRRK2 could dampen a damaging inflammatory response in the brain, LRRK2-IN-1 was also shown to inhibit TNF and CXCL10 in LPS-stimulated astrocytes equally well in both LRRK2 wild type and knock-out cultures, indicating the glaring significant off-target effects of the inhibitor[218].

LRRK2-IN-1 inhibits IFN-γ-dependent induction of LRRK2 in THP-1 differentiated macrophages and human monocyte-derived macrophages[200]. This inhibition was thought to be specific, as other LRRK2 kinase inhibitors do not prevent increased LRRK2 expression after stimulation. However, because of the cross-reactivity of LRRK2-IN-1 with extracellular signal-regulated kinase 5 (ERK5), IFN-γ-induced expression of LRRK2 was proposed and determined to be dependent upon ERK5 levels and activity[200].

A promising new inhibitor, PF-06447475 (PFE475) was recently characterized and shown to be highly specific to LRRK2. *In vivo* studies from the initial characterization of the drug show high blood brain barrier (BBB) permeability and safety. Unfortunately, these studies indicate that the pharmacokinetics (PK) are too high to develop as a therapeutic in the clinic[219]. The next generation following PFE475 is the highly selective LRRK2 kinase inhibitor PF-06685360-00-0011 (PFE360), which has improved potency and greater oral bioavailability. Significant decreases in phosphorylation at both Ser935 and Ser1292 result following plating with 100 nM PFE360 with an IC_{50} determined to be 24 nM for pSer935[220]. Importantly, these drugs decrease phosphorylation while only slightly reducing the levels of total LRRK2 protein

and only cause pathology similar to what is seen in knockout phenotypes at an extremely high dose (IC_{95}) that would never be used clinically[221,222]. Non-human primates treated at low doses that still block LRRK2 kinase activity almost entirely show no lung pathology[221,223]. Because this drug is relatively new, few functional studies have been performed, but it will be a useful drug to provide accurate information on the kinase activity and specific function of LRRK2.

Another possibility for treatment is to knockdown whole LRRK2 protein using an antisense oligonucleotide (ASO). An ASO is a single-stranded synthetic string of nucleotides that can bind to target mRNA, tagging them for degradation by RNase H, and ultimately decreasing total protein levels in the cell[224]. Because early generation kinase inhibitors had substantial off-target effects and some resulted in lung pathology, LRRK2 ASOs were developed as an alternative. ASOs can also be delivered centrally to avoid potential peripheral effects of kinase inhibition. A recent study reports that LRRK2 ASOs successfully attenuated LRRK2 protein expression and resulted in decreased formation of α-syn inclusions in a mouse model using α-syn fibrils to induce DA degeneration[224]. While this is the first study to report these findings, it is an exciting step towards using ASOs as a therapeutic for disease.

The requirement for BBB permeability further complicates the use of LRRK2 inhibitors to treat neuronal dysfunction, but makes ASOs a potentially more attractive treatment. As research supporting the regulatory role of LRRK2 in the peripheral immune system increases, BBB permeability may no longer be necessary for therapeutic use of inhibitors, slightly improving the ease of developing clinically relevant therapies. Currently, there are no clinical trials with LRRK2 inhibitors or ASOs, however large

cohorts of LRRK2 mutations carriers have been identified to expedite the process of future clinical trials[213,221]. With the current information about LRRK2 mutations, specifically G2019S, and the lack of disease-modifying therapies available, the case for LRRK2 modifiers is strong.

1.2f Conclusion

Although the physiological roles of LRRK2 and the molecular mechanism and pathways that link it to PD pathogenesis have yet to be fully defined, it is an important kinase. Elucidating LRRK2 function will give researchers a better understanding of the relationship between chronic inflammatory conditions and age-related neurodegenerative disease. Through the study of LRRK2 mutation carriers both with and without disease, we have gained better understanding of the multiple domains and the complex activities of this large protein in neuronal and non-neuronal cells. With widespread expression in both the immune and nervous systems, LRRK2 remains an interesting, yet challenging, pharmacological target. Through the development of more specific LRRK2 kinase inhibitors and ASOs, the possibility of a disease-modifying therapy for a progressive condition that hasn't seen a new treatment in over 60 years remains bright on the horizon.

1.3 Thesis Aims

The specific aims of this work were to determine if there are changes in LRRK2 expression between healthy controls and individuals with PD and assess if these changes correlate with alterations in immune cell subset frequencies/function. In addition, this work sought to illuminate a potential mechanism by which LRRK2 contributes to

immune function. To investigate these aims, 32 HC and 40 PD individuals were immunophenotyped to assess their immune cell subset frequencies and LRRK2 expression levels. Monocytes and T cells were sorted and then treated with an inflammatory stimulus to determine potential differences in activation response. Finally, NFAT and NF-κB pathways were examined as a potential mechanism contributing to dysregulation of cells in the context of a G2019S mutant LRRK2 mouse model.

1.4 Figures

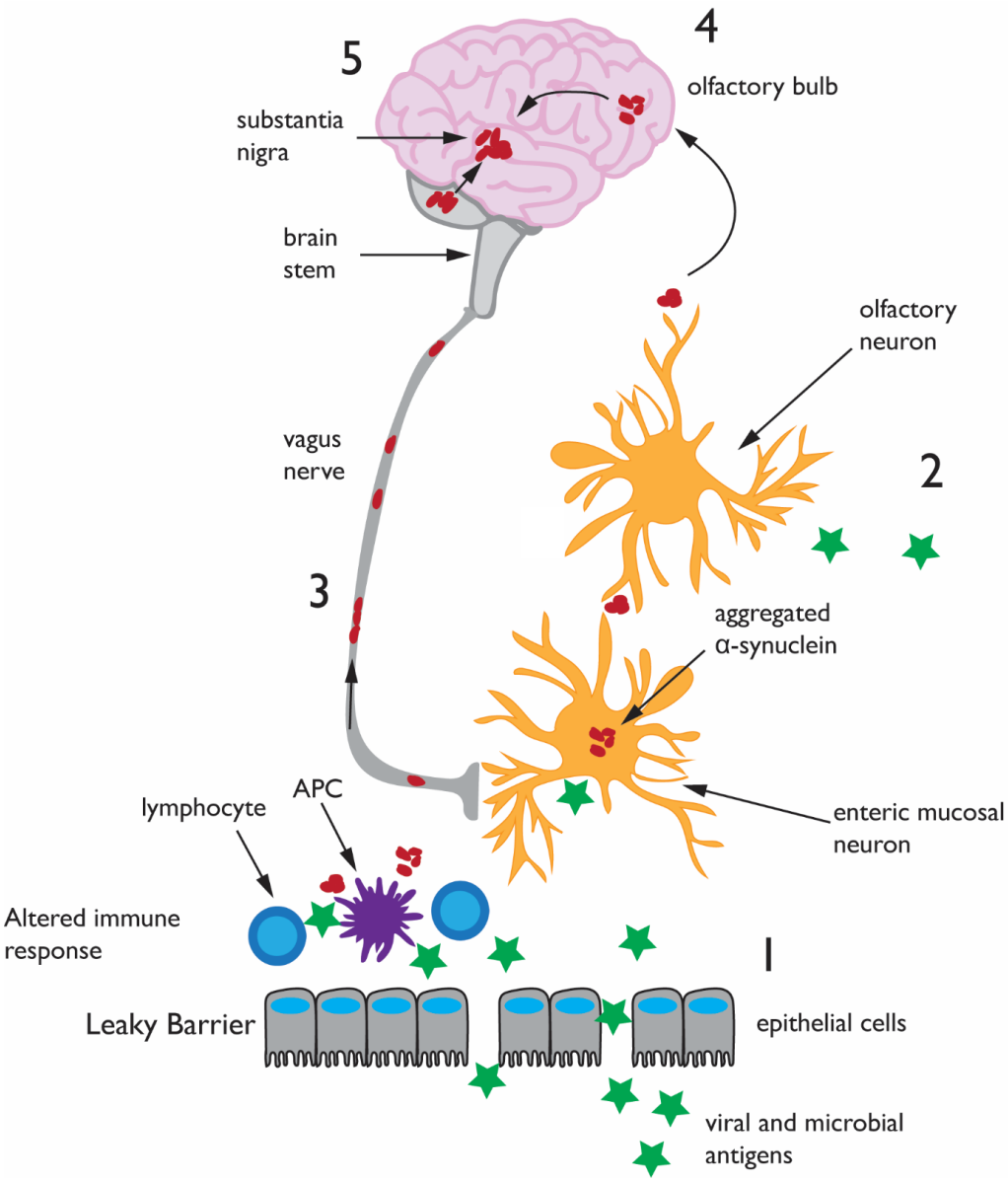

Adapted from Rietdijk CD, et al, *Front Neurol,* 2017, 8:37

Figure 1.1. Schematic of Braak's Hypothesis. Braak's hypothesis proposes that PD begins in the periphery following exposure to antigen via enteric neurons and/or the olfactory bulb (1, 2). Antigen causes the aggregation of synuclein in the periphery and is then transferred to the central nervous system via the vagus nerve (3). Deposition of α-

synuclein aggregates leads to PD by causing the degeneration of dopaminergic neurons in the substantia nigra (4, 5).

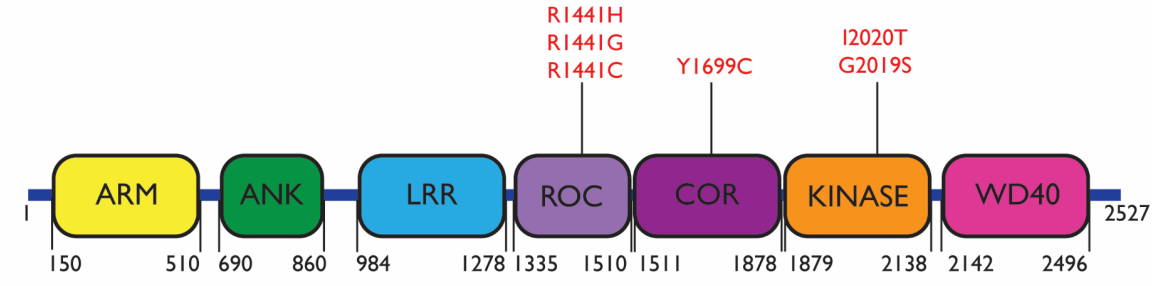

Figure 1.2. The LRRK2 protein has multiple protein binding domains and two enzymatic domains. LRRK2 also has many pathogenic mutations that occur in both enzymatic domains.

Chapter 2: LRRK2 Levels in Immune Cells Are Increased in Parkinson's Disease

Previously published work[105].

2.1 Introduction

Parkinson's disease (PD) is a progressive age-related movement disorder. The histopathological features of PD include degeneration of dopaminergic neurons in the substantia nigra pars compacta (SNpc) and the presence of Lewy bodies (neuronal inclusions of aggregated α-synuclein and other ubiquitinated proteins). Despite decades of extensive study, the etiology of the idiopathic form of PD remains unclear. Thus, the development of new treatments and therapeutics has been slow-paced. In 2004, multiple labs identified mutations in the leucine-rich repeat kinase 2 (*LRRK2*) gene as causative for a dominantly inherited form of PD, leading to an exciting new pathway for researchers to pursue[109,110]. Mutations have also been found in idiopathic cases at rates varying from 0.3-41% depending on the country of origin and ethnicity of the population studied[112]. Due to similarities in the clinical presentation of LRRK2-associated PD and idiopathic PD[111-113]. the study of LRRK2 function has the potential to offer new insight into the mechanisms underlying idiopathic PD etiology.

The *LRRK2* gene is large, containing 51 exons that code for a 2527-amino acid protein of large molecular weight (~286kDa) with several different functional and protein-interacting domains[121,122]. Enzymatic domains include a ROC (Ras of complex) GTPase domain[123] and a serine/threonine kinase domain[124]. There are also multiple protein-interacting domains, including a leucine-rich repeat (LRR) domain, a C-terminal WD40 repeat domain, and armadillo and ankyrin repeat domains[121,122]. Given the multiple, highly diverse enzymatic and protein interacting domains, it is likely that LRRK2 may have different binding partners in different cell types. In support of this,

LRRK2 has been shown *in vitro* to influence regulation of autophagy, macroautophagy[225], ceramide metabolism[226], neurite outgrowth, vesicular trafficking, cytoskeletal components, and cell signaling pathways involving nuclear factor of activated T cells (NFAT), Wnt, and NF-κB[146,149,158,167,168,175].

Multiple mutations and normal genetic variations in the *LRRK2* gene have been associated with disease[180]. The six most common pathogenic mutations in LRRK2 associated with PD[179] reside in the GTPase and kinase domains[181,182]. The most prevalent mutation is the G2019S mutation in the kinase domain[112]. Although mutations in LRRK2 only account for 1-2% of all PD cases, they are particularly prevalent in individuals of Ashkenazi Jewish (29.7%) and North African Arab ancestry (41%)[112]. The penetrance of the most common *LRRK2* mutation (G2019S) ranges from 28% at 54 years of age to 74% at 79 years of age, suggesting that genetic and environmental modifiers influence lifetime risk for PD in individuals with these mutations.

Importantly, LRRK2 is not only expressed in neurons but is also expressed in cells of both the innate and adaptive immune system[166,172]. Interestingly, LRRK2 polymorphisms have been associated with Crohn's disease, an autoimmune inflammatory bowel disease, and leprosy, an infection caused by *Mycobacterium leprae*, supporting a link to immune function[197,198]. LRRK2 is also a member of the receptor interacting protein (RIP) kinase family, which are proteins that detect and respond to cellular stress by regulating cell death and activation of the immune system[119,120]. Pro-inflammatory signals, such as interferon-γ (IFN-γ)[166,173,200], lipopolysaccharide (LPS)[172,201], and IL-1β[167] have been shown to increase LRRK2 expression. Specifically, in $CD14^+$ macrophages, $CD3^+$ T cells, and $CD19^+$ B cells, increases in LRRK2 following IFN-γ

stimulation have been observed[166,173,200]. Also, IFN-γ stimulation was shown to increase LRRK2 mRNA and protein expression in the non-classical $CD14^{+}CD16^{+}$ monocyte population[173]. Pharmacological inhibition of LRRK2 with multiple inhibitors resulted in decreased CD14, CD16, and MHC-II expression, suggesting that LRRK2 may play a significant role in the activation of monocytes via IFN-γ[173]. In addition, use of LRRK2 inhibitors results in decreased LRRK2 protein expression after 24 hrs exposure in PBMCs[227]. Recently, it was reported that increased expression of LRRK2 in monocytes following IFN-γ stimulation occurs via a mechanism involving extracellular signal-related kinase 5 (ERK5) signaling[200].

Despite a growing wealth of evidence that LRRK2 is enriched in both innate and adaptive immune cells[119,120], to date the majority of studies involving LRRK2 and its associated mutations have mainly been assessed for their effects on neuronal function. Given that increased inflammation in the periphery and the brain has been associated with the pathophysiology of PD[100,115-118], it is possible that LRRK2 may play a role in this process and serve as a regulator of inflammatory and immune responses that influence risk for age-related degeneration and risk for PD. Based on the current literature, we hypothesized that LRRK2 expression is increased in cells from PD patients, causing a dysregulation of function and activation in cells of both the innate and adaptive immune system. To test this, we investigated the extent to which various peripheral immune cell types express LRRK2 and inflammatory cytokines under resting conditions and during immune activation in healthy individuals and in patients with idiopathic PD.

2.2 Materials and Methods

2.2a Human subjects

PD patients (40) and age-matched healthy controls (HC) (32) subjects were recruited through the Immune System and Neurological Disease (ISND) Institutional Review Board (IRB)-approved research protocol at the Emory Movement Disorders Clinic and community outreach events. Subjects were excluded based on age (younger than 50 and over 85 years of age), known familial PD mutations and/or other known neurological, chronic or recent infections, or autoimmune comorbidities. Subjects were genotyped for the G2019S LRRK2 mutation (LifeTechnologies #4351378, Grand Island, NY) to exclude individuals with said mutation. Sample size was chosen on the basis of power analyses run by Dr. Holden Maecker in the Human Immune Monitoring Center at Stanford University.

During recruitment, a confidential family history and environmental questionnaire was used to assess history of disease and inflammation/immune-relevant environmental exposures and comorbidities. Caffeine, nonsteroidal anti-inflammatory drug, and nicotine exposure was calculated as milligram-years, milligram-years, and pack-years, respectively. The study populations were balanced with respect to risk factors for PD[86,87,228,229], including age, smoking, nonsteroidal anti-inflammatory drug use, caffeine intake, and rs3129882 (HLA-DRA SNP) genotype (**Table 1**). Study population was not sex-matched: the PD group was predominantly male while HC subjects tended to be more female as they were generally the caregivers; however, when the results are stratified by sex, sex does not account for the differences observed. Clinical severity of PD symptoms was also assessed using Hoehn and Yahr ratings and part II and III of the Unified Parkinson's Disease Rating Scale (UPDRS).

2.2b Human Peripheral Blood Mononuclear Cell (PBMC) isolation, stimulation, and purification

Isolation, stimulation, and purification of peripheral immune cells was performed as previously published in Kannarkat et al. 2015. Briefly, PBMCs were isolated from whole blood using density centrifugation with Ficoll-Paque (GE Healthcare, Uppsala, Sweden). Monocytes and T cells were isolated from PBMCs using positive selection columns with anti-CD14 and anti-CD3 paramagnetic beads, respectively (Miltenyi Biotec, Bergisch Gladbach, Germany). The isolated cell fraction was processed for flow cytometry as follows. Monocytes and T cells were plated for stimulation in a 12-well plate at a density of $1x10^6$ cells per well. Monocytes were plated for 18 or 72 hrs with or without 5 ng/mL IFN-γ (PeproTech, Rocky Hill, NJ, USA). T cells were stimulated for 18 or 72 hrs with or without anti-CD3/CD28 beads (1:1 cells:beads) (Dynabeads® Life Technologies, Grand Island, NY, USA) and 30 U/mL recombinant human IL-2 (Biolegend, San Diego, CA, USA).

2.2c Mouse PBMC isolation

The following mouse strains were obtained from Jackson labs: B6.Cg-Tg(Lrrk2*G2019S)2Yue/J (#012467), B6.Cg-Tg(Lrrk2)6Yue/J (#012466), C57BL/6J (#000664), and C57BL/6-Lrrk2^{tm1Mjfa}/J (#012444). Blood from each mouse (200 µL) was collected in an EDTA vacutainer tube (BD Biosciences) via cheek bleed. Blood was incubated in the dark for 10 minutes at room temperature with 1x RBC lysis buffer

(Biolegend) to lyse red blood cells. Cells were pelleted and resuspended in PBS for flow cytometry processing or lysed in sample buffer for western blot as detailed below.

2.2d Human THP-1 Monocytic Cell Culture and Differentiation

THP-1 cells (ATCC #TIB-202) were maintained in RPMI1640 medium with 2 mM L-glutamine adjusted to contain 1.5 g/L sodium bicarbonate, 4.5 g/L glucose, 10 mM HEPES, and 1 mM sodium pyruvate and supplemented with 10% fetal bovine serum. THP-1 cells were terminally differentiated into macrophages by exposure to 100 nM of phorbol 12-myristate 12- acetate (PMA) (Sigma P-8139) for 72 hrs. Terminal differentiation was confirmed as cells become adherent. Stimulation with 200 U/ml IFN-γ for 18 hrs was performed to further increase LRRK2 protein levels. Trypsin was used to lift the differentiated cells prior to use in western blotting or flow cytometry. For flow cytometry, cells were permeabilized and stained intracellularly with Abcam c41-2 Rb anti-LRRK2 antibody (1:50) and either a FITC-conjugated secondary (1:10,000) or an AlexaFluor-647-conjugated secondary (1:10,000).

2.2e Western Blotting

THP-1 cells and human monocytes were lysed in 4x sample buffer (Bio-Rad, Hercules, CA, USA) and heated at 80°C for 5 min. Proteins were then separated in a 12% polyacrylamide gel (Bio-Rad) by gel electrophoresis and transferred to a 45 μm PVDF membrane (Sigma Aldrich, St Louis, MO, USA). Following transfer, the membrane was cut along the pre-stained standard band indicating 100 kDa molecular weight and incubated in a 5% skim milk blocking solution in 1x tris-buffered saline containing 0.1%

Tween-20 (Sigma Aldrich). The corresponding membrane sections were incubated overnight in blocking solution containing a primary antibody targeting either GAPDH (SC-31915 1:1,000; Santa Cruz Biotechnology, Dallas, TX, USA) or LRRK2 (MJFF c41-2, 1:5,000; Abcam, Cambridge, UK;) at 4°C. Following three 5-min washes in 0.1% TBST with agitation, membrane sections were incubated for one hour at room temperature in either goat anti-rabbit (LRRK2) or rabbit anti-goat (GAPDH) horseradish peroxidase conjugated secondary antibodies (1:1,000; Jackson ImmunoResearch, West Grove, PA, USA) in blocking solution. Membranes were again washed in 0.1% TBST, and imaged using 1:1 dilute SuperSignal West Femto Chemiluminescent Substrate (Thermo Scientific, Waltham, MA, USA). Band intensity was determined using ImageStudio Software (Li-Cor Biosciences, Lincoln, NE, USA). LRRK2 expression (~286 kDa) has been normalized to corresponding GAPDH (~37 kDa).

Mouse PBMCs and T cells, B cells, and monocytes isolated directly from human blood were lysed in 1x Laemmli buffer (40mM NaF, 5% DTT, 1x phosphatase inhibitors, 1x protease inhibitors). Proteins were separated in a 7.5% polyacrylamide gel (Bio-Rad, Hercules, CA, USA) by gel electrophoresis and transferred to 45 μM PVDF membrane (Sigma Aldrich, St Louis, MO, USA). Following transfer, the membrane was cut below the pre-stained 75kDa molecular weight and incubated in 5% milk blocking solution in 1x Tris-buffered saline containing 0.1% Tween-20 (Sigma Aldrich, St Louis, MO, USA) for 1 hour. The corresponding membrane sections were incubated overnight in blocking solution containing primary antibody targeting either LRRK2 (MJFF c41-2, 1:5,000; Abcam, Cambridge, UK) or β-actin (sc-47778 β-Actin (C4) HRP 1:10,000, Santa Cruz Biotechnology) at 4°C. Following three 5-min washes in 1x TBS with 0.1% Tween-20

with agitation, the LRRK2 probed membrane section was incubated overnight in donkey anti-rabbit horseradish peroxidase conjugated secondary antibody (1:5000; Jackson ImmunoResearch, West Grove, PA, USA) in blocking solution at 4°C. Membranes were washed 3 x 5 min in 1x TBS with 0.1% Tween-20, and imaged using Luminata Crescendo Chemiluminescent Substrate (Thermo Scientific).

2.2f Flow Cytometry Analysis

To stain for flow cytometry, 5×10^5 cells per well were washed once with phosphate buffered saline (PBS) and incubated for 30 min at 4°C with LIVE/DEAD Fixable Red (Life Technologies). Cells were incubated in 1x FACS buffer (1% bovine serum albumin, 0.1% sodium azide, and 1 mM EDTA) for 15 min at 37°C with anti-human CCR7:phycoerythrin. Cells were washed and incubated for 20 min at 4°C with surface antibodies detailed in **Table 2**. Cells were intracellularly stained using the Fixation/Permeabilization Stain Kit per manufacturer's protocol (eBiosciences, San Diego, CA, USA). Intracellular cytokine staining (ICS) was performed on T cells stimulated for 18 hrs. Cells were incubated with 5 µg/mL Brefeldin A (Biolegend) for 7 hrs prior to harvest. After harvest, cells were processed according to protocols detailed above. Cells were run immediately on an LSRII instrument (BD Biosciences, Franklin Lakes, NJ, USA). Supra Rainbow Spherobeads (SpheroTech, Lake Forest, IL, USA) and OneComp Beads (eBiosciences) were used to set voltages and compensation settings between cytometry runs. Analysis of flow cytometry data was performed using FlowJo Software v10.X (Ashland, OR, USA). Gates were set according to **Fig 2.1**. Because the LRRK2 antibody is unconjugated, a secondary antibody only control condition was used

to determine nonspecific binding and select for positively stained populations. Conjugated isotype control antibodies were used for the rest of the cellular protein markers stained. Fluorescence minus one controls were used to account for fluorescence spillover between channels. Protein expression levels are reported as median fluorescence intensity (MFI).

2.2g Cell Proliferation Assays

To assess T cell proliferation, cells were stained with CellTrace Violet (Life Technologies) according to manufacturer's protocol and plated for 72 hrs with anti-CD3/CD28 Dynabeads® and 30 U/mL recombinant human IL-2. Unstimulated cells were harvested at 18 hrs post-plating as cells do not remain viable for 72 hrs without stimulation. At harvest, Dynabeads® were removed using magnetic separation, washed, and stained according to the above flow analysis protocol.

2.2h MesoScale Discovery multiplexed immunoassays

Conditioned media from plated cells was collected during cell harvest and stored at -80°C until sample analysis. Media analyte levels were measured in duplicate using 3-plex (IL-2, TNF, and IFN-γ) and 10-plex (IFN-γ, IL-10, IL-12p70, IL-13, IL-1β, IL-2, IL-4, IL-6, IL-8, and TNF) plates on a Sector 2400 instrument (Meso Scale Discovery, Rockville, MD, USA).

2.2i Statistical analyses

A two-tailed Student's t-test was used to make comparisons between HC subjects and PD patients in the immunophenotyping studies. A two-way analysis of variance (ANOVA) followed by Sidak's multiple comparisons post-hoc test was used to compare baseline characteristics of the study population and inducibility of immune response following IFN-γ stimulation in monocytes or anti-CD3/CD28 stimulation in T cells. Data was plotted with means and standard error of the mean. Analysis of covariance (ANCOVA) was used to assess differences in slopes of correlations between HC and PD. Linear regressions were performed to assess correlations of individual slopes of HC and PD. All statistical tests used are indicated in the figure legends. Graphpad Prism Version 6.05 (Prism, La Jolla, CA, USA) software was used to perform all statistical analyses.

2.2j Human subjects research approval

All procedures involving human subjects were approved by the IRB of Emory University in Atlanta, Georgia before study commenced. All participants provided written informed consent and the terms and risks of the study were thoroughly explained before inclusion in the study.

2.3 Results

2.3a Validation of Abcam c41-2 LRRK2 antibody for detection of human LRRK2 by flow cytometry

The c41-2 Abcam LRRK2 (MJFF2) antibody is a rabbit polyclonal antibody used in the studies herein to detect human LRRK2 protein in peripheral immune cell populations. Because the LRRK2 antibody was not conjugated to a fluorophore, a FITC-

conjugated secondary anti-rabbit IgG antibody was used for the flow cytometry studies. Although the manufacturer notes that c41-2 is cross-reactive with mouse LRRK2 protein in western blotting and histological applications, c41-2 only detects mouse LRRK2 when it is highly overexpressed as in the mouse WT-LRRK2- or mouse G2019S-LRRK2-overexpressing BAC transgenic lines **(Fig 2.2a).** In our hands, c41-2 displays minimal cross-reactivity with the mouse LRRK2 protein relative to the human protein in peripheral blood immune cells under conditions for western blotting of SDS-PAGE. Consistent with this, the flow signal from endogenous mouse LRRK2 protein in PBMCs from C57BL/6J mice is indistinguishable from that of PBMCs from LRRK2 KO mice **(Fig 2.2b)**. In addition, there is a minimal shift in the histograms for the PBMCs from the mouse WT LRRK2- or mouse G2019S-LRRK2-overexpressing BAC transgenic mouse lines indicating lack of recognition of mouse LRRK2 via flow cytometry **(Fig 2.2b)**.

To validate the specificity of the LRRK2 antibody for human LRRK2 using flow cytometry applications, we performed experiments in which induction of the human LRRK2 protein was confirmed in both a human monocytic cell line (THP-1) and primary human monocytes using both western blot and flow cytometry under the same experimental conditions. A single immunoreactive band was detectable in immunoblots with the c41-2 LRRK2 antibody in T cells, B cells, and monocytes isolated from human peripheral blood (**Fig2.3a**). Next, naïve THP-1 cells were found to express low amounts of LRRK2 protein. Upon treatment with PMA the cells differentiate into macrophages and following stimulation with IFN-γ, their expression of LRRK2 protein can be shown to increase by western blot (**Fig 2.3b-c**). Importantly, this increase is accompanied by an increase in the LRRK2 signal by flow cytometry (**Fig 2.3d**) using the c41-2 LRRK2

antibody and either of two different secondary antibodies (Alexa-Fluor647 or FITC). In addition, human primary monocytes isolated from peripheral blood were found to express detectable levels of human LRRK2 protein by western blotting with c41-2 (**Fig 2.3a-c**) and by flow cytometry with the same LRRK2 antibody (**Fig 2.3d**). Importantly, the levels of LRRK2 in the primary cells could be increased further by stimulation with IFN-γ as measured by western blot (**Fig 2.3b-c**) and flow cytometry (**Fig 2.3d**).

2.3b PD is associated with increased LRRK2 expression in innate and adaptive immune cells

To investigate if LRRK2 levels differ between specific immune cell populations and between healthy individuals and those with PD, immunophenotyping of peripheral blood was performed in cells from PD and age-matched HC subjects. LRRK2 expression has been reported in both monocytes and B cells[166,172], however, there are conflicting reports as to whether LRRK2 is expressed in T cells[172,173]. To date, the most commonly used approach to ascertain LRRK2 expression levels has been western blotting and quantitative reverse transcriptase-polymerase chain reaction (qRT-PCR). Differences between antibodies and oligonucleotide primers could account for discrepancies between assays and labs. We found that LRRK2 protein levels, reported as MFI, were increased in $CD16^+$ monocytes, T cells, and B cells from PD patients compared to HC (**Fig 2.4a-b**). Importantly, the increase in LRRK2 is not a reflection of overall increases in protein content in immune cells in PD subjects versus HCs as other cell-specific markers such as CD19, CD14, and 4-1BB were not significantly different between HC and PD subjects (**Fig 2.5).**

Given the diverse functions associated with T cell subsets, we determined whether the increased LRRK2 levels in the PD group were altered in all subsets or only specific subsets. The data were stratified by $CD8^+$ effector subsets and $CD4^+$ effector, helper, and regulatory subsets (**Table 3**). We found no significant difference in LRRK2 expression between different T cell subsets, but its levels are globally increased in all subsets in PD patients compared to HC subjects (**Fig 2.4c-e**). One small exception is the $CD4^+$ Teff subset; when comparing the PD and HC subjects the p-value was 0.051. In our study cohort, patients with PD had increased LRRK2 expression in T cells, B cells and a pro-inflammatory subset of monocytes ($CD16^+$).

In addition to protein expression levels in immune cells, we assessed the frequencies of immune cell populations in our subjects. No significant differences between PD and HC in the frequencies of monocytes or B cells were observed (**Fig 2.6a-b**), but PD patients had a significantly decreased T cell frequency compared to HC (**Fig 2.6a**). Consistent with what has been previously reported, it appears that this decrease is due strictly to the $CD4^+$ subset and not to $CD8^+$ T cell frequencies[230] (**Fig 2.6c-e**). In addition, there was a positive correlation between the expression level of LRRK2 and frequency of monocytes in PD patients (**Fig 2.7a**). There was increased LRRK2 expression in subjects with higher frequencies of $CD14^+$ monocytes. Although not reaching significance, there was a trend towards the correlations between LRRK2 expression and $CD14^+$ frequencies between PD and HC being distinctly different (**Fig 2.7a**). Other correlations between LRRK2 level and immune cell frequency were not statistically significant between PD and HC (**Fig 2.7b-d**). In summary, LRRK2 expression is increased in lymphocytes and inflammatory monocytes from PD patients

and the levels of LRRK2 positively correlate with the frequency of monocytes in PD patients.

2.3c LRRK2 expression is induced by inflammatory stimuli in both PD and HC monocytes but shows opposite correlation with MHC-II induction in PD versus HC subjects

There are several reports indicating that LRRK2 expression in immune cells increases following inflammatory stimuli such as IFN-γ or microbial components like LPS[166,172,201,212]. We sought to replicate these data in monocytes and explore whether this paradigm held true in T cells. Cells were plated immediately following isolation from peripheral blood. Monocytes were stimulated with IFN-γ for 18 or 72 hrs. After 18 hrs of stimulation, LRRK2 expression in monocytes was not significantly increased (**Fig 2.8a**). However, by 72 hrs after stimulation, LRRK2 levels in monocytes were significantly increased relative to baseline in both PD and HC populations (**Fig 2.8a**). Major histocompatibility complex class II (MHC-II), also known as Human Leukocyte Antigen (HLA), is the antigen presenting-molecule expressed on cells such as monocytes that activates $CD4^+$ T cells and is up-regulated following an inflammatory stimulus. In humans there are three different isotypes, HLA-DR, -DQ, and -DP, encoded by the MHC-II locus[231]. To determine if there were any alterations in antigen presentation in patients with PD, we assessed expression levels of HLA-DR and -DQ. Both PD and HC groups displayed induction of HLA-DR and -DQ proteins after IFN-γ stimulation with 80-90% of cells being HLA-DR/-DQ double positive (**Fig 2.8b**). Monocytes from both HC subjects and PD patients continued to up-regulate HLA-DQ over time (**Fig 2.8c**).

Both groups also up-regulated HLA-DR over time; however, HC subjects downregulated HLA-DR after 72 hrs while monocytes from PD patients retained expression (**Fig 2.8d**). Furthermore, after 18 hrs of stimulation, LRRK2 levels were positively correlated with HLA-DR MFI (**Fig 2.8e**) in monocytes of PD subjects and negatively correlated with HLA-DQ MFI (**Fig 2.8f**) in monocytes from HC patients. In summary, LRRK2 protein expression was induced in monocytes from both groups after stimulation with IFN-γ at both 18 and 72 hrs post-stimulation. However, LRRK2 expression was positively correlated with MHC-II induction in PD patients and negatively correlated in HC subjects.

2.3d LRRK2 induction is slower in T cells compared to monocytes in both PD and HC subjects

To determine the timing of LRRK2 induction following T cell activation, T cells were stimulated with anti-CD3/CD28-coated beads and IL-2 (a cytokine necessary for T cell activation and proliferation) for 18 or 72 hrs. While 18 hrs of stimulation was not sufficient to induce LRRK2, by 72 hrs LRRK2 levels were significantly increased in both CD4+ and CD8+ T cells in PD and HC groups (Fig 5a). In PD patients, CD4+ T cells displayed a slight but statistically insignificant trend toward increased induction compared to the HC cells at 72 hrs.

2.3e Parkinson's disease is associated with higher LRRK2 induction in proliferating T cells compared to healthy controls

To determine if LRRK2 may be involved in regulation of T cell proliferation, cells were stained with CellTrace Violet, a cell proliferation dye, and analyzed via flow cytometry. Typically, after 72 hrs of stimulation T cells will have divided between three and four times. To simplify this analysis, each cell division was analyzed individually for LRRK2 expression. We found that LRRK2 was upregulated only in the early dividing cells in both PD and HC groups (**Fig 2.9b**). In $CD8^+$ T cells, dividing cells from PD patients had significantly higher levels of LRRK2 compared to dividing cells from HC subjects (**Fig 2.9b**). Importantly, no differences were observed in the percent of $CD4^+$ or $CD8^+$ T cell proliferation or percent of T cells that divided three times between PD and HC subjects (**Fig 2.10a**). Although the relationship between LRRK2 MFI and percentage of proliferated $CD4^+$ T cells was not significantly different between the two groups, the LRRK2 MFI in $CD8^+$ T cells was higher in PD patients than in HC subjects at every percent of proliferated cells (**Fig 2.10b**).

2.3f The T cell activation marker CTLA4 is significantly decreased in T cells of PD patients following stimulation

In addition to proliferation, we also assessed potential differences in activation markers normally up-regulated following stimulation in T cells. If LRRK2 has a role in regulating processes involved in immune cell activation, increased expression levels of LRRK2 should correlate with differential activation of T cells. We looked at two common activation markers: CTLA-4, a negative regulator of activation, and 4-1BB, a receptor that amplifies T cell activation by inducing secretion of IL-2. CTLA-4 competes with CD28 to bind CD80/86 on antigen presenting cells; but while CD28 sends an activating

signal when bound, CTLA-4 sends an inhibitory signal when bound. After the 72 hr stimulation, both PD and HC T cells up-regulated 4-1BB (**Fig 2.5**) and CTLA-4, however CTLA-4 levels in $CD8^+$ T cells of PD patients were significantly lower than those in HCs (**Fig 2.9c**).

2.3g Immune cells from PD patients display similar cellular cytokine expression but increased pro-inflammatory cytokine secretion

We wanted to further explore a potential role for LRRK2 in immune cell activation. Following stimulation, T cells secrete cytokines to further activate the immune cell response[232]. To investigate the hypothesis that LRRK2 expression affects cytokine production, we used intracellular cytokine staining (ICS) to measure cytokine expression in a cell type-specific manner as well as multiplexed immunoassays to measure cytokine secretion into the culture media. Cytokine measurements were performed after 18 hrs of stimulation. Prior to harvest, cells were treated with Brefeldin A, a compound that inhibits protein transport causing vesicle accumulation at the Golgi complex/endoplasmic reticulum[233]. Cells were stained to measure total intracellular protein expression of IFN-γ, TNF, and IL-2. Protein levels of all cytokines were increased with stimulation, but no significant differences were detected between PD and HC groups (**Fig 2.11a-b**).

Multiplexed immunoassays were performed on conditioned media from the 18 hr-stimulated monocyte and 18- and 72 hr-stimulated T cell samples to measure the levels of cytokines secreted into the conditioned media. For 18 hr-stimulated monocytes, cytokine secretion was significantly increased in the PD group for IL-12p70, IL-13, IL-1β, IL-2, IL-4, IL-6, and TNF (**Fig 2.11c**). In 18 hr-stimulated T cells, no significant differences

were detected in levels of secreted IFN-γ and IL-2, but T cells from PD patients secreted significantly more TNF compared to cells from HC subjects (**Fig 2.11d**). Interestingly, at 72 hrs, IL-12p70 was the only cytokine secreted at higher levels in PD T cells compared to HC T cells (**Fig 2.11d**). In summary, several immune cell subsets from PD patients secreted higher cytokines upon stimulation compared to immune cells from HC subjects.

2.3h LRRK2 expression is positively correlated with cytokine expression in PD patients

PD patients had higher LRRK2 expression in cells with a higher amount of intracellular cytokine levels (**Fig 2.12a-b**). T cells from PD patients displayed an association between LRRK2 protein levels and cytokine expression (**Fig 2.12a-b**). LRRK2 protein levels positively correlated with IFN-γ, TNF, and IL-2 expression in T cells from PD patients; however, only IFN-γ expression in $CD4^+$ T cells correlated with LRRK2 protein levels in HC subjects (**Fig 2.12a**). In addition, when comparing the two subject groups for interaction, only the correlation between IL-2 expression in $CD8^+$ T cells and LRRK2 MFI displayed significantly different slopes (**Fig 2.12b**). In summary, LRRK2 levels positively correlated with cytokine expression and secretion in PD but not HC subjects.

2.4 Discussion

Recent new discoveries in immune cells have suggested a potential link for LRRK2 to the regulation of the immune system and modulation of inflammatory responses. Herein, we demonstrate that LRRK2 is expressed in both innate and adaptive human immune cells and is expressed at higher levels in the immune cells of patients with late-onset PD compared to age-matched HC individuals. In addition, LRRK2 is

induced in both human monocytes and T cells following an inflammatory stimulus; and in PD patients there is a positive correlation between LRRK2 levels, MHC-II induction, cytokine expression and secretion levels, and dampened expression of the T cell inhibitory factor CTLA4. Given the established role of LRRK2 as a potential negative regulator of NFAT[168], the differences we observed between PD patients and HC subjects suggest that LRRK2 may be important in the regulation of both innate and adaptive immune cells within the context of PD. Of note, within our study population and similar to other study populations, the PD group was predominantly male while the HC group was predominantly female as they were generally the spouses and caregivers of the PD patients. To ensure that the differences we observed were not due to this unequal sex distribution, results were stratified by sex but did not affect the differences observed between PD and HC groups.

The increased levels of LRRK2 associated with PD suggest that the protein is contributing to disease pathogenesis. $CD14^{+}CD16^{+}$ monocytes are considered to represent a non-classical monocyte population that is characteristically more pro-inflammatory and typically display increased cytokine secretion and greater antigen presentation[234]. Therefore, the finding that LRRK2 levels are notably increased in $CD16^{+}$ monocytes of PD patients may have functional relevance to disease risk or progression given that it was recently reported that IFN-γ induces more LRRK2 in this subset of monocytes compared to classical $CD16^{-}$ monocytes[173]. In addition, it has been shown that circulating monocytes are dysregulated in PD, displaying a hyperactive inflammatory phenotype[235]. The monocyte data taken together with the increased LRRK2 expression in T cells and B cells suggest that following an inflammatory challenge, individuals with PD

will mount an exacerbated inflammatory response compared to healthy individuals that could lead to sustained immune activation and acceleration of disease progression.

In support for the role of LRRK2 in immune cell regulation, we found that LRRK2 protein expression increases in human immune cells following inflammatory challenges. Thereafter, LRRK2 levels continue to increase over time in monocytes. Monocytes are antigen-presenting cells that are critical to the activation of the adaptive immune response by upregulating MHC-II (HLA-DR/-DQ) proteins loaded with antigens that activate $CD4^+$ T cells. Although we observed no differences in the overall extent of MHC-II induction between the PD and HC groups, in HC subjects, LRRK2 expression is negatively correlated with HLA-DQ expression whereas in PD patients, LRRK2 expression is positively correlated with HLA-DR expression. These data suggest that LRRK2 could be regulating the antigen presentation function of human monocytes, and that such regulation is altered in PD patients. Studies have shown that inhibition of LRRK2 kinase activity with the LRRK2-IN1 inhibitor decreased expression of CD14, CD16, and MHC-II in monocytes[173]. However, due to the reported off-target effects of LRRK2-IN1, specifically ERK5 inhibition[217], it is possible that this decrease cannot be attributed wholly to LRRK2 kinase activity. Alternatively, it is possible that LRRK2 localizes and associates with binding partners involved in regulation of antigen presentation and that LRRK2 kinase activity is not required for such interactions. In addition, recent studies suggest that antigen presentation is altered in a subset of individuals with PD in association with a non-coding SNP (*rs 3129882*) in the MHC-II locus that synergizes with environmental exposures to increase risk for PD[84]. Although

the LRRK2 and MHC-II loci are encoded on different chromosomes, perhaps the mechanism of altered antigen presentation increases susceptibility for idiopathic PD.

Previous studies have declared LRRK2 absent or undetectable in T cell populations[173], however, the data presented here definitively demonstrate inducible expression of LRRK2 not just in $CD3^+$ T cells, but also in all functional T cell subsets. There were no significant differences between baseline levels of LRRK2 in subsets of T cells; however, LRRK2 levels were increased in all of the T cells of PD patients relative to those of HC subjects. Given that LRRK2 has been shown to be a negative regulator of NFAT in HEK293T cells[168], and NFAT is a necessary transcription factor for T cell activation, we hypothesize that LRRK2 could also serve as a negative regulator of T cell activation via interaction with NFAT. Induction of LRRK2 was also seen in T cells, but was delayed until 72 hrs and only seen in dividing T cells. PD patients also had greater upregulation of LRRK2 in these dividing T cells, raising the interesting possibility that LRRK2 is essential for T cell division or acting in some sort of regulatory capacity during T cell division.

Markers of T cell activation such as CTLA-4 and 4-1BB are good indicators of proper immune response and regulation. Immune cells upregulate these markers following stimulation to keep the inflammatory response in check. Interestingly, T cells from PD patients have an impaired capacity to upregulate CTLA-4 compared to those from healthy controls. CTLA-4 transcription is controlled by NFAT1 binding to the proximal promoter and is decreased when NFAT is inhibited[236]. Therefore, our findings suggest that in healthy individuals LRRK2 is a negative regulator of T cell activation. Specifically, the increase in LRRK2 induced by stimulation acts to limit NFAT-

dependent transcription, as evidenced by reductions in expression of CTLA-4. In PD patients, alterations in LRRK2 function may translate into poor regulation of T cell responses and result in a pro-inflammatory environment characteristic of PD.

Cytokine secretion by T cells is a necessary step for promoting the immune response, but prolonged secretion and/or increased cytokine levels are hallmarks of inflammatory disease. In the CSF and nigrostriatal regions of PD brains examined at autopsy, the levels of pro-inflammatory cytokines such as IL-1β, TNF, IFN-γ, and IL-6 were increased compared to those of age-matched HC subjects[94,96,98]. In the present studies, monocytes and T cells from PD patients were shown to secrete more pro-inflammatory cytokines than T cells from healthy individuals. In addition, both $CD4^+$ and $CD8^+$ T cells of PD patients expressing higher levels of inflammatory cytokines also expressed higher levels of LRRK2 suggesting that LRRK2 protein expression is associated with the inflammatory response characteristically seen in this neurodegenerative disease. Taken together, our findings suggest that LRRK2 levels in peripheral T cells may serve as a biomarker for diagnosis and monitoring disease progression in PD patients.

The significance of our findings are three-fold. First, the selective induction of LRRK2 in pro-inflammatory monocytes and its potential regulatory role in antigen presentation is a crucial step in activation of the immune response and merits further exploration. Second, defining the kinetics of LRRK2 expression and its regulation in activated T cells is a critical first step toward understanding the role that LRRK2 plays in the adaptive immune system and its potential link to PD pathogenesis. Third, the positive correlations between LRRK2 expression levels in T cell subsets, cytokine expression and

secretion, and T cell activation states suggest that targeting LRRK2 with therapeutic interventions is likely to have direct effects on immune cell function—whether this affords benefit or untoward bystander effects remains to be determined and is prerequisite to advancing LRRK2 kinase inhibitors to clinical trials.

2.5 Figures

	HC	PD	p-value
N	32	40	
Age	65.7±1.86	67.4±1.32	0.46
Sex	24F, 8M	11F, 29M	0.0004
rs3129882 genotype	14AA, 9GG, 9AG	15AA, 13GG, 12AG	0.86
Smoking (pack-yrs)	2.39±1.1	5.88±13.4	0.17
Caffeine (mg-yrs)	10935±1380	12026±1606	0.62
NSAID Use (mg-yrs)	1018±180	981.5±284	0.92
Head Injuries	0.125±0.098	0.45±0.143	0.08

Table 2.1. Demographics of the Study Population. Healthy Controls (HC) and Parkinson's disease (PD) subjects are matched for age, *rs3129882* HLA-DRA genotype, smoking (pack-yrs), caffeine (mg-yrs), NSAID use (mg-yrs), and head injuries. Although the groups are not balanced for sex, these differences do not account for the differences seen in the data.

Marker	Fluorophore	Dilution	Company	Catalog Number
LRRK2	Unconjugated	1:50	abcam	ab133474
F(ab')2 anti-rabbit IgG	FITC	1:50	eBioscience	11-4839
CCR7	PE	1:100	BioLegend	353204
FOXP3	PE	1:20	BD Pharmingen	560046
CD14	PE	1:100	BioLegend	301806
CXCR3	PE	1:20	BioLegend	353706
CD4	PerCP-Cy5.5	1:100	BioLegend	300530
4-1BB	PerCP-Cy5.5	1:20	BioLegend	309814
CD19	PE-Cy7	1:20	BioLegend	302216
CD45RA	PE-Cy7	1:100	eBioscience	25-0458
CCR4	PE-Cy7	1:100	BioLegend	359410
CCR6	PE-Cy7	1:20	BioLegend	353418
CD25	PE-Cy7	1:20	BioLegend	302612
IL-2	PE-Cy7	1:100	BioLegend	500326
HLA-DQ	APC	1:100	eBioscience	17-9881
CD38	APC	1:20	BioLegend	356606
CD127	APC	1:100	BioLegend	351316
TNFa	APC	1:100	BioLegend	502912
CTLA4	APC	1:20	BioLegend	349908
CD8	APC-H7	1:100	BD Pharmingen	560273
CD45RO	APC-Cy7	1:50	BioLegend	304228
IFN-γ	APC-eFluor780	1:20	eBioscience	47-7319
CD3	V450	1:20	BD Horizon	560365
CD8	V450	1:50	eBioscience	48-0087
HLA-DR	V500	1:20	BD Horizon	561224
CD4	BV650	1:100	BioLegend	317436
CD16	AF700	1:20	BioLegend	302026

Table 2.2. Fluorophore-conjugated antibodies used for flow staining and their dilutions.

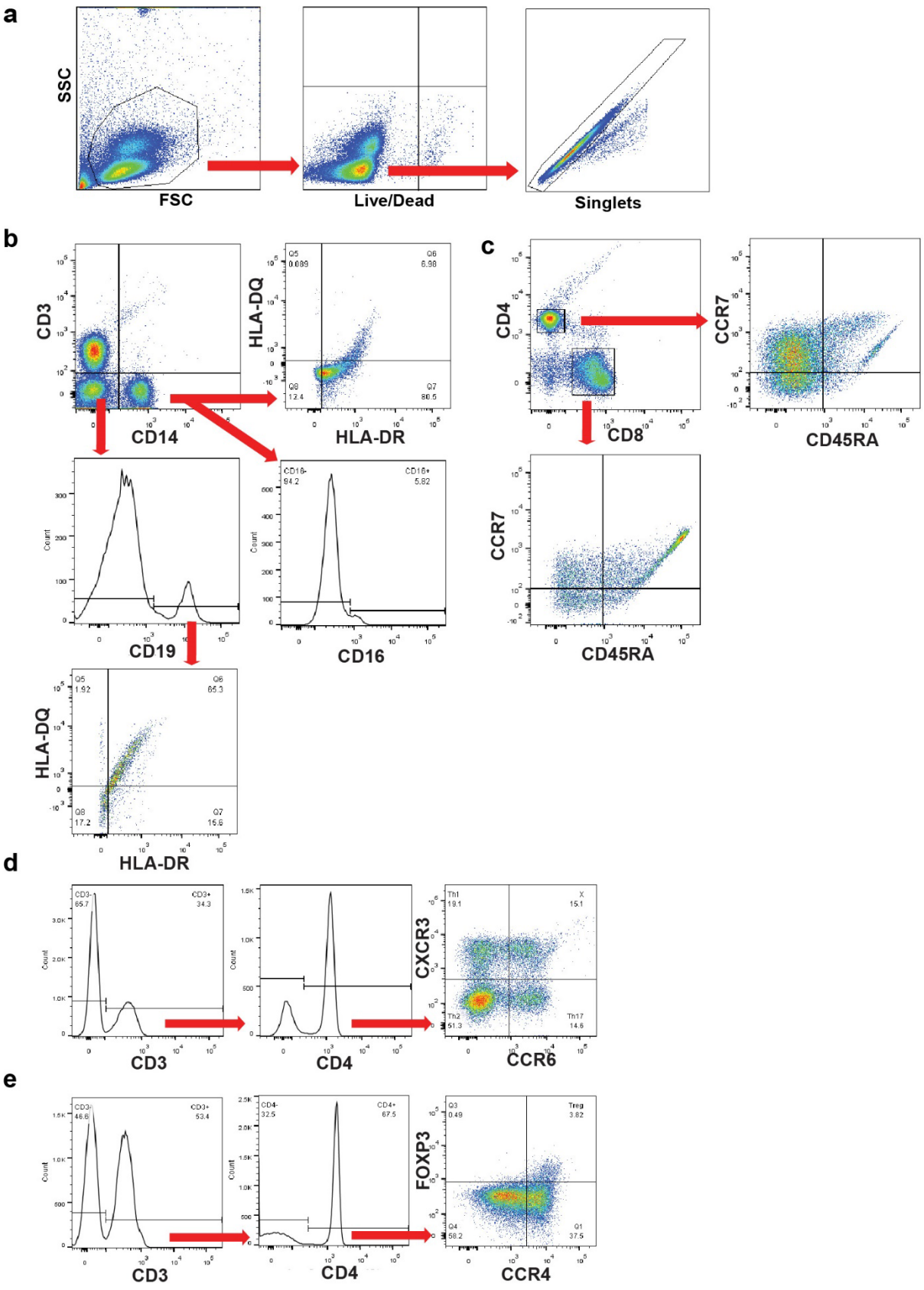
a
SSC
FSC
Live/Dead
Singlets
b
CD3
CD14
HLA-DQ
HLA-DR
CD19
CD16
HLA-DQ
HLA-DR
c
CD4
CD8
CCR7
CD45RA
CCR7
CD45RA
d
CD3
CD4
CXCR3
CCR6
e
CD3
CD4
FOXP3
CCR4

Figure 2.1. Gating Strategy for Flow Cytometry Analysis. Gating for (a) Live/dead and singlet cells, (b) monocytes, (c) Teff cells, (d) T helper cells, and (e) Treg cells. Cells were stained with fluorophore-conjugated antibodies to cell-surface or intracellular markers (See **Table 2**) for flow cytometry and analyzed on a LSR-II flow cytometer (BD Bioscience) after standardization and compensation with Supra Rainbow Sphero beads and OneComp beads. Gates were placed based on staining with isotype control antibodies. Analysis was performed and plots were generated using FlowJo software.

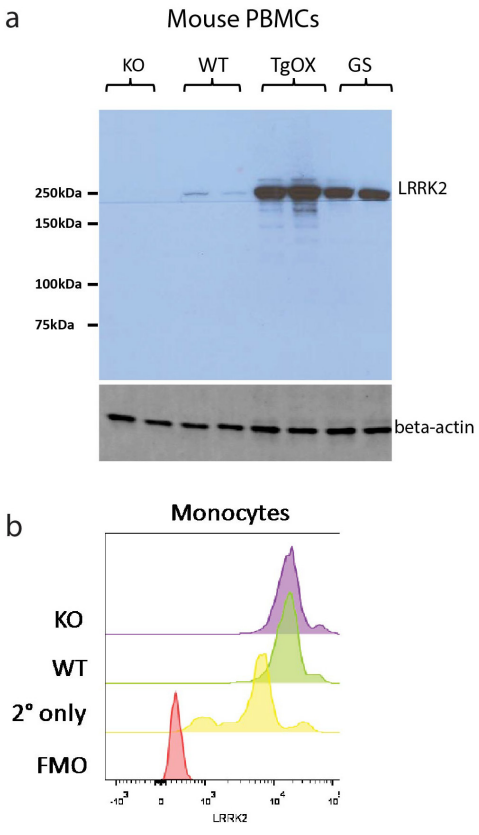

Figure 2.2. The c41-2 LRRK2 antibody does not recognize mouse LRRK2 protein well for flow cytometry. PBMCs from LRRK2 knockout, wild type C57BL/6J, mouse WT-LRRK2 BAC (Tg-OX), or mouse G2019S (GS)-LRRK2-overexpressing were

obtained and processed for western blot analyses (a) or permeabilized and immunolabeled for flow cytometry (b) for detection of LRRK2 with the Abcam c41-2 rabbit polyclonal antibody.

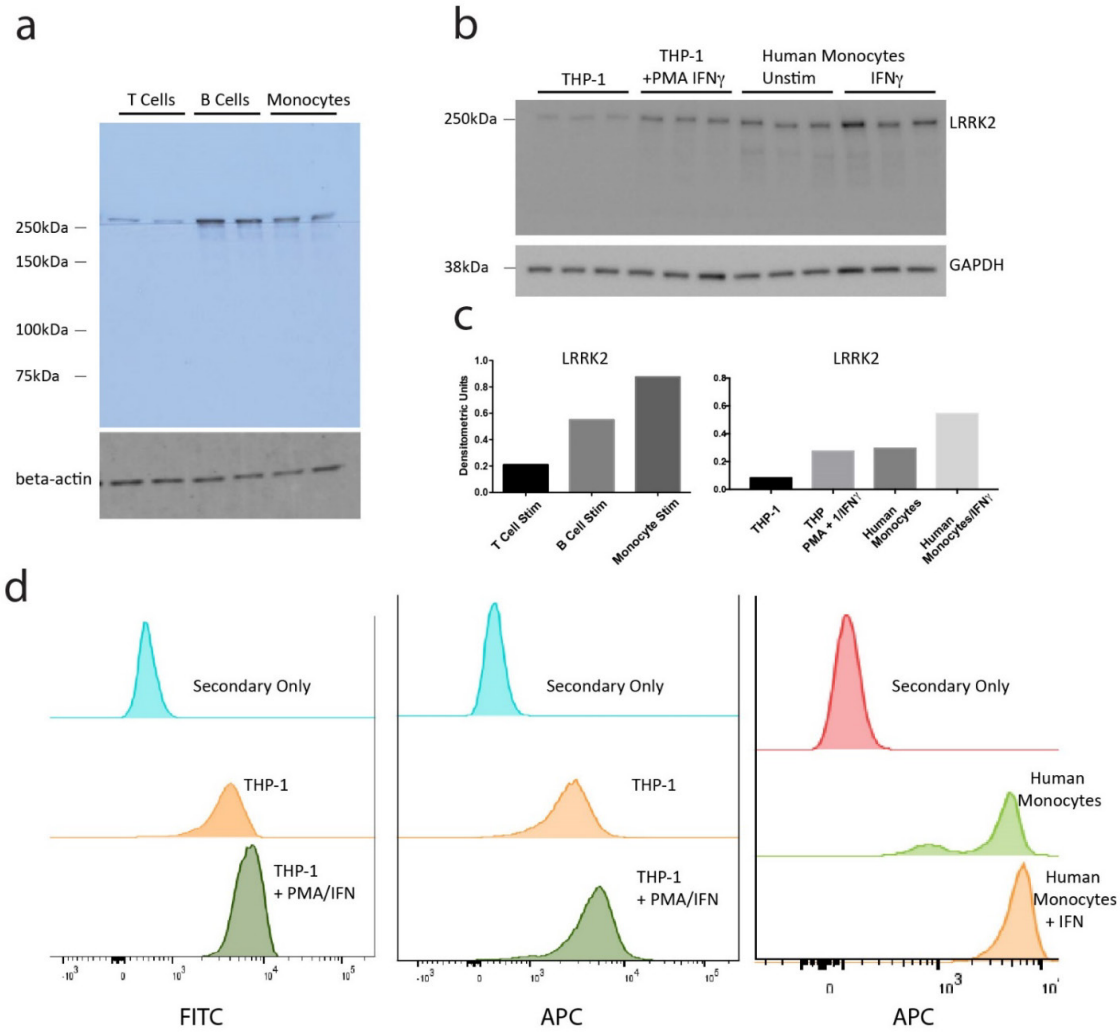

Figure 2.3. Antibody validation for detection of human LRRK2 protein by flow cytometry. (a) The c41-2 LRRK2 antibody detects human LRRK2 protein in human immune cells by western blotting. (b) Increases in human LRRK2 protein in PMA differentiated/IFN-γ-stimulated THP-1 human monocytic cell line, IFN-γ-stimulated human monocytes from peripheral blood are detectable by western blot with the c41-2 LRRK2 antibody. Western blot analysis of LRRK2 levels in naïve THP-1 (n=3) and

PMA-differentiated and IFN-γ-stimulated THP-1 cells (n=3) compared to human primary monocytes from peripheral blood (n=3). (c) Increases in human LRRK2 protein in permeabilized PMA differentiated/IFN-γ-stimulated THP-1 cells are detectable by flow cytometry with the c41-2 LRRK2 antibody and a FITC-conjugated secondary antibody (1:10,000) or an Alexa 647-conjugated secondary (1:10,000).

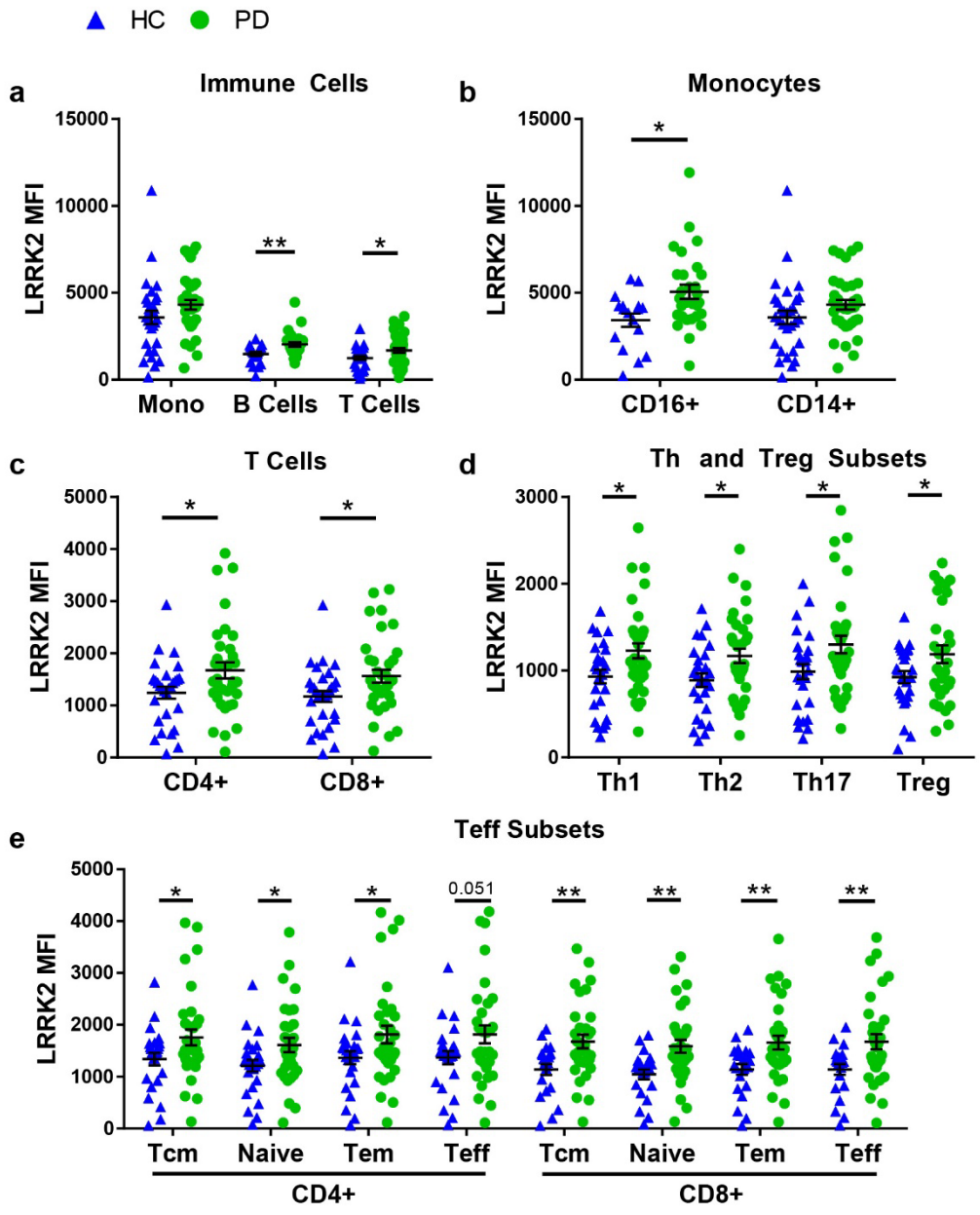

Figure 2.4. LRRK2 expression in T cells, B cells, and a subset of monocytes is increased in PD patients compared to matched HC subjects. (a) LRRK2 median fluorescence intensity (MFI) in monocytes ($t(64)=1.57$, $p=0.122$, HC $n= 30$, PD $n=36$), B cells ($t(47)=3.02$, $p=0.004$, HC $n=21$, PD $n=28$), and T cells ($t(63)=2.35$, $p=0.022$, HC $n=29$, PD $n=36$), (b) a subset of monocytes ($t(44)=2.68$, $p=0.01$, HC $n= 17$, PD $n=29$) (c-e) and T cell subsets ($CD4^+$, $t(61)=2.17$, $p=0.034$, HC $n=29$, PD $n=34$; $CD8^+$, $t(65)=2.39$, $p=0.02$ HC $n=31$, PD $n=36$; T helper HC $n=27$, PD $n=34$: Th1, $t(59)=2.49$, $p=0.016$; Th2, $t(59)=2.41$, $p=0.019$; Th17, $t(59)=2.24$, $p=0.029$; Treg, $t(55)=2.06$, $p=0.044$ HC $n=26$, PD $n=31$; $CD4^+$ effector subsets HC $n=26$, PD $n=33$: Tcm $t(57)=2.08$, $p=0.043$; Naïve $t(57)=2.18$, $p=0.033$; Tem $t(57)=2.02$, $p=0.049$; Teff, $t(57)=1.99$, $p=0.051$; $CD8^+$ effector subsets HC $n=22$, PD $n=33$: Tcm $t(53)=2.95$, $p=0.005$; Naïve $t(53)=3.16$, $p=0.003$; Tem $t(53)=2.81$, $p=0.007$; Teff $t(53)=2.70$, $p=0.009$) was determined flow cytometry staining of total peripheral blood mononuclear cells. Means were plotted with standard error of the mean. Two-tailed Student's t-test between HC and PD was used to test for significance. $*p < 0.05$. $**p < 0.01$.

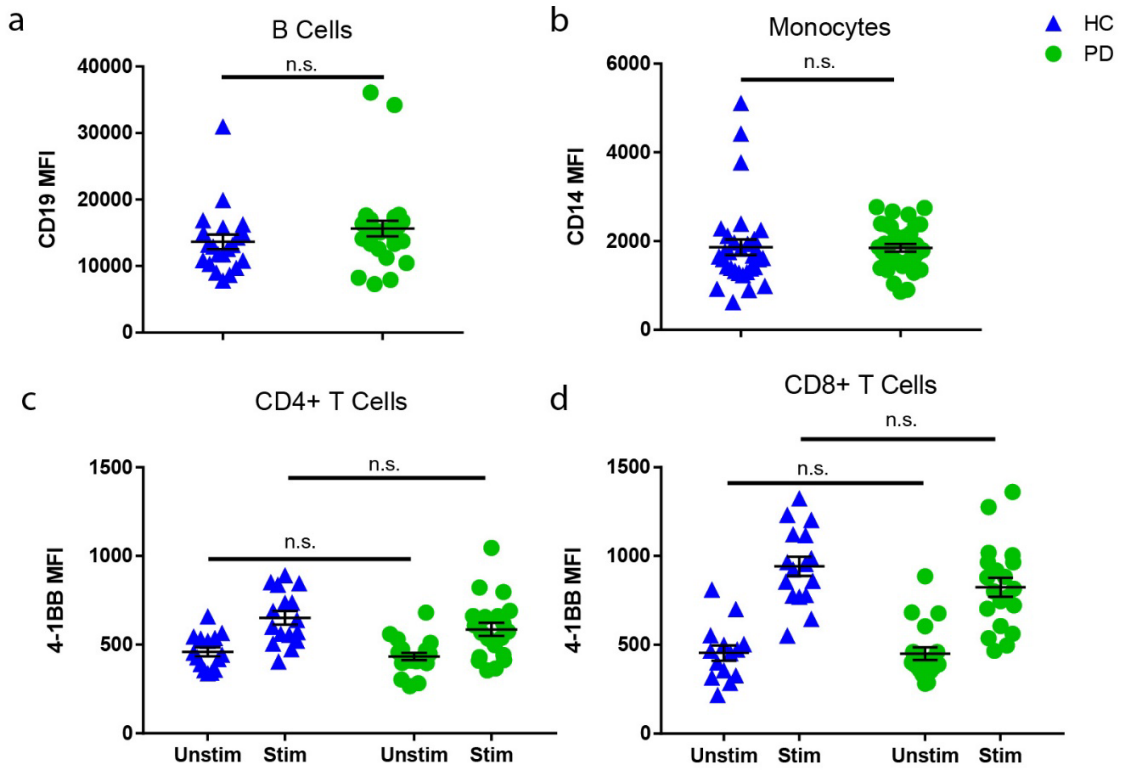

Figure 2.5. Protein levels of cell specific surface markers in B cells, monocytes, and T cells are not different between PD and HC subjects. MFI of (a) CD19 in B cells (p=0.23, HC n=21, PD n=28), (b) CD14 in monocytes (p=0.94, HC n=31, PD n=36), and (c-d) 4-1BB in $CD4^+$ (p=0.16, HC n=16, PD n=20) and $CD8^+$ (p=0.21, HC n=15, PD n=20) T cells.

Immunophenotype of Innate Cells					
Cell	**CD19**	**CD14**	**CD16**	**HLADR**	**HLADQ**
Classical Monocyte	-	+	-	+	+
Non-classical monocyte	-	+	+	+	+
B Cells	+	-	-	+	+

Immunophenotype of Adaptive Cells												
Cell	**CD3**	**CD4**	**CD8**	**CCR7**	**CD45RA**	**CD45RO**	**CXCR3**	**CCR6**	**FOXP3**	**CD25**	**CCR4**	**CD127**
Tcm	+	+	+	+	-							
Teff	+	+	+	-	+							
Tem	+	+	+	-	-							
Tnaive	+	+	+	+	+							
Naïve Treg	+	+				-			+	+	+	-
Memory Treg	+	+				+			+	+	+	-
Th1	+	+				+	+	-				
Th2	+	+				+	-	-				
Th17	+	+				+	-	+				

Table 2.3. Immunophenotypic markers for innate and adaptive immune cells. Innate and adaptive cells were defined using the cell surface markers defined by the Human Immunophenotype Project.

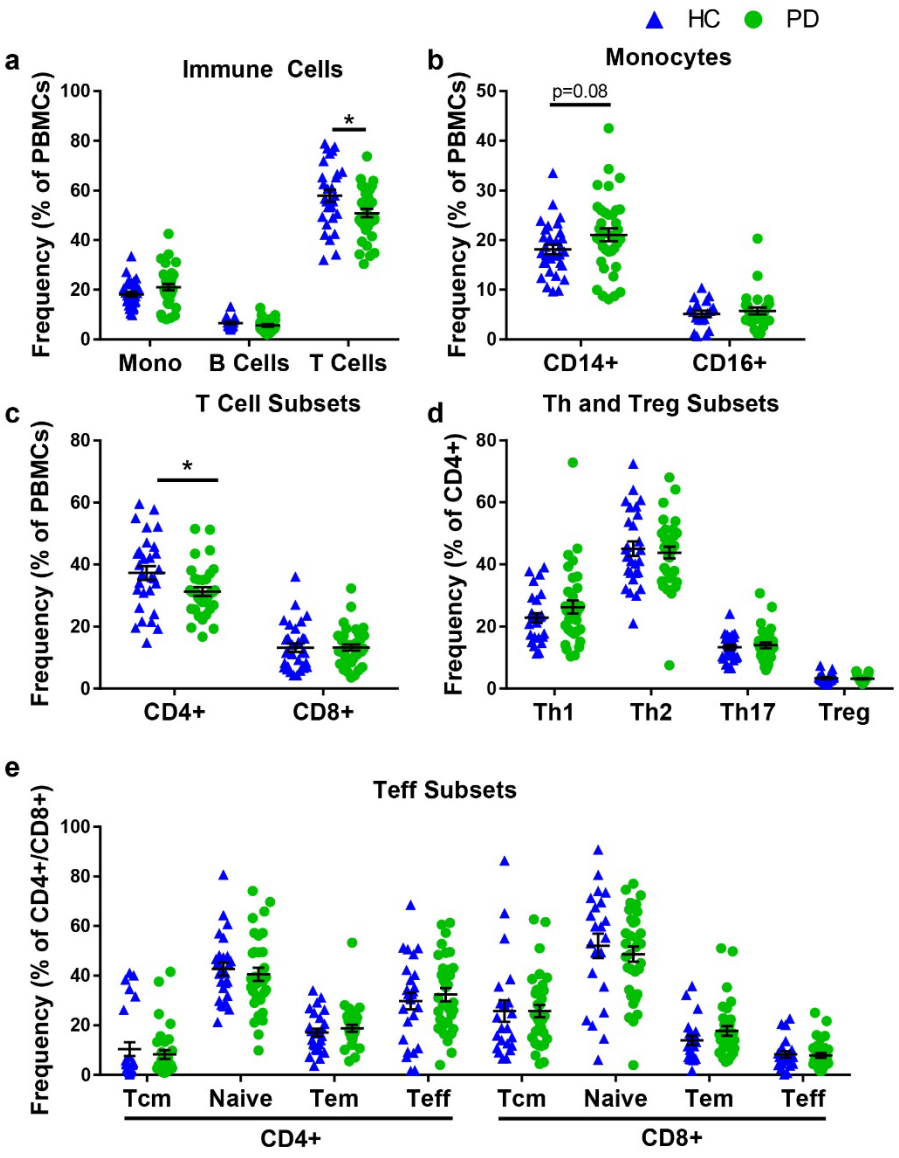

Figure 2.6. T cells frequencies are decreased in subjects with PD relative to HC subjects due to a decrease in CD4$^+$ T cells. (a) Frequencies as percentage of total peripheral blood mononuclear cells of monocytes (p=0.081, HC n= 31, PD n=36), B cells (p>0.05, HC n=22, PD n=28), and T cells (p=0.018, HC n=29, PD n=36), (b) a subset of monocytes (p>0.05, HC n= 18, PD n=29), (c) CD4$^+$ helper subsets (Th1, p>0.05 HC n=27, PD n=34; Th2, p>0.05 HC n=27, PD n=34; Th17, p>0.05 HC n=27, PD n=34; Treg, p>0.05 HC n=26, PD n=31) were determined flow cytometry staining of total

peripheral blood mononuclear cells, and (d) $CD4^+$ (p=0.023, HC n=29, PD n=34) and $CD8^+$ ($CD8^+$, p>0.05 HC n=31, PD n=36) T cells subsets. (e) Frequencies of T cell effector subsets were determined as a percentage of $CD4^+$ ($CD4^+$ HC n=26, PD n=33, Tcm p>0.05; Naïve p>0.05; Tem p>0.05; Teff p>0.05) or $CD8^+$ ($CD8^+$ HC n=22, PD n=33, Tcm p>0.05; Naïve p>0.05; Tem p>0.05; Teff p>0.05) T cells, respectively. Means were plotted with standard error of the mean. Two-tailed Student's t-test between HC and PD was used to test for significance. * $p < 0.05$.

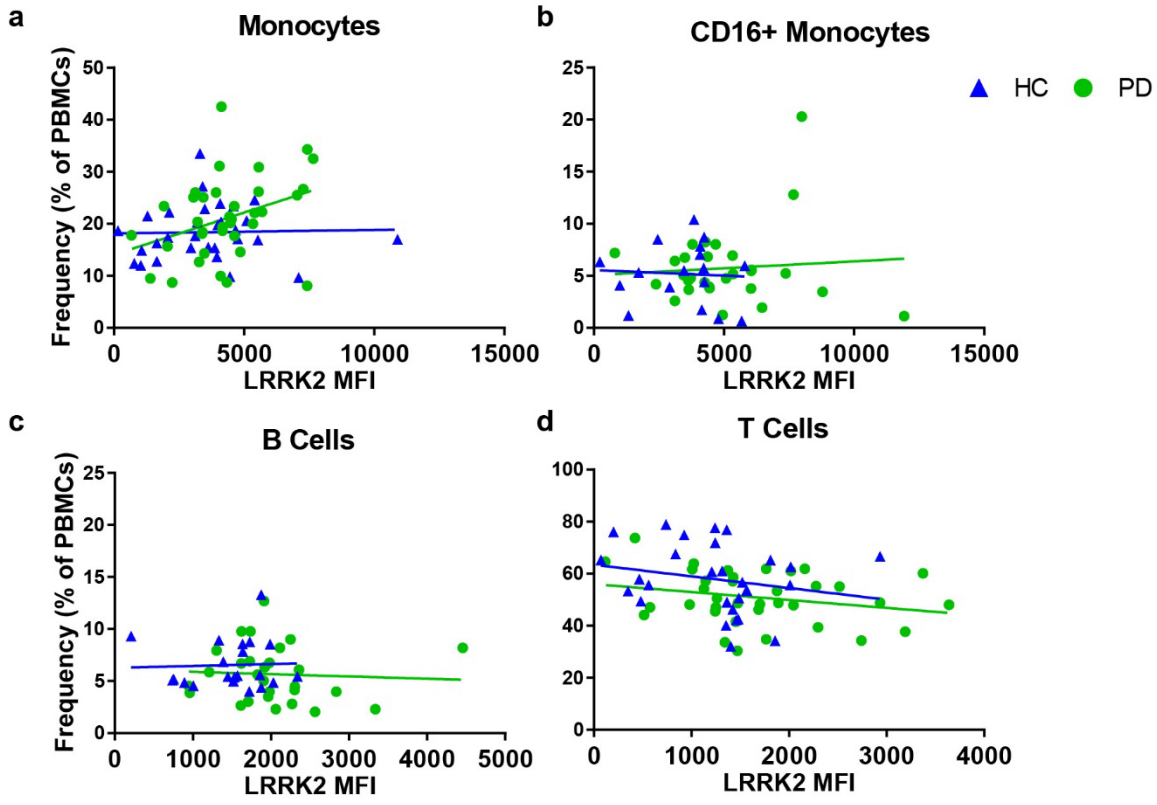

Figure 2.7. LRRK2 expression in monocytes positively correlates with monocyte frequency in PD patients but not in HC subjects. Frequency of (a) monocytes (HC

R^2(30)=0.001, p=0.88; PD R^2(36)=0.125, p=0.034); F(1, 62)=3.23, p=0.077), (b) CD16$^+$ monocytes (HC R^2(17)=0.004, p=0.822, PD R^2(29)=0.006, p=0.684; F(1,42)=0.148, p=0.703), (c) B cells (HC R^2(23)=0.002, p=0.860, PD R^2(28)=0.003, p=0.773; F(1, 45)=0.092, *p=0.763*) and (d) T cells (HC R^2(29)=0.045, p=0.267, PD R^2(37)=0.061, p=0.146; F(1, 61)=0.117, p=0.734) as a percentage of total PBMCs determined by flow cytometry staining were plotted versus LRRK2 median fluorescence intensity (MFI). Means were plotted with standard error of the mean. ANCOVA was performed to assess differences of slopes between HC and PD. Linear regression was used to assess individual correlations of slopes of HC and PD. Significance was set at $p < 0.05$.

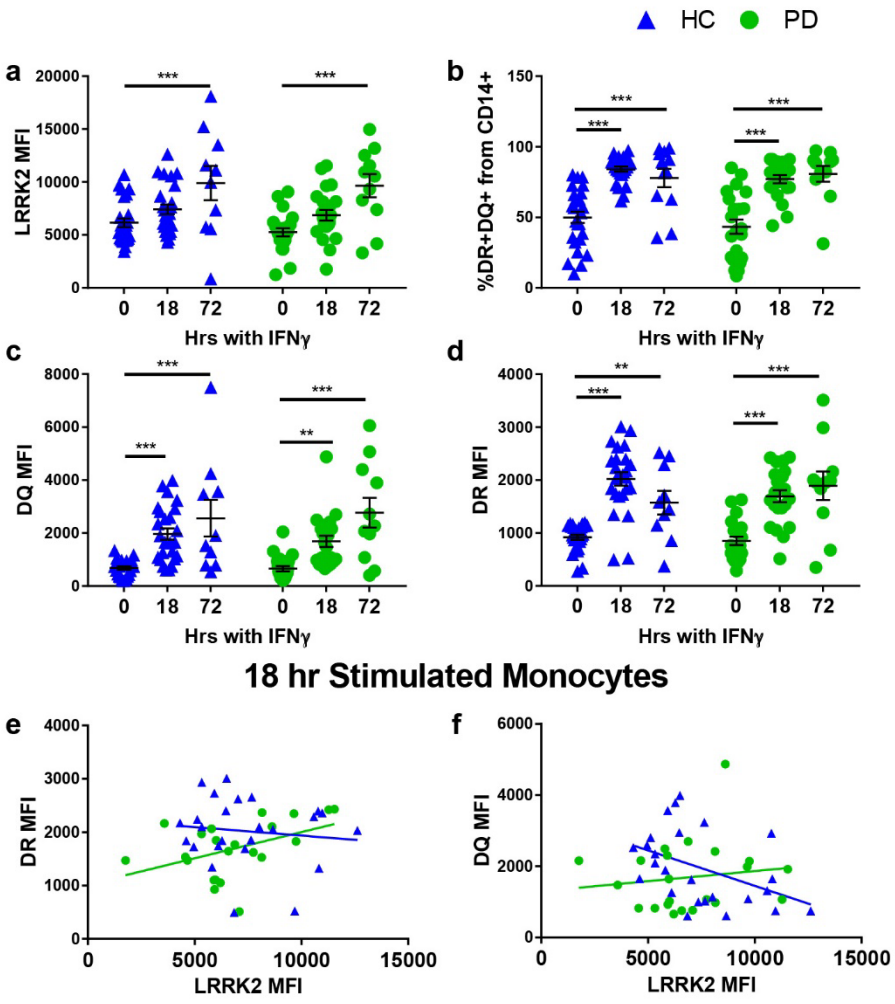

Figure 2.8. The IFNγ-stimulated increase in LRRK2 protein in PD and HC monocytes displays similar kinetics but the correlation between LRRK2 levels and MHC-II expression is different for PD versus HC. (a) LRRK2 induction (HC p=0.0006, PD p<0.0001), (b) %DR^+DQ^+ monocytes (18 and 72 hrs HC p<0.0001, PD p<0.0001), (c) HLA-DQ induction (18 hrs HC p=0.0001, PD p=0.0042; 72 hrs HC p<0.0001, PD p<0.0001), and (d) HLA-DR induction (18 hrs HC p<0.0001, PD p<0.0001; 72 hrs HC p=0.0049, PD p<0.0001) with or without 100 U/mL interferon-γ stimulation for 18 (HC n=25, PD n=22) or 72 hrs (HC n=10, PD n=11) in paramagnetically, positively sorted monocytes was measured by flow cytometry. Means were plotted with standard error of the mean. Two-way ANOVA with Sidak's multiple comparisons post-hoc test was used to test for significance. * P < 0.05, ** P < 0.01, *** P < 0.001. (e) -DR median fluorescence intensity (MFI) (HC R^2(25)=0.013, p=0.580, PD R^2(22)=0.195, p=0.040; F(1,43)=3.16, p=0.083) and (f) -DQ MFI (HC R^2(25)=0.193, p=0.028, PD R^2(22)=0.193, p=0.540; F(1, 43)=4.24, p=0.046) were measured using flow cytometry and plotted against LRRK2 MFI. ANCOVA was performed to assess differences of slopes between HC and PD. Linear regression was used to assess individual correlations of slopes of HC and PD. Significance was set at p < 0.05.

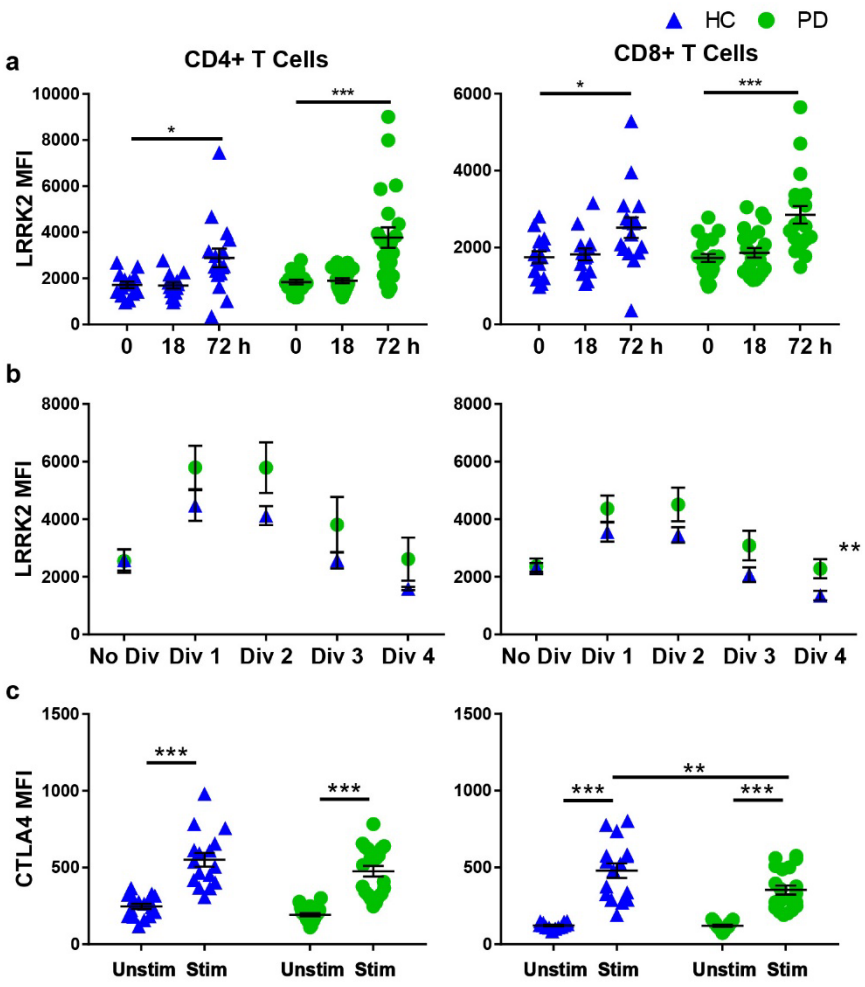

Figure 2.9. The anti-CD3/CD28-stimulated increase in LRRK2 protein in T cells is slower than in monocytes and similar in PD and HC subjects but T cell proliferation is associated with greater increases in LRRK2 protein and dampened expression of the negative regulator of T cell activation CTLA4 in PD subjects. LRRK2 median fluorescence intensity (MFI) of (a) stimulated cells (HC 18 hrs n=14, 72 hrs n=16, p=0.019; PD 18 hrs n=22, 72 hrs n=20, p<0.0001), (b) proliferating cells (CellTrace Violet) (p=0.0045, HC n=12, PD n=11) and (c) CTLA-4 MFI (HC n=16, PD n=20, $CD8^+$ p=0.0034) were measured using flow cytometry following stimulation of paramagnetically, positively selected T cells with 30 U/mL IL-2 and anti-CD3/CD28

stimulation beads for 72 hrs. Means were plotted with standard error of the mean. Two-way ANOVA with Sidak's multiple comparisons post-hoc test was used to test for significance. * $p < 0.05$, ** $p < 0.01$, *** $p < 0.001$.

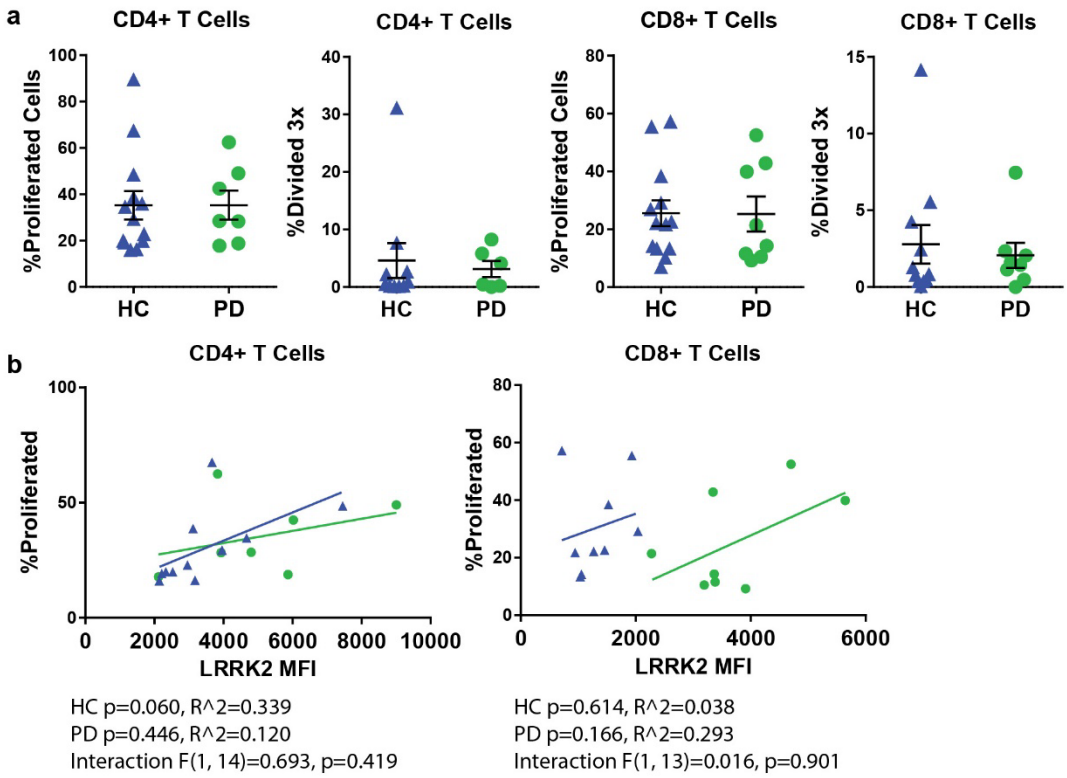

Figure 2.10. Proliferation of T cells from PD and HC subjects is similar after 72 hrs but LRRK2 protein levels show different correlations with percentage of proliferated cells in PD versus HC subjects. Percent of cells that proliferated after 72 hrs of stimulation with CD3/CD28 and IL-2 was calculated using CellTrace Violet and flow cytometry. (a) No differences between HC and PD seen for both $CD4^+$ and $CD8^+$ T cells. The percent of cells that divided at least three times also showed no differences between the two groups. Means were plotted with standard error of the mean. Two-tailed Student's t-test between HC and PD was used to determine significance. $p < 0.05$. (b) Percentage of proliferating cells ($CD4^+$ T cells: HC $R^2(11)=0.339$, $p=0.060$, PD $R^2(7)=0.120$, $p=0.446$; $F(1, 14)=0.693$, $p=0.419$) $CD8^+$ T cells: HC $R^2(9)=0.038$, $p=0.614$, PD $R^2(8)=0.293$, $p=0.166$; $F(1,13)=0.016$, $p=0.901$) versus LRRK2 median fluorescence intensity (MFI) as measured by flow cytometry showed significant

difference for $CD4^+$ T cells between PD and HC. ANCOVA was performed to assess differences of slopes between HC and PD. Linear regression was used to assess individual correlations of slopes of HC and PD. Significance was set at $p < 0.05$.

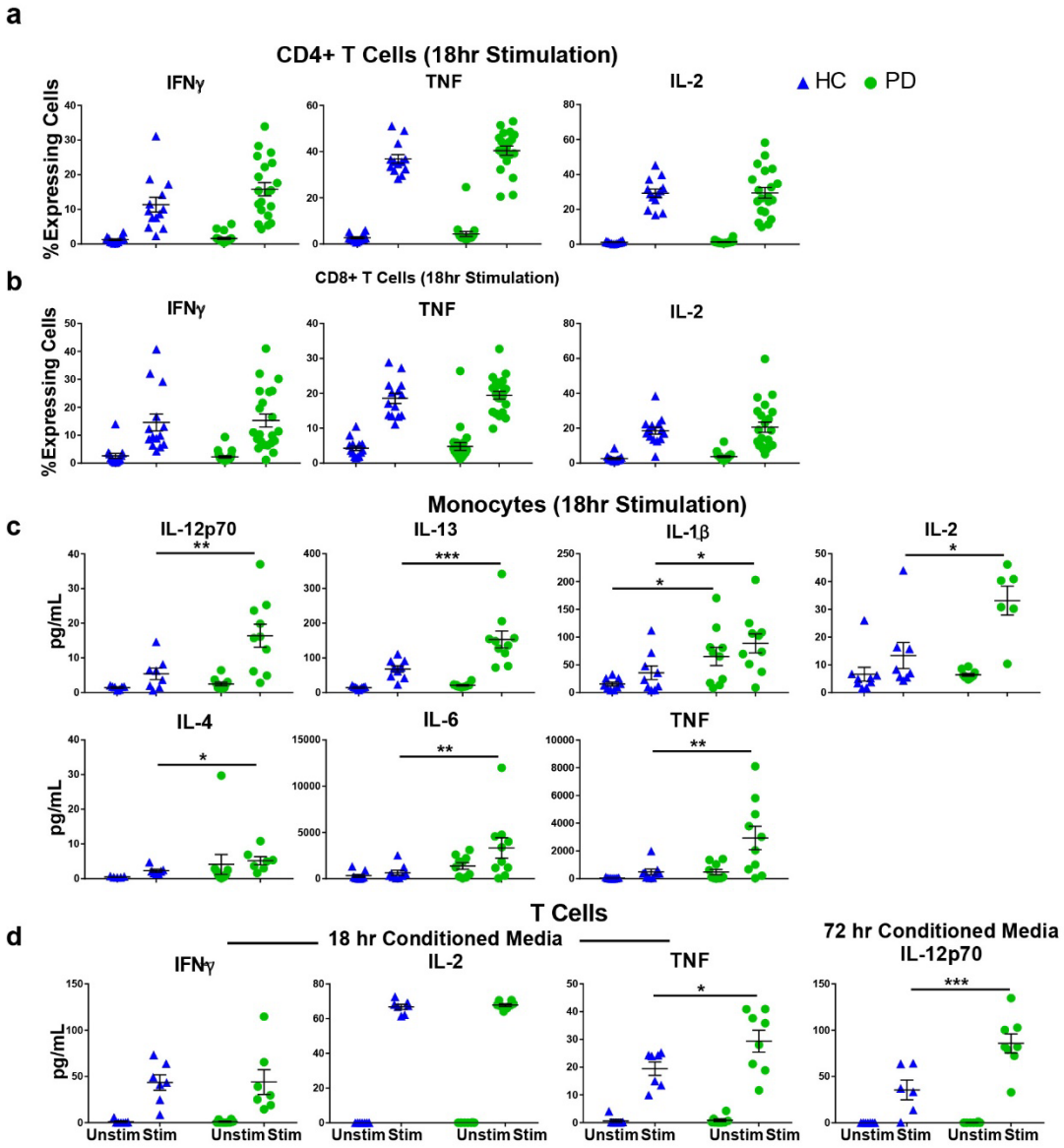

Figure 2.11. Monocytes and T cells from PD patients display increased cellular expression and secretion of pro-inflammatory cytokines in association with higher

LRRK2 protein expression. (a-b) Cytokine expression measured through intracellular cytokine staining measured with flow cytometry (HC n=13, PD n=22), (c) multiplexed immunoassay on conditioned media from 18 hrs stimulated monocytes (HC n=9, PD n=10) and (d) 18 hrs (HC n=7, PD n=8, p=0.0154) and 72 hrs (HC n=7, PD n=8, p=0.0001) stimulated T cells. Means were plotted with standard error of the mean. Two-way ANOVA with Sidak's multiple comparisons post-hoc test was used to test for significance. * $p < 0.05$, ** $p < 0.01$, *** $p < 0.001$.

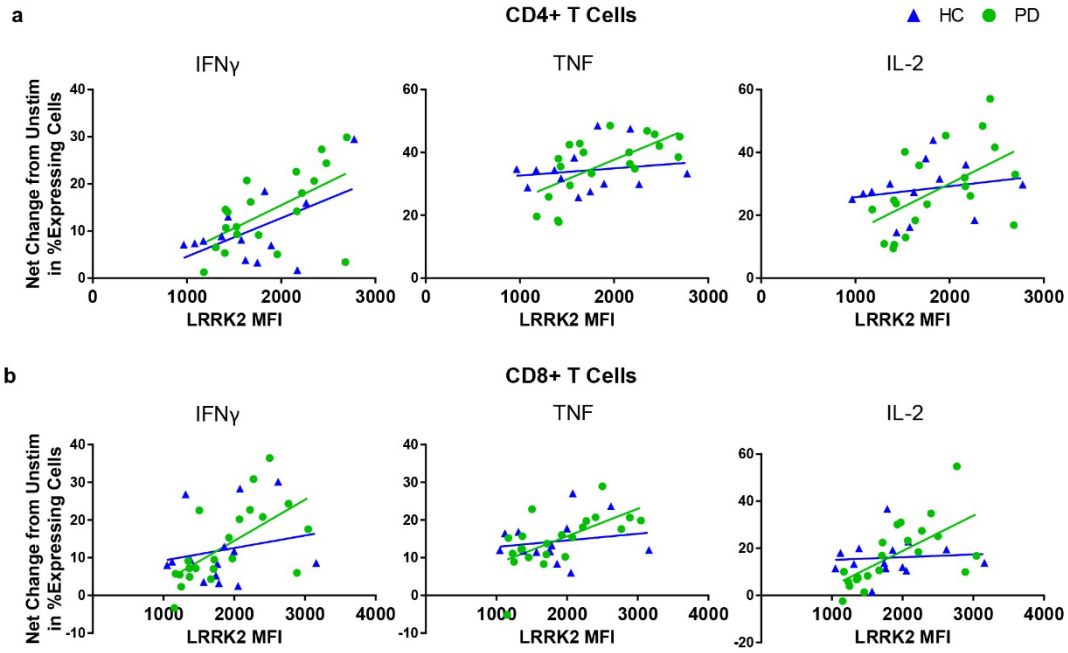

Figure 2.12. LRRK2 protein in stimulated CD4$^+$ and CD8$^+$ T cells from PD patients displays significant positive correlations with cytokine-expression. Fold change in percent of cytokine secretion (IFN-γ, TNF, and IL-2) by (a) CD4+ T cells (IFN-γ: PD $R^2(20)$=0.339, p=0.002, HC $R^2(13)$=0.307, p=0.049; $F(1, 29)$=0.106, p=0.747; TNF: PD $R^2(20)$=0.421, p=0.002, HC $R^2(13)$=0.028, p=0.585; $F(1, 29)$=3.63, p=0.067; IL-2: PD $R^2(20)$=0.293, p=0.0014, HC $R^2(13)$=0.044, p=0.494; $F(1, 29)$=2.19, p=0.150) and (b)

$CD8^+$ T cells (IFN-γ: PD $R^2(22)=0.400$, $p=0.002$, HC $R^2(14)=0.040$, $p=0.494$; $F(1, 32)=2.04$, $p=0.163$; TNF: PD $R^2(22)=0.398$, $p=0.002$, HC $R^2(14)=0.031$, $p=0.549$; $F(1, 32)=2.65$, $p=0.113$; IL-2: PD $R^2(22)=0.430$, $p=0.001$, HC $R^2(14)=0.007$, $p=0.780$; $F(1, 32)=5.46$, $p=0.026$) relative to unstimulated cells plotted against LRRK2 median fluorescence intensity (MFI) of stimulated cells. ANCOVA was performed to assess differences of slopes between HC and PD. Linear regression was used to assess individual correlations of slopes of HC and PD. Significance was set at $p < 0.05$.

Chapter 3. Assessing contribution of LRRK2 kinase activity to immune cell activation via NFAT and NF-κB

3.1 Introduction

Parkinson's disease (PD) is a movement disorder caused by dopaminergic (DA) neuronal degeneration in the substantia nigra that progresses with age. It affects nearly 10 million people worldwide and costs upwards of $25 billion in the United States alone[237]. It is pathologically characterized by the formation of protein aggregates of α-synuclein (α-syn) called Lewy bodies in both the periphery and the brain[89,90]. Clinically, the disease has a pre-motor phase that can begin decades before diagnosis with symptoms that include REM sleep behavior disorder, anosmia, and constipation. Diagnosis occurs after examination where an individual's motor symptoms (muscle rigidity, bradykinesia, shuffling gate, etc.) are rated on a clinical scale[80,81]. While modifiers of disease risk such as cigarette use, caffeine consumption, and NSAID use can have a protective effect against PD, little progress has been made to develop a cure or therapeutic that can halt progression of the disease[86,229].

LRRK2 is a gene that, when mutated, leads to higher susceptibility for development of PD, particularly in Ashkenazi Jewish and North African Arab populations[112]. It encodes a large (~286 kDa) protein with multiple protein interacting domains (WD-40, leucine rich repeat, armadillo, anykrin repeat[122]) and both a Ras of complex (ROC) GTPase[123] and a serine/threonine kinase enzymatic domain[188]. LRRK2 has been implicated in the regulation of many cellular pathways including autophagy[147,238], cytoskeletal remodeling[130,193], lysosomal function, neurite growth[146,149],

and inflammation[166,168,204] making it difficult to pinpoint a specific function. Function is likely cell-type specific and dependent upon the local microenvironment.

Many LRRK2 mutations and polymorphisms have been associated with a range of diseases including PD[110], Crohn's disease[197], and leprosy[199]. The most common pathogenic mutations occur in the GTPase and kinase enzymatic domains. The G2019S mutation in the kinase domain has the highest prevalence and dramatically increases LRRK2 kinase activity compared to wild type protein[174,187]. Recent studies using phosphorylation of Rab as a measure of LRRK2 kinase activity have indicated that pathogenic mutations in both the GTPase and kinase domain enhance LRRK2 kinase activity[125]. Rab GTPases are a family of proteins that regulate vesicular trafficking. Pathogenic LRRK2 mutations increase phosphorylation of Rabs, altering trafficking and contributing to disease.

LRRK2 protein function has been implicated in multiple immune signaling pathways, namely NF-κB and NFAT. The NF-κB transcription factor is essential to immune activation and proliferation. Signaling through the NF-κB pathway results in the production of pro-inflammatory cytokines, chemokines, and adhesions molecules. Multiple studies have linked LRRK2 to regulation of the NF-κB signaling pathway. Silencing of LRRK2 with shRNA significantly reduces the amount of COX-2 (a downstream effector of NF-κB) produced by fibroblasts derived from PD patients[203]. LRRK2 has been shown to phosphorylate RCAN1, a protein inhibitor of phosphatase 3B that positively regulates signaling of inflammatory pathways, leading to increased transcriptional activity of NF-κB and IL-8 production[204]. In addition, LRRK2 has been shown to positively regulate NF-κB signaling in cultured microglia through

downregulation of the inhibitory p50 subunit[205]. Given that NF-κB is a primary signaling pathway related to cellular senescence and IL-6 production with age[10], these studies provide strong evidence that LRRK2 function is contributing to the inflammaging environment that can lead to neurodegeneration.

LRRK2 is also reportedly a negative regulator NFAT signaling. At normal levels of protein expression, LRRK2 interacts with non-coding RNA repressor of NFAT (NRON) to inhibit NFAT activity. A LRRK2 SNP associated with Crohn's disease results in decreased levels of LRRK2 total protein and increased NFAT activity suggesting that the normal function of LRRK2 is to regulate inflammation[168]. While this regulation was reported to be kinase independent, the study did not investigate how a kinase gain-of-function mutation or over-expression of normal LRRK2 would affect NFAT activity. Because both NF-κB and NFAT lead to immune activation and LRRK2 function is implicated to regulate these pathways in opposite directions, there is a balance that must be maintained between them in order to maintain appropriate immune function.

Previous findings have shown that LRRK2 levels are elevated in B cell, T cells, and the pro-inflammatory $CD16^+$ subset of monocytes of individuals with idiopathic Parkinson's disease[105]. Because these PD subjects have no LRRK2-associated mutations, it follows that the normal function of LRRK2 has some important role to play in either the development or progression of PD. Exactly what this role is remains to be determined. Although it is not known for sure, it is likely that increased expression of total protein also results in increased kinase activity. Because kinase activity seems to be the main player in pathogenic mutations, the use of LRRK2 kinase inhibitors to treat disease is an attractive idea. As inhibitors become more specific, their potential use as a

clinical therapeutic increases. Understanding how LRRK2 kinase activity affects immune signaling pathways is an essential step in developing clinical therapeutics to modulate these pathogenic phenotypes.

Herein, we began studies to investigate the extent to which the G2019S kinase gain-of-function mutation contributes to the activation state of NFAT and NF-κB in immune cells. Whiles studies are still ongoing, it appears the G2019S mutation increases transcriptional activity of NFAT while total protein levels of NFAT remain stable. Preliminary results investigating NF-κB function suggest that PBMCs from G2019S mice have higher baseline levels of IκBα and phosphorylated NF-κB p65 subunit. In addition, overexpression of wild type LRRK2 does result in increased phosphorylation at the autophosphorylation site, Ser1292, suggesting that overexpression increases kinase activity.

3.2 Materials and Methods

3.2a Luciferase Assays

Jurkat cells (10,000) were nucleofected with a control plasmid (3 μg), an HA-tagged G2019S-LRRK2 plasmid (10 μg), or an HA-tagged WT-LRRK2 plasmid (6 μg) using the Amaxa nucleofection system, protocol X-005. Cells were then infected for 24 hours with a lenti-NFAT-luciferase reporter plasmid at a multiplicity of infection (MOI) of 50 along with a Renilla control plasmid, MOI 5. Cells were washed and then stimulated with 10 ng/mL of (phorbol 12-myristate 13-acetate) PMA and 0.5 μM ionomycin for 24 hours. Luciferase activity was assessed using the Dual-Glo Luciferase Assay System (Promega, Madison, WI, USA).

3.2b Mouse PBMC and splenocyte isolation

The following mouse strains were obtained from Jackson labs: B6.Cg-Tg(Lrrk2*G2019S)2Yue/J (#012467), B6.Cg-Tg(Lrrk2)6Yue/J (#012466), C57BL/6J (#000664), and C57BL/6-Lrrk2^{tm1Mjfa}/J (#012444). Blood from each mouse (200 µL) was collected in an EDTA vacutainer tube (BD Biosciences) via cheek bleed. Blood was incubated in the dark for 10 minutes at room temperature with 1x RBC lysis buffer (Biolegend) to lyse red blood cells. Cells were pelleted and lysed in sample buffer for western blot as detailed below.

Spleens were dissected and collected into a tube with 1x HBSS (Gibco) following mouse sacrifice. Splenocytes were isolated by mashing the spleen with the back of a 3 mL syringe through a 70 micron filter into a small petri dish. Cells were then resuspended in 1x HBSS and counted.

3.3c Cellular Fractionation

Harvested cells were washed one time with 1x PBS and 1x protease and 1x phosphatase inhibitors. Cells were lysed using Cytoplasmic Lysis Buffer (CLB) (150 mM NaCl, 50 mM Tris pH 7.4, 0.5% Triton X-100, 1x protease inhibitor, 1x phosphatase inhibitor) on ice for varying times (see results) with agitation. Samples were centrifuged at 13,500 g for 15 min at 4°C. Supernatant containing the cytoplasmic fraction was transferred to a new tube. Pellet was washed 1x with CLB and then resuspended in RIPA buffer (50 mM Tris pH 7.4, 100 mM NaCl, 0.1% SDS, 1% Triton-X 100, 1x protease

inhibitor, 1x phosphatase inhibitor). Cells were then sonicated and resuspended in 2x Laemmli with 5% DTT for a final dilution of 1x Laemmli.

3.2d PBMC and Splenocyte Stimulation

For cultured assays, two million splenocytes were plated for 90 minutes with 120 nM PFE360, vehicle, or no treatment with or without 10 ng/mL PMA and 1μM ionomycin in a 24-well plate. For PBMCs, cells were plated in complete Jurkat media and stimulated with 20 ng/mL of recombinant mouse TNF for 30 minutes at 37°C and 5% CO_2. Cells were harvested in 1.5 mL tubes, spun down, and then processed for either western blot or ImageStream® analysis.

3.2e Western Blot

Mouse splenocytes and PBMCs were washed 1x in PBS and then lysed in RIPA buffer with sonication. Cells were then diluted in 2x Laemmli buffer (40mM NaF, 5% DTT, 1x phosphatase inhibitors, 1x protease inhibitors) for a final dilution of 1x Laemmli. Proteins were then separated in a 4-20% polyacrylamide gel (Bio-Rad) by gel electrophoresis and transferred to a 45 μm PVDF membrane (Sigma Aldrich, St Louis, MO, USA) using the Mixed Molecular Weight setting on the TransBlot Turbo system (BioRad). Following transfer, the membrane was cut along the pre-stained standard band indicating 100 kDa molecular weight and incubated in a 5% skim milk blocking solution in 1x tris-buffered saline containing 0.1% Tween-20 (Sigma Aldrich). The corresponding membrane sections were incubated overnight in blocking solution (5% skim milk in TBST) or Signal Enhancer Solution 1 (Millipore) for phospho-antibodies containing a

primary antibody targeting GAPDH (MAB 1:3,000; Millipore), LRRK2 (MJFF c41-2, 1:2,000; Abcam, Cambridge, UK;), pSer1292 (1:2000;Abcam), p-NF-κBp65 (Ser536) (1:1000; Cell Signaling Technology), IκBα (1:500; SantaCruz), or H3 (1:2000; Millipore) at 4°C. Following three 10-min washes in 0.1% TBST with agitation, membrane sections were incubated for one hour at room temperature in either goat anti-rabbit or rabbit anti-goat horseradish peroxidase conjugated secondary antibodies (1:1,000; Jackson ImmunoResearch, West Grove, PA, USA) in blocking solution or Signal Enhancer Solution 2. Membranes were again washed in 0.1% TBST, and imaged using either undilute West Pico Chemisluminescent Substrate or 1:1 dilute SuperSignal West Femto Chemiluminescent Substrate (Thermo Scientific, Waltham, MA, USA). Band intensity was determined using ImageStudio Software (Li-Cor Biosciences, Lincoln, NE, USA). Protein expression levels were normalized to either corresponding GAPDH (~37 kDa) or H3 (~17 kDa).

3.2f ImageStream®

To stain for ImageStream® analysis, 2×10^6 cells per well were resuspended in media and incubated for 25 min at 37°C with Hoechst 33422 (Immunochemistry, Bloomington, MN, USA). Cells were then incubated in 1x FACS buffer (1% bovine serum albumin, 0.1% sodium azide, and 1 mM EDTA) and Mouse Fc block (1:100, eBioscience, San Diego, CA, USA) for 15 min at 4°C. Cells were washed and incubated for 20 min at 4°C with anti-CD3 BV605 (1:20, BioLegend). Cells were intracellularly stained with anti-NFAT1-AF647 (1:40, Cell Signaling) using the Fixation/Permeabilization Stain Kit per manufacturer's protocol (eBiosciences). Cells

were run immediately on an ImageStream®^{X} MarkII instrument (Amnis/Millipore, Billerica, MS, USA) at 60X magnification using extended depth of field (EDF) to improve resolution. Single-stained controls were used to set compensations. Analysis of flow cytometry data was performed using IDEAS® (Amnis/Millipore). Fluorescence minus one controls were used to set gates and account for spillover between channels. Protein expression levels are reported as geometric mean fluorescence intensity (GMFI).

3.2g PFE360 Drug and Vehicle Preparation

PF-06685360-00-0011 (PFE360) was received directly from Pfizer (Groton, CT) and prepared according to manufacturer's protocol. Briefly, use a mortar and pestle to grind PFE360 (MW: 308.35 g/mol) into a fine powder, adding 0.5% methylcellulose dropwise until drug is at a final concentration of 5 mg/mL. Sonicate solution for 15 seconds at 20% power (precipitate will still be visible). Dilute solution to working concentration of 12,000 nM. Final experimental concentration is 120 nM. Vehicle is 0.5% m/v methylcellulose in distilled water and then sterile filtered. Drug is stable in suspension for up to two weeks at 4°C with constant agitation.

3.3 Results

3.3a Optimization of PFE360 for in vitro kinase inhibition studies

If LRRK2 kinase activity is the main contributor its pathogenic phenotype, then inhibition of that activity should restore cells to their normal function. A dose response curve was used to identify the optimal concentration of drug to inhibit LRRK2 kinase activity. Phosphorylation at the Ser1292 site was used to assess levels of kinase activity.

A concentration of 120 nM of PFE360 is the lowest concentration that shows significant downregulation of pSer1292 following 90 minutes of exposure (**Fig 3.1a**). To determine how long kinase inhibition would persist *in vitro,* cells were plated for 6, 18, and 24 hrs. pSer1292 activity was stably decreased with PFE360 for up to 24 hours in culture (**Fig 3.1b**).

3.3a G2019S increases NFAT activity in a transfected T cell line

To explore the effect of LRRK2 kinase activity on NFAT activation in T cells, luciferase reporter assays were used. The Jurkat T cell line was transfected with G2019S-LRRK2 (10μg) or wild type-LRRK2 (6μg) constructs in conjunction with a lenti-NFAT luciferase reporter plasmid (50 MOI). Cells were then stimulated with a cocktail of 10 ng/mL PMA and 0.5 μM ionomycin for 24 hrs to induce NFAT activity. Luciferase activity was normalized to a Renilla control construct and the amount of protein transfected (determined by western blot). Cells transfected with the G2019S plasmid show a greater induction of NFAT activity compared to the cells transfected with a wild type LRRK2 plasmid (**Fig 3.2**). Figure is representative of two separate experiments.

3.3b LRRK2 Wild type overexpressing mice have increased phosphorylation

Given that NFAT activity was significantly increased in G2019S-transfected Jurkats, we wanted to determine whether this phenotype holds true *in vivo*. To do this, we obtained G2019S LRRK2 overexpressing (GSOE) BAC transgenic (tg) mice. To control for overexpression of G2019S-LRRK2 protein we also obtained a LRRK2 wild type overexpressing (WTOE) mouse line that has expression levels consistent with GSOE mice. C57Bl/6J (B6) mice were used as a baseline control. Before checking NFAT

activity, we first sought to determine if the WTOE mice had increased baseline phosphorylation of LRRK2 indicative of altered kinase activity.

While it has been shown that LRRK2 expression levels are altered in PD[105], it is not known whether this increase actually results in increased kinase activity as well. The pSer1292 site is an autophosphorylation site that can be used to monitor LRRK2 kinase activity in cells and tissue[239]. To test whether overexpression of total LRRK2 protein affects its kinase activity, western blots were run to detect pSer1292 in the peripheral blood mononuclear cells (PBMCs) of WTOE mice and compared to those of GSOE and B6 mice.

Cheek blood from two mice of each genotype was obtained and samples were processed for western blot. Samples were blotted for pSer1292 and normalized to a GAPDH loading control. Overexpression of wild type LRRK2 (WTOE) shows an intermediate amount of pSer1292 phosphorylation in between that of the GSOE PBMCs with the highest level of phosphorylation and B6 with the lowest level (**Fig 3.3**).

3.3c Optimizing Fractionation for NFAT1 Translocation Studies

Because primary T cells are difficult to transfect, we sought to assess NFAT1 activity via cellular fractionation studies. Following stimulation, NFAT is dephosphorylated and translocates into the nucleus where it binds DNA to initiate transcription of inflammatory response mediators. Separating cells into a nuclear and cytoplasmic fraction to blot for NFAT1 would allow for quantification of nuclear translocation of NFAT1.

Fractionation optimization was performed in the THP-1, human monocytic cell line using a protocol developed by the Kukar lab. To ensure full fractionation and limit potential contamination between fractions, a time course was done to determine the best amount of time to leave cells in cytoplasmic lysis buffer. THP-1 cells fractionated cleanly showing no GAPDH in the nuclear fraction and very little histone-H3 in the cytoplasmic fraction. There were no differences in quality of fractionation between cellular lysis for 5 min or 10 min, so 5 min was chosen as the optimal lysis time (**Fig 3.4a**). The next set of fractionation studies were performed in both primary T cells and the Jurkat T cell line. A time course to determine peak nuclear translocation NFAT1 following PMA and ionomycin stimulation was performed. Peak translocation generally occurs between 10 and 30 minutes, so this study assessed time points in that range and longer time points that would allow for collection of media for cytokine quantification—5 min, 10 min, 20 min (**Fig 3.4b-c**), 30 min, 1 hr, 2 hr, 18 hrs, and 72 hrs (data not shown) were chosen. Unfortunately, the fractionation protocol yielded inconsistent results between various Jurkat samples. In some samples, the fractionation was clean and there was no contamination of histone H3 in the cytoplasmic fraction or GAPDH in the nuclear fraction. In other samples, there was substantial contamination and the fractions where not clearly separated into nuclear and cytoplasmic (**Fig 3.4c**). In addition, there were issues in the detection of increases in NFAT1 protein and nuclear translocation following stimulation (**Fig 3.4b-c**). These issues could be due to fractionation, the quality of the antibody, or sample processing. It is unlikely that timing was an issue given what has been previously published[240] and the range of time points assessed.

3.3d Optimizing ImageStream® to Quantify Nuclear Translocation of NFAT

Because of the variability seen using biochemical techniques, we sought an alternative assay that combines both flow cytometry and microscopy to quantify NFAT1 translocation into the nucleus. The ImageStream® Mark II machine is capable of detecting fluorescently tagged protein markers in addition to taking a picture of each cell as it passes through the fluidics at a magnification as high as 60X.

In order to assess differences in nuclear translocation of NFAT1, total splenocytes were isolated from GSOE, WTOE, and B6 mice. Cells were then plated at a concentration of 2 million cells/mL and stimulated with a cocktail of 10 ng/mL PMA and 1 μM ionomycin for 90 minutes. In order to maximize use of splenocytes from these animals, cells were also plated with or without 120 nM PFE360 to assess contribution of LRRK2 kinase activity to any potential differences. Following treatment, cells were harvested and stained with both CD3 and NFAT1 antibodies plus a nuclear stain.

Analysis of NFAT1 expression and nuclear translocation was performed using the IDEAS software. Cells were first gated on CD3 to ensure assessment of a homogenous T cell population. The staining of NFAT1 (red) and CD3 (orange) was very clear and polarization of the TCR could be seen in stimulated cells indicating proper response to stimulus (**Fig 3.5a**). The DNA stain was not very clear and thus there was no way to quantify NFAT1 translocation into the nucleus; however, NFAT1 induction following stimulation was consistent across all genotypes and inhibition of LRRK2 kinase activity does not affect total NFAT1 protein levels (**Fig 3.5b**). Follow-up experiments with a different nuclear stain are currently in progress.

To get the most information from each sample, we sought to determine success of kinase inhibition via flow cytometry to avoid having to do side-by-side westerns. We attempted to stain for phosphorylated LRRK2 and visualize levels with flow cytometry. Because pSer1292 has very low stoichiometry, pSer935, which has higher levels than pSer1292, but is still diminished by kinase inhibition, was used as a functional readout. Unfortunately, pSer935 levels were barely higher than the secondary only control and there were no differences between B6 and GSOE mice treated with or without PFE360 (**Fig 3.5c**) and it was determined that phosphorylation status could not be obtained by flow cytometry.

3.3e Gain-of-function G2019S LRRK2 mutation has increased basal levels of NF-kB signaling proteins

To test the effect of the G2019S mutation on NF-κB activity, PBMCs from GSOE, WTOE, and B6 mice and stimulated with 20 ng/mL recombinant mouse TNF for 30 minutes. A western blot was run to determine phosphorylation of the p65 subunit and degradation of IκBα as a measure of NF-κB activation. Interestingly, p-p65 levels and IκBα levels appear to be increased at baseline compared to WTOE and B6 levels (**Fig 3.6)**. Because there are only two samples per genotype, meaningful statistics cannot be run, but the preliminary results are intriguing and merit further exploration.

Another potentially interesting trend is that p-p65 levels the GSOE sample actually go down in response to TNF in contrast to WTOE and B6 (**Fig 3.6**). Following stimulation with TNF, it is expected that p-p65 would increase as an indication of NF-κB activation, as was seen in the WTOE and B6 samples, albeit at low levels. A time course

to determine peak time of p-p65 activation and IκBα degradation will need to be performed to better understand these data. It is also notable that pSer1292 levels are not altered by TNF stimulation for 30 minutes.

3.4 Discussion

A previous report states that a kinase dead mutant of LRRK2 does not alter NFAT activity[168]; however, a gain-of-function mutation was never studied. Because LRRK2 can dimerize following auto-phosphorylation[138,175] it's possible that a kinase gain-of-function increases the dimerized form of protein detracting from its ability to properly regulate NFAT activity. While the bulk of these data are preliminary and studies are ongoing, the *in vitro* studies with the Jurkat cell line suggest that G2019S LRRK2 does in fact, increase NFAT activity.

Because of prior studies indicating increased total LRRK2 protein expression in immune cells of PD subjects, we wanted to determine if an increase in total protein also meant increased kinase function. Phosphorylation of pSer1292[239] and Rab proteins[150] are an accepted functional readout for LRRK2 kinase activity. In this study, we used pSer1292 detection on western blot as an indicator, but attempts to validate antibodies for flow cytometry were unsuccessful. Future studies could potentially use phosphorylation of Rab proteins to assess LRRK2 kinase activity and take advantage of other techniques such as flow cytometry. Phosphorylation levels of pSer910 and pSer935 correlate with total LRRK2 protein levels[241]. Although neither of these sites are considered to be an autophosphorylation site, they both decrease in response to treatment with LRRK2 kinase inhibitors. Given these data, it follows that a WTOE would have increased

phosphorylation compared to a cell expressing normal levels of LRRK2. In fact, mouse PBMCs from a WTOE line have an intermediate amount of pSer1292 in between that of GSOE and B6 mice. This finding is exciting because it supports the idea that LRRK2 kinase inhibitors could be used a potential therapeutic not just for those with a mutation, but also for those with idiopathic PD.

To fully investigate the extent to which a gain-of-function mutation contributes to increased inflammation, we sought to assess differences in NFAT nuclear translocation and activity following inflammatory stimulus. Western blotting was the first method used, but consistent, clean fractionation of cells proved elusive. Use of a quality-controlled store-bought kit in lieu of homemade buffers and reagents may mitigate these issues for future studies. Due to these complications, it was decided to use the ImageStream® platform to image cells and gather flow cytometry data. Preliminary results suggest that this will be a powerful way to answer these questions. Difficulty with the DNA stain prevented acquisition of translocation data, but imaging of NFAT1 total protein was robust and suggests that there are no alterations in induction of total NFAT1 following stimulation. Use of a DAPI nuclear stain instead of Hoescht 33342 should improve the quality of DNA staining using the ImageStream®. Follow-up functional studies and validation of nuclear translocation will provide evidence to answer the questions of whether NFAT activity is altered as a result of LRRK2 kinase activity.

Because of the multiple studies implicating LRRK2 function in NF-κB signaling pathways in monocytes[203-205,242], we sought to assess potential differences in signaling of G2019S cells. Most studies have focused strictly on comparing LRRK2 knockout or knockdown cells to wild type while very little has been done to determine effect of gain-

of-function mutations on NF-κB signaling. A recent study derived iPSC-neurons from dermal fibroblasts of PD subjects with G2019S mutations and found that translocation of the NF-κB p65 subunit and overall NF-κB activity was diminished compared to healthy controls. Intriguingly, they found no alterations in baseline levels of NF-κB activity by luciferase assay or IκBα degradation by western blot. However, another study done in human umbilical vein endothelial cells found that overexpression of wild type LRRK2 and G2019S-LRRK2 resulted in increased nuclear translocation of p65 and increased phosphorylation of IκBα[167]. Taken together, these data suggest a differential regulation of NF-κB signaling dependent upon cell type. While the data presented herein are extremely preliminary with a small sample, it is interesting that the p-p65 and IκBα levels appear to be much higher at baseline in the G2019S mice compared to WTOE and B6. Increasing the sample size, fractionating cells to quantify nuclear translocation of NF-κB, and assessing overall NF-κB activity with a luciferase assay will help to determine which cell specific differences in regulation are true for immune cells.

Sustained NF-κB activity in neurons is thought to enhance memory and protect against apoptosis and neurotoxicity[243]. NF-κB activation is much more tightly regulated in immune cells as the signaling cascade results in production of inflammatory species that can be damaging to the tissue environment with prolonged exposure. Defects in NF-κB signaling in G2019S neurons could prove to be detrimental to neuronal health, while dysregulation of NF-κB in immune cells could contribute to the inflammatory milieu accelerating neurodegeneration. The data presented herein suggests that LRRK2 is contributing to a dysregulation resulting in increased NF-κB for immune cells.

Studies investigating potential differences in immunophenotype of human subjects with or without the G2019S mutation and with or without PD are currently ongoing. It is too early to speculate about the data, but in conjunction with continued investigation into immune defects in inflammatory signaling cascades, these studies are an important next step in determining the specific function of LRRK2 in immune cells and how it contributes to development of PD.

3.5 Figures

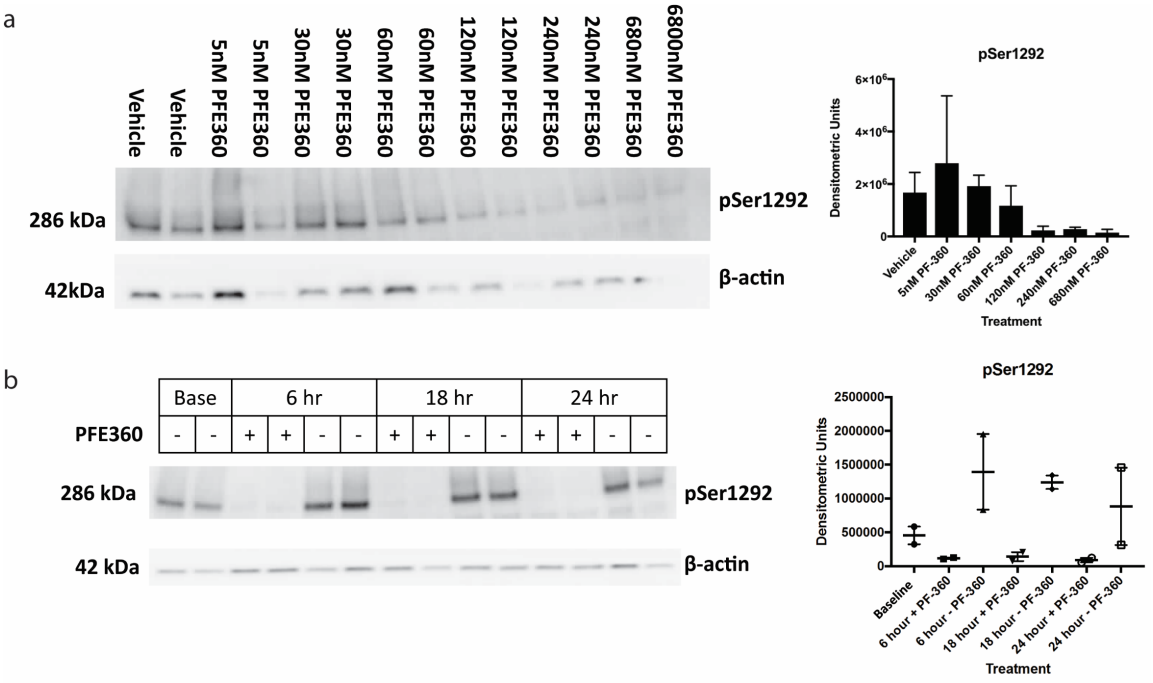

Figure 3.1. PFE360 kinase inhibitor works optimally at 120 nM and is stable in culture for up to 24 hours. GSOE mouse splenocytes were treated with (a) varying concentrations of PFE360 to determine the lowest dose that will still knock down most of the phosphorylation at pSer1292 and (b) left in culture for up to 24 hours to see how long inhibition was stable in culture. Data generated by Mary Herrick (Neuroscience Graduate Student) and Dr. María Elizabeth DeSousa Rodrigues (Post-doctoral Fellow).

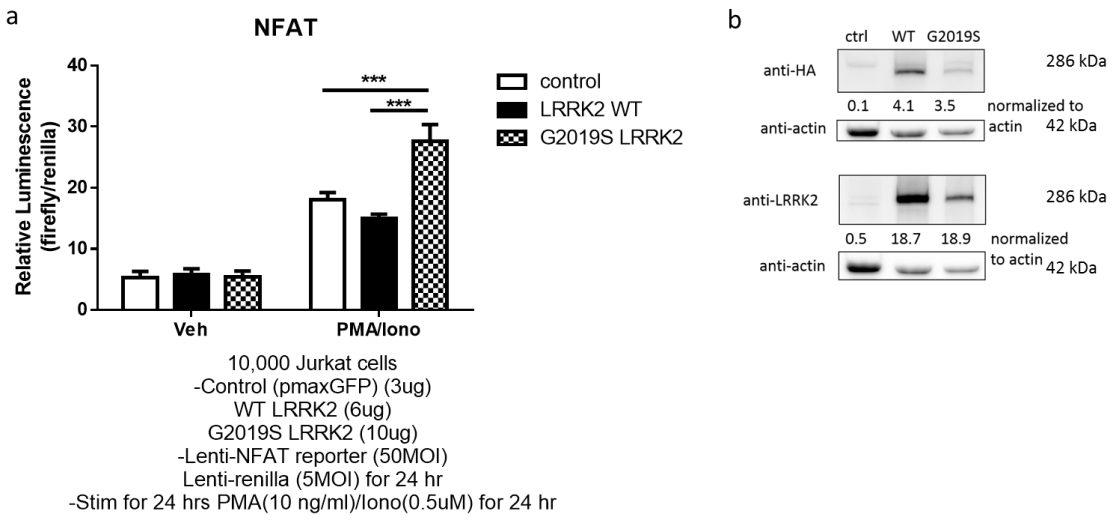

Figure 3.2. G2019S mutation increases NFAT activity following stimulation. 10,000 Jurkat cells were plated and transfected with a G2019S or WT LRRK2 construct. Cells were infected with a lenti-NFAT luciferase reporter plasmid and stimulated with PMA and ionomycin. Data generated by Dr. Jae-Kyung Lee, former Assistant Professor of Physiology at Emory University and now at the University of Georgia in Athens,GA.

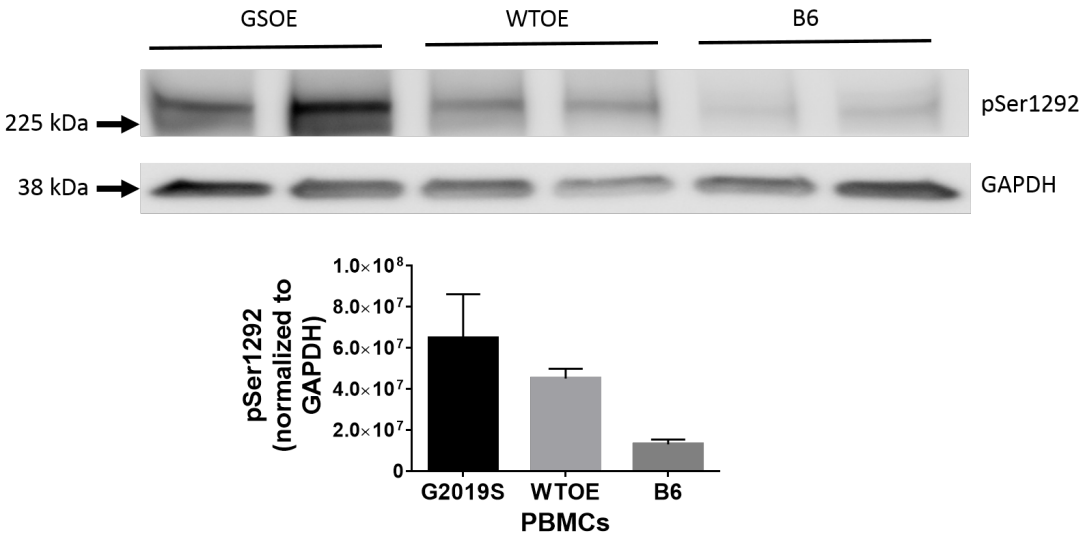

Figure 3.3. LRRK2 wild type overexpressing mice have an intermediate level of pSer1292 phosphorylation. PBMCs from GSOE, WTOE, and B6 mice were obtained and processed for western blot analysis of LRRK2 pSer1292. Quantification was normalized to GAPDH loading control. N = 2 per genotype.

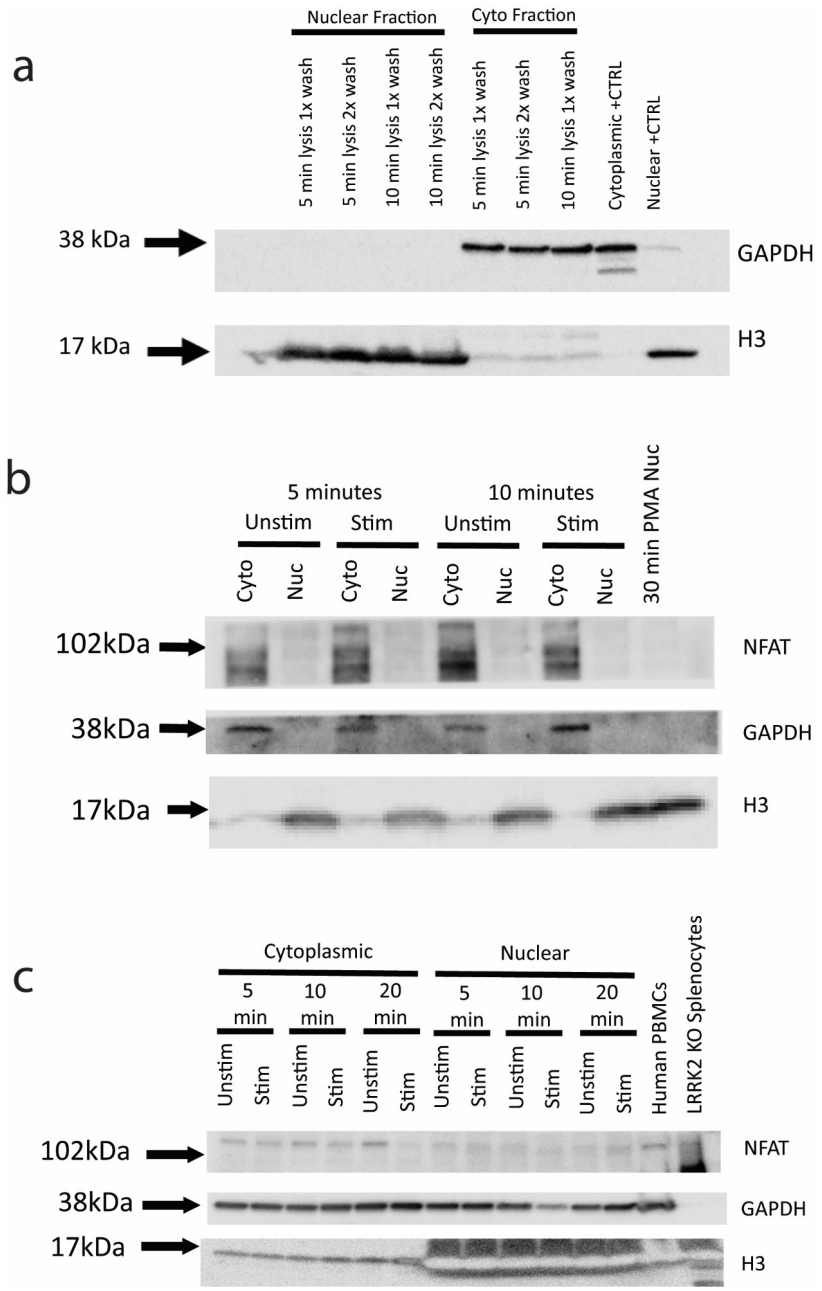

Figure 3.4. Cellular fractionation yields inconsistent results. Fractionation of (a) THP-1 cells, (b) primary mouse T cells, and (c) Jurkat T cells under various stimulation conditions yield variable results.

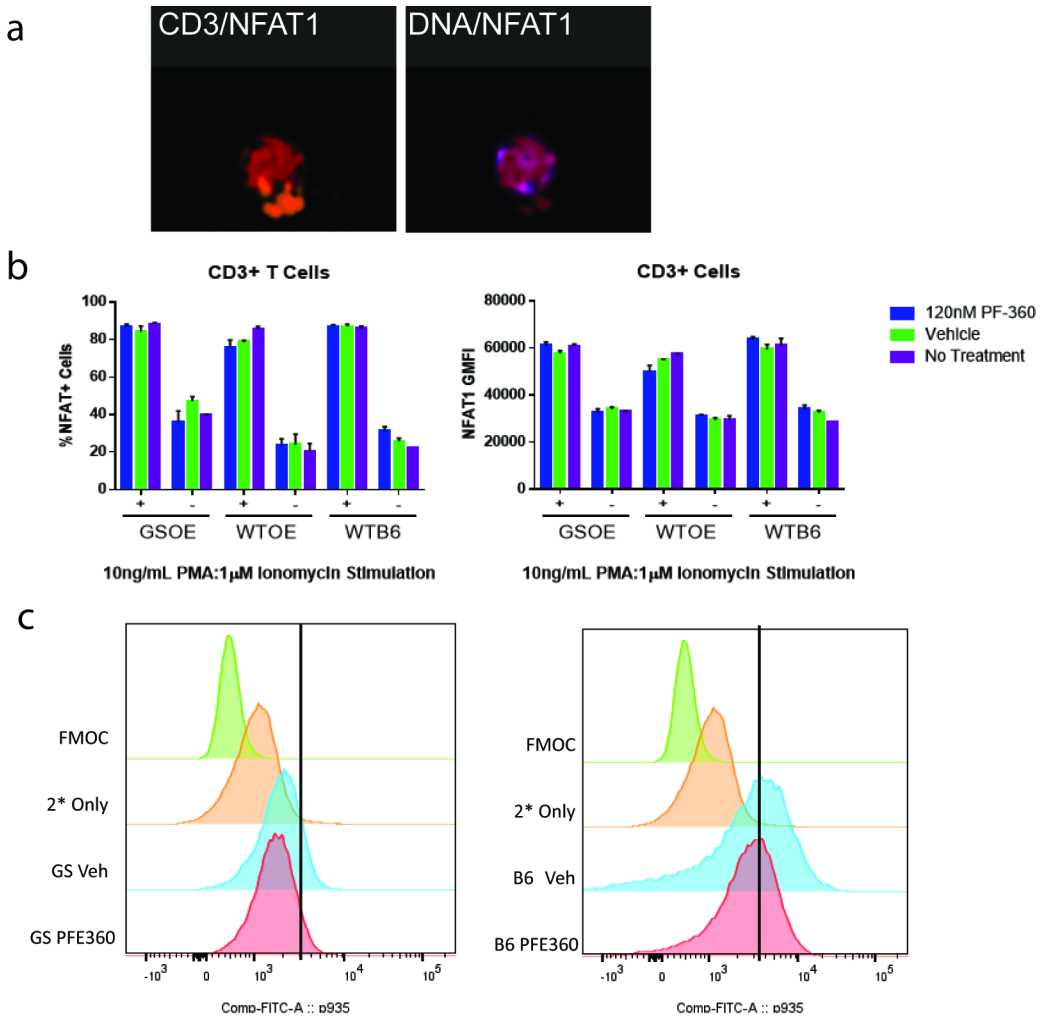

Figure 3.5. Gain of function LRRK2 mutation does not alter NFAT protein following stimulation. Total splenocytes (a-b) were stimulated with 10 ng/mL PMA + 1 μM ionomycin and treated with or without 120 nM PFE360 for 90 minutes. In (a) CD3 is orange, NFAT is red, and DNA is purple. N = 1 per genotype with a technical duplicate. (c) pSer935 levels by flow cytometry of splenocytes from GSOE and B6 mice.

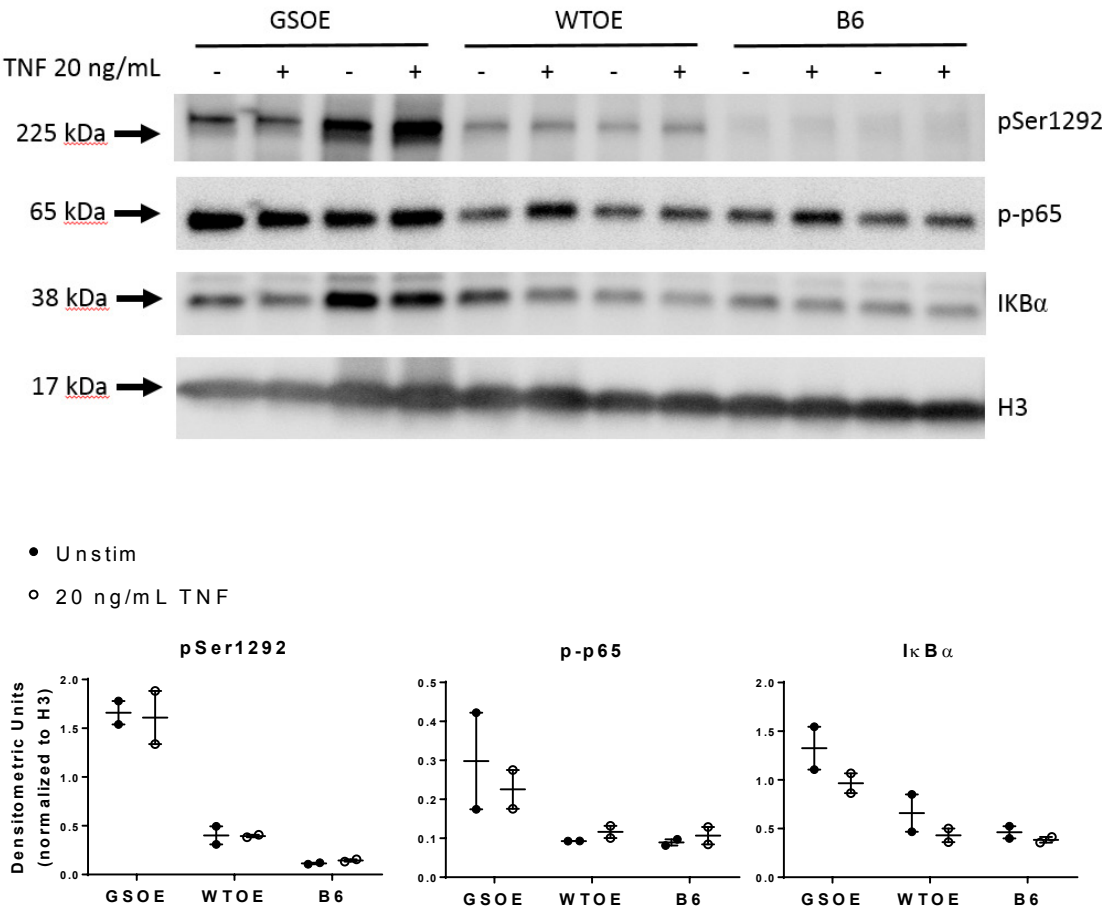

Figure 3.6. GSOE mice have increased basal expression of p-p65 and IκBα. PBMCs were isolated from mice and stimulated with 20 ng/mL TNF for 30 minutes. Samples were processed for (a) western blot analyses and then (b) quantified using ImageStudio. N= 2 per genotype.

Chapter 4: Future Directions and Implications for Clinical Treatment

4.1 Introduction

Parkinson's disease (PD) is a progressive neurodegenerative disease that affects more than 10 million of people around the world and costs approximately $25 billion per year in the United States alone[237]. LRRK2 mutations account for 1-2% of all PD cases, but up to 40% of cases in Ashkenazi Jewish and North African Arab populations[112]. Because LRRK2-associated PD closely resembles the idiopathic form of the disease, it is useful to study development and progression. Determining the ways in which LRRK2 contributes to PD can illuminate new insights and lead to improved therapeutics.

This work demonstrates that LRRK2 expression is elevated in the immune cells of individuals with idiopathic PD compared to the HC group. While LRRK2 was not elevated in the broad $CD14^+$ population, it was increased in the $CD16^+$ pro-inflammatory subset. Both B and T cells also have increased expression of LRRK2. Intriguingly, expression levels were globally upregulated in all T cell subsets examined ($CD4^+$, $CD8^+$, Tcm, Teff, Tem, Tnaive, Th1, Th2, Th17, and Treg). LRRK2 expression is also inducible in both monocytes and T cells following inflammatory stimulus with IFN-γ and engagement of the TCR, respectively.

Interestingly, expression of LRRK2 protein positively correlates with HLA-DR expression in PD subjects, but negatively correlates with HLA-DQ in HC subjects. These data suggest that there is a complex interplay between antigen presentation with specific MHC-II and LRRK2 regulation. Following IFN-γ stimulation, monocytes from PD subjects secreted greater levels of inflammatory cytokines compared to HC. It is possible that upregulation of LRRK2 leads to increased cytokine secretion that then affects MHC-

II expression levels. It will be important to determine if LRRK2 protein levels are specifically contributing to upregulation of MHC-II protein levels or simply contributing to the inflammatory environment that leads to increased upregulation of MHC-II.

T cell proliferation and activation is an essential process in generating an effective immune response. Equally important is making sure that the immune response turns off following clearance of the foreign antigen to limit long-term inflammation. In this study, CTLA-4 levels were dampened in $CD8^+$ T cells from PD subjects compared to HC. In conjunction with the decrease in CTLA-4, LRRK2 expression is increased in dividing $CD8^+$ T cells. For PD subjects, both $CD4^+$ and $CD8^+$ T cells expressing higher levels of cytokines also have higher levels of LRRK2 expression, while HC subjects only have a positive correlation with IFN-γ expression in their $CD4^+$ T cells. Finally, compared to HC T cells, PD T cells secreted higher levels of both TNF and IL-12p70 following TCR stimulation.

In addition to these studies, preliminary data using a G2019S overexpressing (GSOE) mouse line indicate that there may also be defects in the regulation of NFAT and NF-κB in immune cells. G2019S vectors resulted in increased NFAT transcriptional activity by luciferase assay, while PBMCs from GSOE mice showed higher baseline levels of NF-κB phospho-p65 expression compared to wild type LRRK overexpressing (WTOE) and wild type (B6) mice. While these data need to replicated, further exploration into these pathways is merited.

4.2 Future Directions

This work highlights the differences in LRRK2 expression levels and immune activation between individuals with Parkinson's disease compared to healthy controls. The finding that LRRK2 protein is increased in subjects with PD indicates that LRRK2 is playing a role in disease pathogenesis. Whether LRRK2 contributes to the development of the disease or is upregulated as a result of disease remains to be determined. Identifying a definitive biomarker or using screenings for non-motor symptoms to catch "at-risk" individuals earlier in life will allow us to determine at what point LRRK2 protein is being upregulated, whether this increase in protein also results in an increase in kinase activity, and how these changes contribute to disease.

Future studies are needed to parse out the exact mechanism in which LRRK2 is acting to contribute to development and progression of PD. Currently, studies to immunophenotype individuals with the G2019S mutation both with and without PD and individuals lacking the mutation with and without PD are underway (see **Appendix II**). Because of the lab's ongoing studies involving the high risk MHCII single nucleotide polymorphism (SNP) *rs3129882* (see **Appendix I**) and the data suggesting dysregulation of antigen presentation in PD subjects with increased LRRK2 protein expression (**Ch 2**), it would be useful to investigate potential contribution of LRRK2 to *rs3129882* genotype. Some preliminary data has been generated from the studies detailed here suggesting that there are alterations in LRRK2 protein levels depending upon *rs3129882* genotype and disease status (see **Appendix II**) that bear further investigation. The validation of reagents and optimization of methods from this work paved the way to begin these more in-depth studies. Similar to what was done in idiopathic PD versus HC patients (**Ch 2**), blood is obtained from subjects and baseline immune activation and induction of

activation following inflammatory stimulus is assessed. Results from these studies will allow determination of PD-related differences versus LRRK2 mutation-related differences.

Assessing differences in NFAT and NF-κB transcriptional activity in immune cells of subjects both with or without PD and with or without G2019S mutations will provide further insight into the mechanism of increased inflammation associated with PD. Further optimizing ImageStream® studies will be essential to imaging NFAT translocation in these cells. In addition, western blot and luciferase reporter assays would also be informative for both NFAT and NF-κB. In addition to determining transcriptional differences, experiments to quantify downstream signaling cytokines and effectors must be done. Following plating and stimulation of cells, a multiplexed immunoassay approach such as MESO to quantify secreted cytokine levels or intracellular cytokine staining for a cell specific assessment of cytokine production could be performed.

If significant alterations in inflammatory response are seen in GS patients, it would also be useful to determine if these increases are a direct result of kinase activity and could be dampened by kinase inhibition. Treating PD GS blood with the LRRK2 kinase inhibitor PFE360 to see if the alterations in cytokine levels and immune cell activation can be brought back down to normal levels would provide essential evidence that LRRK2 kinase inhibitors will be useful as a clinical treatment. A longitudinal study of "at-risk" (both from a non-motor standpoint and those with a GS mutation) individuals charting LRRK2 levels over time would be extremely informative to identify at what point LRRK2 becomes upregulated compared to healthy controls. Does the immunophenotype of an at-risk individual change over time? How does LRRK2

influence this? These are important questions that this type of longitudinal study will be able to answer.

In addition to studying the periphery, mouse models can be used to investigate alterations in immune cell trafficking into the brain and activation of resident cells like microglia. Little is known about how the immune system is affected long-term by overexpression of either wild type or G2019S LRRK2. A longitudinal study to assess alterations in immunophenotype for both of these models would be beneficial to the field; however, given that LRRK2-associated PD has an average onset later than that of idiopathic PD, it is likely that these models won't show much pathology until very late in life. Gaining further insight into the mechanism of immune alterations related to LRRK2 in PD could assist in developing better therapeutics and treatment strategies.

4.3 LRRK2 Contribution to Parkinson's Disease

Contrary to prior studies reporting little to no expression of LRRK2 in T cells, this work firmly establishes LRRK2 expression in T cells, albeit at a level lower than that of monocytes and B cells. Because of this long-held belief, there are very few studies investigating the effect LRRK2 has on T cell function; however, LRRK2 has been shown to be a negative regulator of NFAT[168], a signaling pathway very important to proper T cell function. This work is the first to establish that LRRK2 expression can be induced by engagement of the T cell receptor (TCR). Interestingly, LRRK2 was only upregulated after 72 hours of stimulation, suggesting that it is important for the later effector functions of T cells. Given the recent report that T cells can respond to MHC-II:α-synuclein peptide complexes[106] in conjunction with data suggesting LRRK2 regulates

formation of α-syn inclusions[224,244] and can be induced by TCR stimulation there is support for the idea that LRRK2 is contributing to T cell function.

Importantly, basal expression of LRRK2 was upregulated in all T cell subsets in PD subjects compared to HC. Because of the diverse range of function for each subset, this suggests that whatever role LRRK2 is playing in T cells, it is a function irrelevant of T cell phenotype. LRRK2 is either providing a different function to each cell subset, or it is playing a regulatory role essential to T cell function and/or in response to disease. Given that this work shows LRRK2 is upregulated specifically in the pro-inflammatory subset of monocytes, B cells, and all T cell subsets, it is not surprising that there are few inflammatory differences between idiopathic PD subjects and those with LRRK2-G2019S PD[245]. It is not yet known whether the upregulation of LRRK2 is a result of disease or if it is a contributor to disease.

LRRK2 expression is higher in the pro-inflammatory non-classical subset of monocytes expressing CD16. Compared to classical monocytes, non-classical monocytes have increased production of both TNF and IL-12 and little-to-no production of IL-10[234]. They also have increased expression of HLA-DR with a greater capacity to present antigen to T cells. The $CD14^{+}CD16^{+}$ subset migrates differently than the classical subset, as non-classical monocytes do not respond to the chemokine CCL2, but do migrate towards CX3CL1[246]. Interestingly, stimulating monocytes with IFN-γ increases LRRK2 protein levels and induces a shift from $CD14^{+}CD16^{-}$ to the more pro-inflammatory $CD14^{+}CD16^{+}$. In addition, this shift could be attenuated by treatment with the LRRK2 kinase inhibitor LRRK2-IN-1[173]. While LRRK2-IN-1 does have some off-target effects,

the study suggests that LRRK2 is participating in the maturation of monocyte and the switch to a pro-inflammatory phenotype.

These data are consistent with the finding that $CD14^{+}CD16^{+}$ monocytes from PD subjects have increased LRRK2 expression compared to HC (**Ch 2**). Monocytes were the only immune subset that showed a positive correlation with cell frequency and LRRK2 expression. Expression of HLA-DR in PD monocytes also positively correlated with LRRK2 expression. Because non-classical monocytes have increased expression of HLA-DR, it follows that PD monocytes more readily switch to a pro-inflammatory phenotype compared to HC. While it is not known exactly what is being presented, MHC-II upregulation is indicative of increased inflammation not seen in healthy individuals. Since LRRK2-IN-1 is capable of mitigating this shift, it's likely that more specific inhibitors would have a similar effect and therefore could be used to dampen inflammation in both idiopathic and familial PD.

This work also shows that LRRK2 levels positively correlate with T cell production of cytokines in PD, but not HC subjects. In addition, cytokine secretion from monocytes was heightened compared to HC monocytes following stimulation. These variations between PD and HC are likely due in part to LRRK2 regulation of both the NFAT and NF-κB inflammatory signaling pathways. Together, these pathways are responsible for initiating an inflammatory response in the form of secretion of cytokines and chemokines. LRRK2 has been shown to negatively regulate NFAT activity in a non-coding RNA repressor of NFAT (NRON) dependent manner[168]. Absence of LRRK2 results in increased NFAT activity and inflammation. While kinase dead mutants showed no alterations in inflammation, kinase gain-of-function mutations were not assessed.

Because LRRK2 is capable of diverse function depending on phosphorylation state, increased kinase activity could still contribute to dysregulation via dimerization and trafficking to a different cellular compartment[138,175,176]. As evidenced in chapter 3, G2019S constructs can increase NFAT activity compared to wild type LRRK2 constructs, suggesting that there is differential regulation of inflammation that is likely phosphorylation dependent.

NF-κB signaling results in production of pro-inflammatory mediators such as IL-1β, IL-6, and COX2. While NF-κB signaling is important to maintain neuronal health[243], dysregulated signaling in immune cells can result in a cytotoxic environment ultimately resulting in pathology and disease. LRRK2 has been shown positively regulate NF-κB in microglia by down-regulating phosphorylation of the p50 inhibitory subunit. Microglia from LRRK2 knockout mice and BV2 cells treated with LRRK2 kinase inhibitors both showed diminished expression of IL-1β and COX2 following LPS stimulation. In addition, LRRK2 KO BMDMs have diminished NF-κB activation in response to LPS and muramyl dipeptide, a NOD2 activating protein[247]. In our hands, PBMCs from G2019S mice have increased basal levels of p-p65 and IκBα compared to both wild type overexpressing and wild type normal mice, suggesting that these cells are primed for an inflammatory response. Interestingly, iPSCs derived from G2019S dermal fibroblasts showed diminished NF-κB signaling compared to wild type LRRK2 iPSCs[242]. At baseline, G2019S iPSC neurons had an increased nuclear p65; however, following stimulation, there was significantly less nuclear p65 in the G2019S neurons compared to wild type[242]. Given the divergent function of NF-κB in neurons and immune cells, it follows that dysregulation of signaling with mutations would be cell type dependent.

While it is not yet known if treatment with kinase inhibitors can rescue defects in neuronal signaling, there is evidence to suggest that inhibition of kinase activity can dampen the response back to normal levels in immune cells[205].

The case for use of LRRK2 kinase inhibitors and centrally delivered antisense oligonucleotides (ASO) is strong. Given the data presented herein, the non-mutant form of LRRK2 is contributing to idiopathic PD, suggesting that LRRK2 modifying therapies would be useful for both idiopathic and familial forms of the disease. In the past few years, LRRK2 kinase inhibitors have become far more specific[221]. While high doses are still capable of inducing pathology, clinical doses would be much lower and mitigate these effects. The use of ASOs to knockdown total protein instead of kinase activity is an attractive alternative. While normal LRRK2 is likely playing an essential regulatory role, treating dysregulation with knockdown of total protein would likely need to be targeted to avoid deleterious side effects. That being said, early investigations into their use are promising: α-syn levels are higher in neurons of G2019S patients[152,202,244] and knock-down of LRRK2 using an intracerebral ventricular injection of ASOs results in a decrease in α-syn levels and increase in tyrosine hydroxylase-positive dopaminergic neurons[224,242]. Whether pathology associate with LRRK2 is kinase dependent, protein level dependent, or both, kinase inhibitors and the newly reported use of ASOs[224] could both be effective therapies.

Multiple studies have assessed inflammatory differences between asymptomatic G2019S mutation carriers and both G2019S PD subjects and idiopathic subjects. Some studies report no differences in inflammatory cytokines between asymptomatic carriers and controls[248]. However, another study found that asymptomatic G2019S mutation

carriers show increased levels of IL-1β with a subgroup showing an even greater pro-inflammatory profile, including increased IL-6, TNF, MCP-1, IL-10, and IL-12[245]. Because there are sex differences in cytokine profiles, differences could be due to the demographics of the cohort. In addition, one study found a high inflammatory subgroup indicating that there is substantial variability even among mutation carriers. Interestingly, after development of PD, G2019S carriers and idiopathic PD subjects have a mostly similar inflammatory profile. G2019S carriers do have increased CSF vascular endothelial growth factor (VEGF) and IL-8, and higher serum levels of platelet derived growth factor (PDGF) compared to idiopathic PD subjects, but there were no differences in the rest of the inflammatory markers tested[245]. The overall inflammatory profiles of idiopathic PD and LRRK2 G2019S PD are likely similar due to the upregulation of LRRK2 following disease development. Once an individual develops PD, it is likely that any inflammatory differences seen between LRRK2 G2019S asymptomatic carriers and asymptomatic healthy controls become undetectable.

Despite decades of research into the development and pathology of disease, little clinical progress has been made in finding a cure or preventative treatment. Success of clinical trials for new therapeutics has been limited, likely due to the fact that they don't account for biological variability between individuals. In recent years, there has been an uptick in discussion of personalized medicine to improve the effectiveness of specific treatments[249]. Characterizing factors such as genetics, microbiome, environmental exposure, and immunophenotype increase the likelihood of identifying a specific treatment that an individual will respond to. In addition, finding a definitive set of biomarkers that can predict progression to disease would allow us to follow "at-risk"

individuals and provide them with interventional therapeutics lowering their risk for development of disease. In the future, knowing an individual's total LRRK2 protein levels and phosphorylation state could determine if they are a candidate for the use of LRRK2 inhibitors or ASOs.

4.4 Conclusions

Mutations in the LRRK2 protein are the most common genetically inherited form of PD. The fact that these mutations contribute to not just familial, but also idiopathic PD makes these mutations an interesting model to study the development and progression of the disease over time. This novel work demonstrates that LRRK2 protein levels are increased in the context of idiopathic PD, suggesting that kinase inhibition could prove to be a successful therapeutic for all individuals with PD, not just those with a mutant form. As LRRK2 kinase inhibitors get more specific, future studies investigating the mechanism of kinase inhibition are published, and biomarkers for the early detection of PD become available, we may be able to prevent or slow the development and progression of disease with age.

REFERENCES CITED

1 Cook, D. A. & Tansey, M. G. in *Neuroimmune Pharmacology* (eds Tsuneya Ikezu & Howard E. Gendelman) 107-116 (Springer International Publishing, 2017).

2 Coppe, J. P. *et al.* Senescence-associated secretory phenotypes reveal cell-nonautonomous functions of oncogenic RAS and the p53 tumor suppressor. *PLoS Biol* **6**, 2853-2868, doi:10.1371/journal.pbio.0060301 (2008).

3 Fagiolo, U. *et al.* Increased cytokine production in mononuclear cells of healthy elderly people. *Eur J Immunol* **23**, 2375-2378, doi:10.1002/eji.1830230950 (1993).

4 Mariani, E. *et al.* Simultaneous evaluation of circulating chemokine and cytokine profiles in elderly subjects by multiplex technology: relationship with zinc status. *Biogerontology* **7**, 449-459, doi:10.1007/s10522-006-9060-8 (2006).

5 Wei, J., Xu, H., Davies, J. L. & Hemmings, G. P. Increase of plasma IL-6 concentration with age in healthy subjects. *Life Sci* **51**, 1953-1956 (1992).

6 Ferrucci, L. *et al.* The origins of age-related proinflammatory state. *Blood* **105**, 2294-2299, doi:10.1182/blood-2004-07-2599 (2005).

7 Ershler, W. B. Interleukin-6: a cytokine for gerontologists. *J Am Geriatr Soc* **41**, 176-181 (1993).

8 Maggio, M., Guralnik, J. M., Longo, D. L. & Ferrucci, L. Interleukin-6 in aging and chronic disease: a magnificent pathway. *J Gerontol A Biol Sci Med Sci* **61**, 575-584 (2006).

9 Nelson, G., Kucheryavenko, O., Wordsworth, J. & von Zglinicki, T. The senescent bystander effect is caused by ROS-activated NF-kappaB signalling. *Mech Ageing Dev*, doi:10.1016/j.mad.2017.08.005 (2017).

10 Chien, Y. *et al.* Control of the senescence-associated secretory phenotype by NF-kappaB promotes senescence and enhances chemosensitivity. *Genes Dev* **25**, 2125-2136, doi:10.1101/gad.17276711 (2011).

11 Coder, B. D., Wang, H., Ruan, L. & Su, D.-M. Thymic Involution Perturbs Negative Selection Leading to Autoreactive T Cells That Induce Chronic Inflammation. *Journal of immunology (Baltimore, Md. : 1950)* **194**, 5825-5837, doi:10.4049/jimmunol.1500082 (2015).

12 Chinta, S. J. *et al.* Cellular senescence and the aging brain. *Exp Gerontol* **68**, 3-7, doi:10.1016/j.exger.2014.09.018 (2015).

13 Salminen, A. *et al.* Astrocytes in the aging brain express characteristics of senescence-associated secretory phenotype. *Eur J Neurosci* **34**, 3-11, doi:10.1111/j.1460-9568.2011.07738.x (2011).

14 Dykstra, B., Olthof, S., Schreuder, J., Ritsema, M. & de Haan, G. Clonal analysis reveals multiple functional defects of aged murine hematopoietic stem cells. *The Journal of Experimental Medicine* **208**, 2691-2703, doi:10.1084/jem.20111490 (2011).

15 Beerman, I. *et al.* Functionally distinct hematopoietic stem cells modulate hematopoietic lineage potential during aging by a mechanism of clonal expansion.

Proceedings of the National Academy of Sciences of the United States of America **107**, 5465-5470, doi:10.1073/pnas.1000834107 (2010).

16 Pang, W. W. *et al.* Human bone marrow hematopoietic stem cells are increased in frequency and myeloid-biased with age. *Proceedings of the National Academy of Sciences of the United States of America* **108**, 20012-20017, doi:10.1073/pnas.1116110108 (2011).

17 Seidler, S., Zimmermann, H. W., Bartneck, M., Trautwein, C. & Tacke, F. Age-dependent alterations of monocyte subsets and monocyte-related chemokine pathways in healthy adults. *BMC Immunol* **11**, 30, doi:10.1186/1471-2172-11-30 (2010).

18 Hearps, A. C. *et al.* Aging is associated with chronic innate immune activation and dysregulation of monocyte phenotype and function. *Aging Cell* **11**, 867-875, doi:10.1111/j.1474-9726.2012.00851.x (2012).

19 Nyugen, J., Agrawal, S., Gollapudi, S. & Gupta, S. Impaired Functions of Peripheral Blood Monocyte Subpopulations in Aged Humans. *Journal of Clinical Immunology* **30**, 806-813, doi:10.1007/s10875-010-9448-8 (2010).

20 Jing, Y. *et al.* Aging is associated with a numerical and functional decline in plasmacytoid dendritic cells, whereas myeloid dendritic cells are relatively unaltered in human peripheral blood. *Hum Immunol* **70**, 777-784, doi:10.1016/j.humimm.2009.07.005 (2009).

21 Perez-Cabezas, B. *et al.* Reduced numbers of plasmacytoid dendritic cells in aged blood donors. *Exp Gerontol* **42**, 1033-1038, doi:10.1016/j.exger.2007.05.010 (2007).

22 Agrawal, A. *et al.* Altered innate immune functioning of dendritic cells in elderly humans: a role of phosphoinositide 3-kinase-signaling pathway. *Journal of immunology* **178**, 6912-6922 (2007).

23 Pinti, M. *et al.* Aging of the immune system: Focus on inflammation and vaccination. *Eur J Immunol* **46**, 2286-2301, doi:10.1002/eji.201546178 (2016).

24 van Duin, D. *et al.* Age-Associated Defect in Human TLR-1/2 Function. *The Journal of Immunology* **178**, 970 (2007).

25 Qian, F. *et al.* Age-associated elevation in TLR5 leads to increased inflammatory responses in the elderly. *Aging Cell* **11**, 104-110, doi:10.1111/j.1474-9726.2011.00759.x (2012).

26 van Duin, D. *et al.* Prevaccine Determination of the Expression of Costimulatory B7 Molecules in Activated Monocytes Predicts Influenza Vaccine Responses in Young and Older Adults. *The Journal of Infectious Diseases* **195**, 1590-1597, doi:10.1086/516788 (2007).

27 Birjandi, S. Z., Ippolito, J. A., Ramadorai, A. K. & Witte, P. L. Alterations in marginal zone macrophages and marginal zone B cells in old mice. *Journal of immunology* **186**, 3441-3451, doi:10.4049/jimmunol.1001271 (2011).

28 Liang, S., Domon, H., Hosur, K. B., Wang, M. & Hajishengallis, G. Age-related alterations in innate immune receptor expression and ability of macrophages to respond to pathogen challenge in vitro. *Mech Ageing Dev* **130**, 538-546, doi:10.1016/j.mad.2009.06.006 (2009).

29 Aprahamian, T., Takemura, Y., Goukassian, D. & Walsh, K. Ageing is associated with diminished apoptotic cell clearance in vivo. *Clin Exp Immunol* **152**, 448-455, doi:10.1111/j.1365-2249.2008.03658.x (2008).

30 Janssen, N. *et al.* Responses of Dendritic Cells to TLR-4 Stimulation Are Maintained in the Elderly and Resist the Effects of CMV Infection Seen in the Young. *J Gerontol A Biol Sci Med Sci* **71**, 1117-1123, doi:10.1093/gerona/glv119 (2016).

31 Panda, A. *et al.* Age-associated decrease in TLR function in primary human dendritic cells predicts influenza vaccine response. *Journal of immunology* **184**, 2518-2527, doi:10.4049/jimmunol.0901022 (2010).

32 Bhushan, M. *et al.* Tumour necrosis factor-alpha-induced migration of human Langerhans cells: the influence of ageing. *Br J Dermatol* **146**, 32-40 (2002).

33 Shaw, A. C., Goldstein, D. R. & Montgomery, R. R. Age-dependent dysregulation of innate immunity. *Nature reviews. Immunology* **13**, 875-887, doi:10.1038/nri3547 (2013).

34 Sapey, E. *et al.* Phosphoinositide 3-kinase inhibition restores neutrophil accuracy in the elderly: toward targeted treatments for immunosenescence. *Blood* **123**, 239-248, doi:10.1182/blood-2013-08-519520 (2014).

35 Nomellini, V. *et al.* Dysregulation of neutrophil CXCR2 and pulmonary endothelial icam-1 promotes age-related pulmonary inflammation. *Aging Dis* **3**, 234-247 (2012).

36 Butcher, S. K. *et al.* Senescence in innate immune responses: reduced neutrophil phagocytic capacity and CD16 expression in elderly humans. *J Leukoc Biol* **70**, 881-886 (2001).

37 Emanuelli, G. *et al.* Influence of age on polymorphonuclear leukocytes in vitro: phagocytic activity in healthy human subjects. *Gerontology* **32**, 308-316 (1986).

38 Tseng, C. W. *et al.* Innate immune dysfunctions in aged mice facilitate the systemic dissemination of methicillin-resistant S. aureus. *PloS one* **7**, e41454, doi:10.1371/journal.pone.0041454 (2012).

39 Martinon, F., Burns, K. & Tschopp, J. The inflammasome: a molecular platform triggering activation of inflammatory caspases and processing of proIL-beta. *Mol Cell* **10**, 417-426 (2002).

40 Stout-Delgado, H. W., Vaughan, S. E., Shirali, A. C., Jaramillo, R. J. & Harrod, K. S. Impaired NLRP3 inflammasome function in elderly mice during influenza infection is rescued by treatment with nigericin. *Journal of immunology* **188**, 2815-2824, doi:10.4049/jimmunol.1103051 (2012).

41 Youm, Y. H. *et al.* Canonical Nlrp3 inflammasome links systemic low-grade inflammation to functional decline in aging. *Cell Metab* **18**, 519-532, doi:10.1016/j.cmet.2013.09.010 (2013).

42 Arnold, C. R., Wolf, J., Brunner, S., Herndler-Brandstetter, D. & Grubeck-Loebenstein, B. Gain and Loss of T Cell Subsets in Old Age—Age-Related Reshaping of the T Cell Repertoire. *Journal of Clinical Immunology* **31**, 137-146, doi:10.1007/s10875-010-9499-x (2011).

43 Yanes, R. E., Gustafson, C. E., Weyand, C. M. & Goronzy, J. J. Lymphocyte generation and population homeostasis throughout life. *Seminars in Hematology* **54**, 33-38, doi:http://dx.doi.org/10.1053/j.seminhematol.2016.10.003 (2017).

44 Wang, C. *et al.* Effects of aging, cytomegalovirus infection, and EBV infection on human B cell repertoires. *Journal of immunology* **192**, 603-611, doi:10.4049/jimmunol.1301384 (2014).

45 Colonna-Romano, G. *et al.* A double-negative (IgD-CD27-) B cell population is increased in the peripheral blood of elderly people. *Mech Ageing Dev* **130**, 681-690, doi:10.1016/j.mad.2009.08.003 (2009).

46 Pritz, T. *et al.* Plasma cell numbers decrease in bone marrow of old patients. *Eur J Immunol* **45**, 738-746, doi:10.1002/eji.201444878 (2015).

47 Steinmann, G. G., Klaus, B. & Muller-Hermelink, H. K. The involution of the ageing human thymic epithelium is independent of puberty. A morphometric study. *Scand J Immunol* **22**, 563-575 (1985).

48 Coder, B. & Su, D.-M. Thymic involution beyond T-cell insufficiency. *Oncotarget* **6**, 21777-21778 (2015).

49 Sauce, D. *et al.* Evidence of premature immune aging in patients thymectomized during early childhood. *J Clin Invest* **119**, 3070-3078, doi:10.1172/JCI39269 (2009).

50 Briceno, O. *et al.* Reduced naive CD8(+) T-cell priming efficacy in elderly adults. *Aging Cell* **15**, 14-21, doi:10.1111/acel.12384 (2016).

51 Li, G. *et al.* Decline in miR-181a expression with age impairs T cell receptor sensitivity by increasing DUSP6 activity. *Nature medicine* **18**, 1518-1524, doi:10.1038/nm.2963 (2012).

52 Johnson, P. L., Goronzy, J. J. & Antia, R. A population biological approach to understanding the maintenance and loss of the T-cell repertoire during aging. *Immunology* **142**, 167-175, doi:10.1111/imm.12244 (2014).

53 Richner, J. M. *et al.* Age-Dependent Cell Trafficking Defects in Draining Lymph Nodes Impair Adaptive Immunity and Control of West Nile Virus Infection. *PLoS Pathog* **11**, e1005027, doi:10.1371/journal.ppat.1005027 (2015).

54 Vallejo, A. N., Schirmer, M., Weyand, C. M. & Goronzy, J. J. Clonality and longevity of CD4+CD28null T cells are associated with defects in apoptotic pathways. *Journal of immunology* **165**, 6301-6307 (2000).

55 van der Geest, K. S. *et al.* Aging disturbs the balance between effector and regulatory CD4+ T cells. *Exp Gerontol* **60**, 190-196, doi:10.1016/j.exger.2014.11.005 (2014).

56 Raynor, J., Lages, C. S., Shehata, H., Hildeman, D. A. & Chougnet, C. A. Homeostasis and function of regulatory T cells in aging. *Curr Opin Immunol* **24**, 482-487, doi:10.1016/j.coi.2012.04.005 (2012).

57 Gregg, R. *et al.* The number of human peripheral blood CD4+ CD25high regulatory T cells increases with age. *Clin Exp Immunol* **140**, 540-546, doi:10.1111/j.1365-2249.2005.02798.x (2005).

58 Parish, S. T. *et al.* Adenosine deaminase modulation of telomerase activity and replicative senescence in human CD8 T lymphocytes. *Journal of immunology* **184**, 2847-2854, doi:10.4049/jimmunol.0903647 (2010).

59 Weng, N. P., Akbar, A. N. & Goronzy, J. CD28(-) T cells: their role in the age-associated decline of immune function. *Trends in immunology* **30**, 306-312, doi:10.1016/j.it.2009.03.013 (2009).

60 Koch, S. *et al.* Multiparameter flow cytometric analysis of CD4 and CD8 T cell subsets in young and old people. *Immun Ageing* **5**, 6, doi:10.1186/1742-4933-5-6 (2008).
61 Brenchley, J. M. *et al.* Expression of CD57 defines replicative senescence and antigen-induced apoptotic death of CD8+ T cells. *Blood* **101**, 2711-2720, doi:10.1182/blood-2002-07-2103 (2003).
62 Henson, S. M., Macaulay, R., Riddell, N. E., Nunn, C. J. & Akbar, A. N. Blockade of PD-1 or p38 MAP kinase signaling enhances senescent human CD8(+) T-cell proliferation by distinct pathways. *Eur J Immunol* **45**, 1441-1451, doi:10.1002/eji.201445312 (2015).
63 Kipnis, J., Cohen, H., Cardon, M., Ziv, Y. & Schwartz, M. T cell deficiency leads to cognitive dysfunction: implications for therapeutic vaccination for schizophrenia and other psychiatric conditions. *Proceedings of the National Academy of Sciences of the United States of America* **101**, 8180-8185, doi:10.1073/pnas.0402268101 (2004).
64 Wolf, S. A. *et al.* CD4-positive T lymphocytes provide a neuroimmunological link in the control of adult hippocampal neurogenesis. *Journal of immunology* **182**, 3979-3984, doi:10.4049/jimmunol.0801218 (2009).
65 Derecki, N. C. *et al.* Regulation of learning and memory by meningeal immunity: a key role for IL-4. *J Exp Med* **207**, 1067-1080, doi:10.1084/jem.20091419 (2010).
66 Ellwardt, E., Walsh, J. T., Kipnis, J. & Zipp, F. Understanding the Role of T Cells in CNS Homeostasis. *Trends in immunology* **37**, 154-165, doi:10.1016/j.it.2015.12.008 (2016).
67 Louveau, A. *et al.* Structural and functional features of central nervous system lymphatic vessels. *Nature* **523**, 337-341, doi:10.1038/nature14432 (2015).
68 Ginhoux, F. & Merad, M. [Microglia arise from extra-embryonic yolk sac primitive progenitors]. *Med Sci (Paris)* **27**, 719-724, doi:10.1051/medsci/2011278013 (2011).
69 Alliot, F., Godin, I. & Pessac, B. Microglia derive from progenitors, originating from the yolk sac, and which proliferate in the brain. *Brain Res Dev Brain Res* **117**, 145-152 (1999).
70 Ransohoff, R. M. A polarizing question: do M1 and M2 microglia exist? *Nature neuroscience* **19**, 987-991, doi:10.1038/nn.4338 (2016).
71 Deleidi, M., Jaggle, M. & Rubino, G. Immune aging, dysmetabolism, and inflammation in neurological diseases. *Front Neurosci* **9**, 172, doi:10.3389/fnins.2015.00172 (2015).
72 Flanary, B. E., Sammons, N. W., Nguyen, C., Walker, D. & Streit, W. J. Evidence that aging and amyloid promote microglial cell senescence. *Rejuvenation Res* **10**, 61-74, doi:10.1089/rej.2006.9096 (2007).
73 Sheng, J. G., Mrak, R. E. & Griffin, W. S. Enlarged and phagocytic, but not primed, interleukin-1 alpha-immunoreactive microglia increase with age in normal human brain. *Acta neuropathologica* **95**, 229-234 (1998).
74 Sheffield, L. G. & Berman, N. E. Microglial expression of MHC class II increases in normal aging of nonhuman primates. *Neurobiology of aging* **19**, 47-55 (1998).

75 Winkler, E. A., Sengillo, J. D., Bell, R. D., Wang, J. & Zlokovic, B. V. Blood-spinal cord barrier pericyte reductions contribute to increased capillary permeability. *J Cereb Blood Flow Metab* **32**, 1841-1852, doi:10.1038/jcbfm.2012.113 (2012).

76 Lucin, K. M. & Wyss-Coray, T. Immune activation in brain aging and neurodegeneration: too much or too little? *Neuron* **64**, 110-122, doi:10.1016/j.neuron.2009.08.039 (2009).

77 Anthony, D. C., Bolton, S. J., Fearn, S. & Perry, V. H. Age-related effects of interleukin-1 beta on polymorphonuclear neutrophil-dependent increases in blood-brain barrier permeability in rats. *Brain : a journal of neurology* **120 (Pt 3)**, 435-444 (1997).

78 Norden, D. M., Muccigrosso, M. M. & Godbout, J. P. Microglial priming and enhanced reactivity to secondary insult in aging, and traumatic CNS injury, and neurodegenerative disease. *Neuropharmacology* **96**, 29-41, doi:10.1016/j.neuropharm.2014.10.028 (2015).

79 Montagne, A. *et al.* Blood-brain barrier breakdown in the aging human hippocampus. *Neuron* **85**, 296-302, doi:10.1016/j.neuron.2014.12.032 (2015).

80 Brooks, D. J. The early diagnosis of parkinson's disease. *Annals of neurology* **44**, S10-S18, doi:10.1002/ana.410440704 (1998).

81 Samii, A., Nutt, J. G. & Ransom, B. R. Parkinson's disease. *Lancet* **363**, 1783-1793, doi:10.1016/S0140-6736(04)16305-8 (2004).

82 Puschmann, A. New Genes Causing Hereditary Parkinson's Disease or Parkinsonism. *Current neurology and neuroscience reports* **17**, 66, doi:10.1007/s11910-017-0780-8 (2017).

83 Langston, J. W., Ballard, P., Tetrud, J. W. & Irwin, I. Chronic Parkinsonism in humans due to a product of meperidine-analog synthesis. *Science* **219**, 979-980 (1983).

84 Kannarkat, G. T. *et al.* Common genetic variant association with altered HLA expression, synergy with pyrethroid exposure, and risk for Parkinson’s disease: an observational and case–control study. *npj Parkinson's Disease* **1**, 15002, doi:10.1038/npjparkd.2015.2 (2015).

85 Tanner, C. M. *et al.* Rotenone, paraquat, and Parkinson's disease. *Environ Health Perspect* **119**, 866-872, doi:10.1289/ehp.1002839 (2011).

86 Hernán, M. A., Takkouche, B., Caamaño-Isorna, F. & Gestal-Otero, J. J. A meta-analysis of coffee drinking, cigarette smoking, and the risk of Parkinson's disease. *Annals of neurology* **52**, 276-284, doi:10.1002/ana.10277 (2002).

87 Chen, H., Zhang, S. M., Hernán, M. A. & et al. NOnsteroidal anti-inflammatory drugs and the risk of parkinson disease. *Archives of Neurology* **60**, 1059-1064, doi:10.1001/archneur.60.8.1059 (2003).

88 Braak, H., Rub, U., Gai, W. P. & Del Tredici, K. Idiopathic Parkinson's disease: possible routes by which vulnerable neuronal types may be subject to neuroinvasion by an unknown pathogen. *J Neural Transm (Vienna)* **110**, 517-536, doi:10.1007/s00702-002-0808-2 (2003).

89 Braak, H. *et al.* Staging of brain pathology related to sporadic Parkinson's disease. *Neurobiology of aging* **24**, 197-211 (2003).

90 Rietdijk, C. D., Perez-Pardo, P., Garssen, J., van Wezel, R. J. & Kraneveld, A. D. Exploring Braak's Hypothesis of Parkinson's Disease. *Front Neurol* **8**, 37, doi:10.3389/fneur.2017.00037 (2017).

91 Shannon, K. M. *et al.* Alpha-synuclein in colonic submucosa in early untreated Parkinson's disease. *Movement disorders : official journal of the Movement Disorder Society* **27**, 709-715, doi:10.1002/mds.23838 (2012).

92 Visanji, N. P., Brooks, P. L., Hazrati, L. N. & Lang, A. E. The prion hypothesis in Parkinson's disease: Braak to the future. *Acta Neuropathol Commun* **1**, 2, doi:10.1186/2051-5960-1-2 (2013).

93 Block, M. L., Zecca, L. & Hong, J. S. Microglia-mediated neurotoxicity: uncovering the molecular mechanisms. *Nat Rev Neurosci* **8**, 57-69, doi:10.1038/nrn2038 (2007).

94 Mogi, M. *et al.* Interleukin-1 beta, interleukin-6, epidermal growth factor and transforming growth factor-alpha are elevated in the brain from parkinsonian patients. *Neurosci Lett* **180**, 147-150 (1994).

95 Mogi, M., Harada, M., Kondo, T., Riederer, P. & Nagatsu, T. Brain beta 2-microglobulin levels are elevated in the striatum in Parkinson's disease. *J Neural Transm Park Dis Dement Sect* **9**, 87-92 (1995).

96 Blum-Degen, D. *et al.* Interleukin-1 beta and interleukin-6 are elevated in the cerebrospinal fluid of Alzheimer's and de novo Parkinson's disease patients. *Neurosci Lett* **202**, 17-20 (1995).

97 McGuire, S. O. *et al.* Tumor necrosis factor alpha is toxic to embryonic mesencephalic dopamine neurons. *Experimental neurology* **169**, 219-230, doi:10.1006/exnr.2001.7688 (2001).

98 Mount, M. P. *et al.* Involvement of interferon-gamma in microglial-mediated loss of dopaminergic neurons. *The Journal of neuroscience : the official journal of the Society for Neuroscience* **27**, 3328-3337, doi:10.1523/JNEUROSCI.5321-06.2007 (2007).

99 Tansey, M. G. & Goldberg, M. S. Neuroinflammation in Parkinson's disease: its role in neuronal death and implications for therapeutic intervention. *Neurobiology of disease* **37**, 510-518, doi:10.1016/j.nbd.2009.11.004 (2010).

100 McGeer, P. L., Itagaki, S., Boyes, B. E. & McGeer, E. G. Reactive microglia are positive for HLA-DR in the substantia nigra of Parkinson's and Alzheimer's disease brains. *Neurology* **38**, 1285-1291 (1988).

101 McGeer, P. L., Schwab, C., Parent, A. & Doudet, D. Presence of reactive microglia in monkey substantia nigra years after 1-methyl-4-phenyl-1,2,3,6-tetrahydropyridine administration. *Annals of neurology* **54**, 599-604, doi:10.1002/ana.10728 (2003).

102 Lawson, L. J., Perry, V. H., Dri, P. & Gordon, S. Heterogeneity in the distribution and morphology of microglia in the normal adult mouse brain. *Neuroscience* **39**, 151-170 (1990).

103 Brochard, V. *et al.* Infiltration of CD4+ lymphocytes into the brain contributes to neurodegeneration in a mouse model of Parkinson disease. *J Clin Invest* **119**, 182-192, doi:10.1172/JCI36470 (2009).

104 Harms, A. S. *et al.* MHCII is required for alpha-synuclein-induced activation of microglia, CD4 T cell proliferation, and dopaminergic neurodegeneration. *The*

Journal of neuroscience : the official journal of the Society for Neuroscience **33**, 9592-9600, doi:10.1523/JNEUROSCI.5610-12.2013 (2013).

105 Cook, D. A. *et al.* LRRK2 levels in immune cells are increased in Parkinson's disease. *NPJ Parkinsons Dis* **3**, 11, doi:10.1038/s41531-017-0010-8 (2017).

106 Sulzer, D. *et al.* T cells from patients with Parkinson's disease recognize alpha-synuclein peptides. *Nature* **546**, 656-661, doi:10.1038/nature22815 (2017).

107 Caggiu, E. *et al.* Homologous HSV1 and alpha-synuclein peptides stimulate a T cell response in Parkinson's disease. *J Neuroimmunol* **310**, 26-31, doi:10.1016/j.jneuroim.2017.06.004 (2017).

108 Matsumoto, J. *et al.* Transmission of alpha-synuclein-containing erythrocyte-derived extracellular vesicles across the blood-brain barrier via adsorptive mediated transcytosis: another mechanism for initiation and progression of Parkinson's disease? *Acta Neuropathol Commun* **5**, 71, doi:10.1186/s40478-017-0470-4 (2017).

109 Paisan-Ruiz, C. *et al.* Cloning of the gene containing mutations that cause PARK8-linked Parkinson's disease. *Neuron* **44**, 595-600, doi:10.1016/j.neuron.2004.10.023 (2004).

110 Zimprich, A. *et al.* Mutations in LRRK2 cause autosomal-dominant parkinsonism with pleomorphic pathology. *Neuron* **44**, 601-607, doi:10.1016/j.neuron.2004.11.005 (2004).

111 Aasly, J. O. *et al.* Clinical features of LRRK2-associated Parkinson's disease in central Norway. *Annals of neurology* **57**, 762-765, doi:10.1002/ana.20456 (2005).

112 Thaler, A., Ash, E., Gan-Or, Z., Orr-Urtreger, A. & Giladi, N. The LRRK2 G2019S mutation as the cause of Parkinson's disease in Ashkenazi Jews. *Journal of neural transmission* **116**, 1473-1482, doi:10.1007/s00702-009-0303-0 (2009).

113 Haugarvoll, K. *et al.* Lrrk2 R1441C parkinsonism is clinically similar to sporadic Parkinson disease. *Neurology* **70**, 1456-1460, doi:10.1212/01.wnl.0000304044.22253.03 (2008).

114 Kumari, U. & Tan, E. K. LRRK2 in Parkinson's disease: genetic and clinical studies from patients. *FEBS Journal* **276**, 6455-6463, doi:10.1111/j.1742-4658.2009.07344.x (2009).

115 Russo, I., Bubacco, L. & Greggio, E. LRRK2 and neuroinflammation: partners in crime in Parkinson's disease? *Journal of Neuroinflammation* **11**, 52 (2014).

116 Pradhan, S. & Andreasson, K. Commentary: Progressive inflammation as a contributing factor to early development of Parkinson's disease. *Experimental neurology* **241**, 148-155, doi:http://dx.doi.org/10.1016/j.expneurol.2012.12.008 (2013).

117 Neumann, H., Kotter, M. R. & Franklin, R. J. M. Debris clearance by microglia: an essential link between degeneration and regeneration. *Brain : a journal of neurology* **132**, 288-295 (2009).

118 Whitton, P. S. Inflammation as a causative factor in the aetiology of Parkinson's disease. *British Journal of Pharmacology* **150**, 963-976, doi:10.1038/sj.bjp.0707167 (2007).

119 Meylan, E. & Tschopp, J. The RIP kinases: crucial integrators of cellular stress. *Trends in biochemical sciences* **30**, 151-159, doi:10.1016/j.tibs.2005.01.003 (2005).

120 Zhang, D., Lin, J. & Han, J. Receptor-interacting protein (RIP) kinase family. *Cell Mol Immunol* **7**, 243-249 (2010).
121 Funayama, M. *et al.* A new locus for Parkinson's disease (PARK8) maps to chromosome 12p11.2-q13.1. *Annals of neurology* **51**, 296-301 (2002).
122 Mata, I. F., Wedemeyer, W. J., Farrer, M. J., Taylor, J. P. & Gallo, K. A. LRRK2 in Parkinson's disease: protein domains and functional insights. *Trends in neurosciences* **29**, 286-293, doi:10.1016/j.tins.2006.03.006 (2006).
123 Guo, L. *et al.* The Parkinson's disease-associated protein, leucine-rich repeat kinase 2 (LRRK2), is an authentic GTPase that stimulates kinase activity. *Experimental cell research* **313**, 3658-3670, doi:10.1016/j.yexcr.2007.07.007 (2007).
124 Gilsbach, B. K. *et al.* Roco kinase structures give insights into the mechanism of Parkinson disease-related leucine-rich-repeat kinase 2 mutations. *Proceedings of the National Academy of Sciences* **109**, 10322-10327, doi:10.1073/pnas.1203223109 (2012).
125 Steger, M. *et al.* Phosphoproteomics reveals that Parkinson's disease kinase LRRK2 regulates a subset of Rab GTPases. *Elife* **5**, doi:10.7554/eLife.12813 (2016).
126 Ito, G. *et al.* Phos-tag analysis of Rab10 phosphorylation by LRRK2: a powerful assay for assessing kinase function and inhibitors. *The Biochemical journal* **473**, 2671-2685, doi:10.1042/BCJ20160557 (2016).
127 Toyofuku, T., Morimoto, K., Sasawatari, S. & Kumanogoh, A. Leucine-Rich Repeat Kinase 1 Regulates Autophagy through Turning On TBC1D2-Dependent Rab7 Inactivation. *Mol Cell Biol* **35**, 3044-3058, doi:10.1128/MCB.00085-15 (2015).
128 Dodson, M. W., Zhang, T., Jiang, C., Chen, S. & Guo, M. Roles of the Drosophila LRRK2 homolog in Rab7-dependent lysosomal positioning. *Human molecular genetics* **21**, 1350-1363, doi:10.1093/hmg/ddr573 (2012).
129 Cooper, A. A. *et al.* Alpha-synuclein blocks ER-Golgi traffic and Rab1 rescues neuron loss in Parkinson's models. *Science* **313**, 324-328, doi:10.1126/science.1129462 (2006).
130 Drolet, R. E., Sanders, J. M. & Kern, J. T. Leucine-rich repeat kinase 2 (LRRK2) cellular biology: a review of recent advances in identifying physiological substrates and cellular functions. *Journal of neurogenetics* **25**, 140-151, doi:10.3109/01677063.2011.627072 (2011).
131 Kamikawaji, S., Ito, G. & Iwatsubo, T. Identification of the autophosphorylation sites of LRRK2. *Biochemistry* **48**, 10963-10975, doi:10.1021/bi9011379 (2009).
132 Li, X., Moore, D. J., Xiong, Y., Dawson, T. M. & Dawson, V. L. Reevaluation of Phosphorylation Sites in the Parkinson Disease-associated Leucine-rich Repeat Kinase 2. *Journal of Biological Chemistry* **285**, 29569-29576, doi:10.1074/jbc.M110.127639 (2010).
133 Greggio, E. *et al.* The Parkinson's disease kinase LRRK2 autophosphorylates its GTPase domain at multiple sites. *Biochemical and biophysical research communications* **389**, 449-454, doi:http://dx.doi.org/10.1016/j.bbrc.2009.08.163 (2009).

134 Gloeckner, C. J. *et al.* The Parkinson disease causing LRRK2 mutation I2020T is associated with increased kinase activity. *Human molecular genetics* **15**, 223-232, doi:10.1093/hmg/ddi439 (2006).
135 Webber, P. J. *et al.* Autophosphorylation in the Leucine-Rich Repeat Kinase 2 (LRRK2) GTPase Domain Modifies Kinase and GTP-Binding Activities. *Journal of Molecular Biology* **412**, 94-110, doi:http://dx.doi.org/10.1016/j.jmb.2011.07.033 (2011).
136 Bosgraaf, L. & Van Haastert, P. J. Roc, a Ras/GTPase domain in complex proteins. *Biochimica et biophysica acta* **1643**, 5-10 (2003).
137 Biosa, A. *et al.* GTPase activity regulates kinase activity and cellular phenotypes of Parkinson's disease-associated LRRK2. *Human molecular genetics* **22**, 1140-1156, doi:10.1093/hmg/dds522 (2013).
138 Sen, S., Webber, P. J. & West, A. B. Dependence of Leucine-rich Repeat Kinase 2 (LRRK2) Kinase Activity on Dimerization. *Journal of Biological Chemistry* **284**, 36346-36356, doi:10.1074/jbc.M109.025437 (2009).
139 Haebig, K. *et al.* ARHGEF7 (BETA-PIX) Acts as Guanine Nucleotide Exchange Factor for Leucine-Rich Repeat Kinase 2. *PloS one* **5**, e13762, doi:10.1371/journal.pone.0013762 (2010).
140 Xiong, Y., Yuan, C., Chen, R., Dawson, T. M. & Dawson, V. L. ArfGAP1 Is a GTPase Activating Protein for LRRK2: Reciprocal Regulation of ArfGAP1 by LRRK2. *The Journal of Neuroscience* **32**, 3877-3886, doi:10.1523/jneurosci.4566-11.2012 (2012).
141 Stafa, K. *et al.* GTPase Activity and Neuronal Toxicity of Parkinson's Disease–Associated LRRK2 Is Regulated by ArfGAP1. *PLoS Genet* **8**, e1002526, doi:10.1371/journal.pgen.1002526 (2012).
142 Gómez-Suaga, P. *et al.* Novel insights into the neurobiology underlying LRRK2-linked Parkinson's disease. *Neuropharmacology* **85**, 45-56, doi:http://dx.doi.org/10.1016/j.neuropharm.2014.05.020 (2014).
143 Reyniers, L. *et al.* Differential protein-protein interactions of LRRK1 and LRRK2 indicate roles in distinct cellular signaling pathways. *Journal of neurochemistry*, doi:10.1111/jnc.12798 (2014).
144 Nichols, R. J. *et al.* 14-3-3 binding to LRRK2 is disrupted by multiple Parkinson's disease-associated mutations and regulates cytoplasmic localization. *The Biochemical journal* **430**, 393-404, doi:10.1042/BJ20100483 (2010).
145 Dzamko, N. *et al.* Inhibition of LRRK2 kinase activity leads to dephosphorylation of Ser(910)/Ser(935), disruption of 14-3-3 binding and altered cytoplasmic localization. *The Biochemical journal* **430**, 405-413, doi:10.1042/BJ20100784 (2010).
146 Plowey, E. D., Cherra, S. J., Liu, Y.-J. & Chu, C. T. Role of autophagy in G2019S-LRRK2-associated neurite shortening in differentiated SH-SY5Y cells. *Journal of neurochemistry* **105**, 1048-1056, doi:10.1111/j.1471-4159.2008.05217.x (2008).
147 Gómez-Suaga, P. *et al.* Leucine-rich repeat kinase 2 regulates autophagy through a calcium-dependent pathway involving NAADP. *Human molecular genetics* **21**, 511-525, doi:10.1093/hmg/ddr481 (2012).

148 Tong, Y. *et al.* Loss of leucine-rich repeat kinase 2 causes age-dependent bi-phasic alterations of the autophagy pathway. *Molecular Neurodegeneration* **7**, 2-2, doi:10.1186/1750-1326-7-2 (2012).
149 Ramonet, D. *et al.* Dopaminergic Neuronal Loss, Reduced Neurite Complexity and Autophagic Abnormalities in Transgenic Mice Expressing G2019S Mutant LRRK2. *PloS one* **6**, e18568, doi:10.1371/journal.pone.0018568 (2011).
150 Beilina, A. *et al.* Unbiased screen for interactors of leucine-rich repeat kinase 2 supports a common pathway for sporadic and familial Parkinson disease. *Proceedings of the National Academy of Sciences of the United States of America* **111**, 2626-2631, doi:10.1073/pnas.1318306111 (2014).
151 Chia, R. *et al.* Phosphorylation of LRRK2 by casein kinase 1alpha regulates trans-Golgi clustering via differential interaction with ARHGEF7. *Nature communications* **5**, 5827, doi:10.1038/ncomms6827 (2014).
152 Sanchez-Danes, A. *et al.* Disease-specific phenotypes in dopamine neurons from human iPS-based models of genetic and sporadic Parkinson's disease. *EMBO Mol Med* **4**, 380-395, doi:10.1002/emmm.201200215 (2012).
153 Bravo-San Pedro, J. M. *et al.* The LRRK2 G2019S mutant exacerbates basal autophagy through activation of the MEK/ERK pathway. *Cellular and molecular life sciences : CMLS* **70**, 121-136, doi:10.1007/s00018-012-1061-y (2013).
154 Kett, L. R. *et al.* LRRK2 Parkinson disease mutations enhance its microtubule association. *Human molecular genetics* **21**, 890-899, doi:10.1093/hmg/ddr526 (2012).
155 Gillardon, F. Leucine-rich repeat kinase 2 phosphorylates brain tubulin-beta isoforms and modulates microtubule stability--a point of convergence in parkinsonian neurodegeneration? *Journal of neurochemistry* **110**, 1514-1522, doi:10.1111/j.1471-4159.2009.06235.x (2009).
156 Parisiadou, L. *et al.* Phosphorylation of ezrin/radixin/moesin proteins by LRRK2 promotes the rearrangement of actin cytoskeleton in neuronal morphogenesis. *The Journal of neuroscience : the official journal of the Society for Neuroscience* **29**, 13971-13980, doi:10.1523/JNEUROSCI.3799-09.2009 (2009).
157 Esteves, A. R. & Cardoso, S. M. LRRK2 at the Crossroad Between Autophagy and Microtubule Trafficking: Insights into Parkinson's Disease. *Neuroscientist*, doi:10.1177/1073858415616558 (2016).
158 Berwick, D. C. & Harvey, K. LRRK2 functions as a Wnt signaling scaffold, bridging cytosolic proteins and membrane-localized LRP6. *Human molecular genetics* **21**, 4966-4979, doi:10.1093/hmg/dds342 (2012).
159 Berwick, D. C. & Harvey, K. The regulation and deregulation of Wnt signaling by PARK genes in health and disease. *Journal of Molecular Cell Biology* **6**, 3-12, doi:10.1093/jmcb/mjt037 (2014).
160 Staal, F. J., Luis, T. C. & Tiemessen, M. M. WNT signalling in the immune system: WNT is spreading its wings. *Nature reviews. Immunology* **8**, 581-593, doi:10.1038/nri2360 (2008).
161 Sancho, R. M., Law, B. M. H. & Harvey, K. Mutations in the LRRK2 Roc-COR tandem domain link Parkinson's disease to Wnt signalling pathways. *Human molecular genetics* **18**, 3955-3968, doi:10.1093/hmg/ddp337 (2009).

162 Salasova, A. *et al.* A proteomic analysis of LRRK2 binding partners reveals interactions with multiple signaling components of the WNT/PCP pathway. *Mol Neurodegener* **12**, 54, doi:10.1186/s13024-017-0193-9 (2017).

163 Berwick, D. C. *et al.* Pathogenic LRRK2 variants are gain-of-function mutations that enhance LRRK2-mediated repression of beta-catenin signaling. *Mol Neurodegener* **12**, 9, doi:10.1186/s13024-017-0153-4 (2017).

164 Yang, S.-H., Sharrocks, A. D. & Whitmarsh, A. J. MAP kinase signalling cascades and transcriptional regulation. *Gene* **513**, 1-13, doi:http://dx.doi.org/10.1016/j.gene.2012.10.033 (2013).

165 White, L. R., Toft, M., Kvam, S. N., Farrer, M. J. & Aasly, J. O. MAPK-pathway activity, Lrrk2 G2019S, and Parkinson's disease. *Journal of neuroscience research* **85**, 1288-1294, doi:10.1002/jnr.21240 (2007).

166 Gardet, A. *et al.* LRRK2 is involved in the IFN-gamma response and host response to pathogens. *Journal of immunology* **185**, 5577-5585, doi:10.4049/jimmunol.1000548 (2010).

167 Hongge, L., Kexin, G., Xiaojie, M., Nian, X. & Jinsha, H. The Role of LRRK2 in the Regulation of Monocyte Adhesion to Endothelial Cells. *Journal of molecular neuroscience : MN*, doi:10.1007/s12031-014-0312-9 (2014).

168 Liu, Z. *et al.* The kinase LRRK2 is a regulator of the transcription factor NFAT that modulates the severity of inflammatory bowel disease. *Nature immunology* **12**, 1063-1070, doi:10.1038/ni.2113 (2011).

169 Westerlund, M. *et al.* Developmental regulation of leucine-rich repeat kinase 1 and 2 expression in the brain and other rodent and human organs: Implications for Parkinson's disease. *Neuroscience* **152**, 429-436, doi:10.1016/j.neuroscience.2007.10.062 (2008).

170 Miklossy, J. *et al.* LRRK2 expression in normal and pathologic human brain and in human cell lines. *Journal of neuropathology and experimental neurology* **65**, 953-963, doi:10.1097/01.jnen.0000235121.98052.54 (2006).

171 Taymans, J. M., Van den Haute, C. & Baekelandt, V. Distribution of PINK1 and LRRK2 in rat and mouse brain. *Journal of neurochemistry* **98**, 951-961, doi:10.1111/j.1471-4159.2006.03919.x (2006).

172 Hakimi, M. *et al.* Parkinson's disease-linked LRRK2 is expressed in circulating and tissue immune cells and upregulated following recognition of microbial structures. *Journal of neural transmission* **118**, 795-808, doi:10.1007/s00702-011-0653-2 (2011).

173 Thevenet, J., Pescini Gobert, R., Hooft van Huijsduijnen, R., Wiessner, C. & Sagot, Y. J. Regulation of LRRK2 expression points to a functional role in human monocyte maturation. *PloS one* **6**, e21519, doi:10.1371/journal.pone.0021519 (2011).

174 West, A. B. *et al.* Parkinson's disease-associated mutations in leucine-rich repeat kinase 2 augment kinase activity. *Proceedings of the National Academy of Sciences of the United States of America* **102**, 16842-16847, doi:10.1073/pnas.0507360102 (2005).

175 Schapansky, J., Nardozzi, J. D., Felizia, F. & LaVoie, M. J. Membrane recruitment of endogenous LRRK2 precedes its potent regulation of autophagy. *Human molecular genetics* **23**, 4201-4214, doi:10.1093/hmg/ddu138 (2014).

176 Berger, Z., Smith, K. A. & Lavoie, M. J. Membrane localization of LRRK2 is associated with increased formation of the highly active LRRK2 dimer and changes in its phosphorylation. *Biochemistry* **49**, 5511-5523, doi:10.1021/bi100157u (2010).

177 Blesa, J. & Przedborski, S. PARKINSON'S DISEASE: ANIMAL MODELS AND DOPAMINERGIC CELL VULNERABILITY. *Frontiers in Neuroanatomy* **8**, doi:10.3389/fnana.2014.00155 (2014).

178 Martin, I., Kim, J. W., Dawson, V. L. & Dawson, T. M. LRRK2 pathobiology in Parkinson's disease. *Journal of neurochemistry* **131**, 554-565, doi:10.1111/jnc.12949 (2014).

179 Rudenko, I. N. & Cookson, M. R. Heterogeneity of leucine-rich repeat kinase 2 mutations: genetics, mechanisms and therapeutic implications. *Neurotherapeutics : the journal of the American Society for Experimental NeuroTherapeutics* **11**, 738-750, doi:10.1007/s13311-014-0284-z (2014).

180 Brice, A. Genetics of Parkinson's disease: LRRK2 on the rise. *Brain : a journal of neurology* **128**, 2760-2762, doi:10.1093/brain/awh676 (2005).

181 Rideout, H. J. & Stefanis, L. The neurobiology of LRRK2 and its role in the pathogenesis of Parkinson's disease. *Neurochemical research* **39**, 576-592, doi:10.1007/s11064-013-1073-5 (2014).

182 Greggio, E. & Cookson, M. R. Leucine-rich repeat kinase 2 mutations and Parkinson's disease: three questions. *ASN neuro* **1**, doi:10.1042/AN20090007 (2009).

183 Lewis, P. A. *et al.* The R1441C mutation of LRRK2 disrupts GTP hydrolysis. *Biochemical and biophysical research communications* **357**, 668-671, doi:10.1016/j.bbrc.2007.04.006 (2007).

184 Tong, Y. *et al.* R1441C mutation in LRRK2 impairs dopaminergic neurotransmission in mice. *Proceedings of the National Academy of Sciences* **106**, 14622-14627, doi:10.1073/pnas.0906334106 (2009).

185 Gotthardt, K., Weyand, M., Kortholt, A., Van Haastert, P. J. M. & Wittinghofer, A. Structure of the Roc–COR domain tandem of C. tepidum, a prokaryotic homologue of the human LRRK2 Parkinson kinase. *The EMBO journal* **27**, 2239-2249 (2008).

186 Nixon-Abell, J. *et al.* Protective LRRK2 R1398H Variant Enhances GTPase and Wnt Signaling Activity. *Frontiers in molecular neuroscience* **9**, 18, doi:10.3389/fnmol.2016.00018 (2016).

187 Greggio, E. *et al.* Kinase activity is required for the toxic effects of mutant LRRK2/dardarin. *Neurobiology of disease* **23**, 329-341, doi:10.1016/j.nbd.2006.04.001 (2006).

188 Gilsbach, B. K. & Kortholt, A. Structural biology of the LRRK2 GTPase and kinase domains: implications for regulation. *Frontiers in molecular neuroscience* **7**, 32, doi:10.3389/fnmol.2014.00032 (2014).

189 Smith, W. W. *et al.* Kinase activity of mutant LRRK2 mediates neuronal toxicity. *Nature neuroscience* **9**, 1231-1233, doi:10.1038/nn1776 (2006).

190 Sharma, S. *et al.* LRRK2 expression in idiopathic and G2019S positive Parkinson's disease subjects: a morphological and quantitative study.

Neuropathology and applied neurobiology **37**, 777-790, doi:10.1111/j.1365-2990.2011.01187.x (2011).

191 West, A. B. *et al.* Parkinson's disease-associated mutations in LRRK2 link enhanced GTP-binding and kinase activities to neuronal toxicity. *Human molecular genetics* **16**, 223-232, doi:10.1093/hmg/ddl471 (2007).

192 Imai, Y. *et al.* Phosphorylation of 4E-BP by LRRK2 affects the maintenance of dopaminergic neurons in Drosophila. *The EMBO journal* **27**, 2432-2443, doi:10.1038/emboj.2008.163 (2008).

193 Jaleel, M. *et al.* LRRK2 phosphorylates moesin at threonine-558: characterization of how Parkinson's disease mutants affect kinase activity. *The Biochemical journal* **405**, 307-317, doi:10.1042/BJ20070209 (2007).

194 Anand, V. S. *et al.* Investigation of leucine-rich repeat kinase 2 : enzymological properties and novel assays. *The FEBS journal* **276**, 466-478, doi:10.1111/j.1742-4658.2008.06789.x (2009).

195 Luzón-Toro, B., de la Torre, E. R., Delgado, A., Pérez-Tur, J. & Hilfiker, S. Mechanistic insight into the dominant mode of the Parkinson's disease-associated G2019S LRRK2 mutation. *Human molecular genetics* **16**, 2031-2039 (2007).

196 Ray, S. *et al.* The Parkinson disease-linked LRRK2 protein mutation I2020T stabilizes an active state conformation leading to increased kinase activity. *The Journal of biological chemistry* **289**, 13042-13053, doi:10.1074/jbc.M113.537811 (2014).

197 Barrett, J. C. *et al.* Genome-wide association defines more than 30 distinct susceptibility loci for Crohn's disease. *Nature genetics* **40**, 955-962, doi:10.1038/ng.175 (2008).

198 Zhang, F.-R. *et al.* Genomewide Association Study of Leprosy. *New England Journal of Medicine* **361**, 2609-2618, doi:doi:10.1056/NEJMoa0903753 (2009).

199 Wang, D. *et al.* Association of the LRRK2 genetic polymorphisms with leprosy in Han Chinese from Southwest China. *Genes and immunity*, doi:10.1038/gene.2014.72 (2014).

200 Kuss, M., Adamopoulou, E. & Kahle, P. J. Interferon-gamma induces leucine-rich repeat kinase LRRK2 via extracellular signal-regulated kinase ERK5 in macrophages. *Journal of neurochemistry* **129**, 980-987, doi:10.1111/jnc.12668 (2014).

201 Moehle, M. S. *et al.* LRRK2 inhibition attenuates microglial inflammatory responses. *The Journal of neuroscience : the official journal of the Society for Neuroscience* **32**, 1602-1611, doi:10.1523/JNEUROSCI.5601-11.2012 (2012).

202 Reinhardt, P. *et al.* Genetic correction of a LRRK2 mutation in human iPSCs links parkinsonian neurodegeneration to ERK-dependent changes in gene expression. *Cell stem cell* **12**, 354-367, doi:10.1016/j.stem.2013.01.008 (2013).

203 Lopez de Maturana, R. *et al.* Leucine-rich repeat kinase 2 modulates cyclooxygenase 2 and the inflammatory response in idiopathic and genetic Parkinson's disease. *Neurobiology of aging* **35**, 1116-1124, doi:10.1016/j.neurobiolaging.2013.11.018 (2014).

204 Han, K. A. *et al.* Leucine-Rich Repeat Kinase 2 (LRRK2) Stimulates IL-1beta-Mediated Inflammatory Signaling through Phosphorylation of RCAN1. *Front Cell Neurosci* **11**, 125, doi:10.3389/fncel.2017.00125 (2017).

205 Russo, I. *et al.* Leucine-rich repeat kinase 2 positively regulates inflammation and down-regulates NF-κB p50 signaling in cultured microglia cells. *Journal of Neuroinflammation* **12**, 230, doi:10.1186/s12974-015-0449-7 (2015).

206 Daher, J. P., Volpicelli-Daley, L. A., Blackburn, J. P., Moehle, M. S. & West, A. B. Abrogation of alpha-synuclein-mediated dopaminergic neurodegeneration in LRRK2-deficient rats. *Proceedings of the National Academy of Sciences of the United States of America* **111**, 9289-9294, doi:10.1073/pnas.1403215111 (2014).

207 Ness, D. *et al.* Leucine-rich repeat kinase 2 (LRRK2)-deficient rats exhibit renal tubule injury and perturbations in metabolic and immunological homeostasis. *PloS one* **8**, e66164, doi:10.1371/journal.pone.0066164 (2013).

208 Tong, Y. & Shen, J. Genetic analysis of Parkinson's disease-linked leucine-rich repeat kinase 2. *Biochemical Society transactions* **40**, 1042-1046, doi:10.1042/BST20120112 (2012).

209 Herzig, M. C. *et al.* LRRK2 protein levels are determined by kinase function and are crucial for kidney and lung homeostasis in mice. *Human molecular genetics* **20**, 4209-4223, doi:10.1093/hmg/ddr348 (2011).

210 Baptista, M. A. S. *et al.* Loss of Leucine-Rich Repeat Kinase 2 (LRRK2) in Rats Leads to Progressive Abnormal Phenotypes in Peripheral Organs. *PloS one* **8**, e80705, doi:10.1371/journal.pone.0080705 (2013).

211 Miklavc, P. *et al.* Surfactant Secretion in LRRK2 Knock-Out Rats: Changes in Lamellar Body Morphology and Rate of Exocytosis. *PloS one* **9**, e84926, doi:10.1371/journal.pone.0084926 (2014).

212 Gillardon, F., Schmid, R. & Draheim, H. Parkinson's disease-linked leucine-rich repeat kinase 2(R1441G) mutation increases proinflammatory cytokine release from activated primary microglial cells and resultant neurotoxicity. *Neuroscience* **208**, 41-48, doi:10.1016/j.neuroscience.2012.02.001 (2012).

213 West, A. B. Ten Years and Counting: Moving Leucine-Rich Repeat Kinase 2 Inhibitors to the Clinic. *Movement disorders : official journal of the Movement Disorder Society*, doi:10.1002/mds.26075 (2014).

214 Peng, Y.-H. *et al.* Protein Kinase Inhibitor Design by Targeting the Asp-Phe-Gly (DFG) Motif: The Role of the DFG Motif in the Design of Epidermal Growth Factor Receptor Inhibitors. *Journal of Medicinal Chemistry* **56**, 3889-3903, doi:10.1021/jm400072p (2013).

215 Kramer, T., Lo Monte, F., Göring, S., Okala Amombo, G. M. & Schmidt, B. Small Molecule Kinase Inhibitors for LRRK2 and Their Application to Parkinson's Disease Models. *ACS Chemical Neuroscience* **3**, 151-160, doi:10.1021/cn200117j (2012).

216 Kethiri, R. R. & Bakthavatchalam, R. Leucine-rich repeat kinase 2 inhibitors: a review of recent patents (2011 – 2013). *Expert Opinion on Therapeutic Patents* **24**, 745-757, doi:doi:10.1517/13543776.2014.907275 (2014).

217 Deng, X. *et al.* Characterization of a selective inhibitor of the Parkinson's disease kinase LRRK2. *Nat Chem Biol* **7**, 203-205, doi:http://www.nature.com/nchembio/journal/v7/n4/abs/nchembio.538.html#supplementary-information (2011).

218 Luerman, G. C. *et al.* Phosphoproteomic evaluation of pharmacological inhibition of leucine-rich repeat kinase 2 reveals significant off-target effects of LRRK-2-IN-1. *Journal of neurochemistry* **128**, 561-576, doi:10.1111/jnc.12483 (2014).
219 Henderson, J. L. *et al.* Discovery and Preclinical Profiling of 3-[4-(Morpholin-4-yl)-7H-pyrrolo[2,3-d]pyrimidin-5-yl]benzonitrile (PF-06447475), a Highly Potent, Selective, Brain Penetrant, and in Vivo Active LRRK2 Kinase Inhibitor. *J Med Chem* **58**, 419-432, doi:10.1021/jm5014055 (2015).
220 Thirstrup, K. *et al.* Selective LRRK2 kinase inhibition reduces phosphorylation of endogenous Rab10 and Rab12 in human peripheral mononuclear blood cells. *Sci Rep* **7**, 10300, doi:10.1038/s41598-017-10501-z (2017).
221 West, A. B. Achieving neuroprotection with LRRK2 kinase inhibitors in Parkinson disease. *Experimental neurology*, doi:10.1016/j.expneurol.2017.07.019 (2017).
222 Daher, J. P. *et al.* Leucine-rich Repeat Kinase 2 (LRRK2) Pharmacological Inhibition Abates alpha-Synuclein Gene-induced Neurodegeneration. *The Journal of biological chemistry* **290**, 19433-19444, doi:10.1074/jbc.M115.660001 (2015).
223 Fuji, R. N. *et al.* Effect of selective LRRK2 kinase inhibition on nonhuman primate lung. *Sci Transl Med* **7**, 273ra215, doi:10.1126/scitranslmed.aaa3634 (2015).
224 Zhao, H. T. *et al.* LRRK2 Antisense Oligonucleotides Ameliorate alpha-Synuclein Inclusion Formation in a Parkinson's Disease Mouse Model. *Mol Ther Nucleic Acids* **8**, 508-519, doi:10.1016/j.omtn.2017.08.002 (2017).
225 Manzoni, C. *et al.* mTOR independent regulation of macroautophagy by Leucine Rich Repeat Kinase 2 via Beclin-1. *Scientific Reports* **6**, 35106, doi:10.1038/srep35106

http://www.nature.com/articles/srep35106#supplementary-information (2016).
226 Ferrazza, R. *et al.* LRRK2 deficiency impacts ceramide metabolism in brain. *Biochemical and biophysical research communications* **478**, 1141-1146, doi:http://dx.doi.org/10.1016/j.bbrc.2016.08.082 (2016).
227 Perera, G., Ranola, M., Rowe, D. B., Halliday, G. M. & Dzamko, N. Inhibitor treatment of peripheral mononuclear cells from Parkinson's disease patients further validates LRRK2 dephosphorylation as a pharmacodynamic biomarker. *Scientific Reports* **6**, 31391, doi:10.1038/srep31391

http://www.nature.com/articles/srep31391#supplementary-information (2016).
228 Chen, H. *et al.* Smoking duration, intensity, and risk of Parkinson disease. *Neurology* **74**, 878-884, doi:10.1212/WNL.0b013e3181d55f38 (2010).
229 Gagne, J. J. & Power, M. C. Anti-inflammatory drugs and risk of Parkinson disease: A meta-analysis. *Neurology* **74**, 995-1002, doi:10.1212/WNL.0b013e3181d5a4a3 (2010).
230 Saunders, J. A. *et al.* CD4+ regulatory and effector/memory T cell subsets profile motor dysfunction in Parkinson's disease. *Journal of neuroimmune pharmacology : the official journal of the Society on NeuroImmune Pharmacology* **7**, 927-938, doi:10.1007/s11481-012-9402-z (2012).

231 Waldburger, J. M. *et al.* Lessons from the bare lymphocyte syndrome: molecular mechanisms regulating MHC class II expression. *Immunol Rev* **178**, 148-165 (2000).
232 Guermonprez, P., Valladeau, J., Zitvogel, L., Thery, C. & Amigorena, S. Antigen presentation and T cell stimulation by dendritic cells. *Annu Rev Immunol* **20**, 621-667, doi:10.1146/annurev.immunol.20.100301.064828 (2002).
233 Chardin, P. & McCormick, F. Brefeldin A: the advantage of being uncompetitive. *Cell* **97**, 153-155 (1999).
234 Ziegler-Heitbrock, L. The CD14+ CD16+ blood monocytes: their role in infection and inflammation. *J Leukoc Biol* **81**, 584-592, doi:10.1189/jlb.0806510 (2007).
235 Grozdanov, V. *et al.* Inflammatory dysregulation of blood monocytes in Parkinson's disease patients. *Acta neuropathologica* **128**, 651-663, doi:10.1007/s00401-014-1345-4 (2014).
236 Gibson, H. M. *et al.* Induction of the CTLA-4 Gene in Human Lymphocytes Is Dependent on NFAT Binding the Proximal Promoter. *The Journal of Immunology* **179**, 3831-3840, doi:10.4049/jimmunol.179.6.3831 (2007).
237 Dorsey, E. R. *et al.* Projected number of people with Parkinson disease in the most populous nations, 2005 through 2030. *Neurology* **68**, 384-386, doi:10.1212/01.wnl.0000247740.47667.03 (2007).
238 Alegre-Abarrategui, J. *et al.* LRRK2 regulates autophagic activity and localizes to specific membrane microdomains in a novel human genomic reporter cellular model. *Human molecular genetics* **18**, 4022-4034, doi:10.1093/hmg/ddp346 (2009).
239 Sheng, Z. *et al.* Ser1292 autophosphorylation is an indicator of LRRK2 kinase activity and contributes to the cellular effects of PD mutations. *Sci Transl Med* **4**, 164ra161, doi:10.1126/scitranslmed.3004485 (2012).
240 Maguire, O., Tornatore, K. M., O'Loughlin, K. L., Venuto, R. C. & Minderman, H. Nuclear translocation of nuclear factor of activated T cells (NFAT) as a quantitative pharmacodynamic parameter for tacrolimus. *Cytometry A* **83**, 1096-1104, doi:10.1002/cyto.a.22401 (2013).
241 Dzamko, N., Chua, G., Ranola, M., Rowe, D. B. & Halliday, G. M. Measurement of LRRK2 and Ser910/935 phosphorylated LRRK2 in peripheral blood mononuclear cells from idiopathic Parkinson's disease patients. *J Parkinsons Dis* **3**, 145-152, doi:10.3233/JPD-130174 (2013).
242 Lopez de Maturana, R. *et al.* Mutations in LRRK2 impair NF-kappaB pathway in iPSC-derived neurons. *J Neuroinflammation* **13**, 295, doi:10.1186/s12974-016-0761-x (2016).
243 Kaltschmidt, B. & Kaltschmidt, C. NF-kappaB in the nervous system. *Cold Spring Harb Perspect Biol* **1**, a001271, doi:10.1101/cshperspect.a001271 (2009).
244 Volpicelli-Daley, L. A. *et al.* G2019S-LRRK2 Expression Augments alpha-Synuclein Sequestration into Inclusions in Neurons. *The Journal of neuroscience : the official journal of the Society for Neuroscience* **36**, 7415-7427, doi:10.1523/JNEUROSCI.3642-15.2016 (2016).
245 Dzamko, N., Rowe, D. B. & Halliday, G. M. Increased peripheral inflammation in asymptomatic leucine-rich repeat kinase 2 mutation carriers. *Movement disorders*

: official journal of the Movement Disorder Society **31**, 889-897, doi:10.1002/mds.26529 (2016).
246 Ziegler-Heitbrock, L. Monocyte subsets in man and other species. *Cell Immunol* **289**, 135-139, doi:10.1016/j.cellimm.2014.03.019 (2014).
247 Yan, R. & Liu, Z. LRRK2 enhances Nod1/2-mediated inflammatory cytokine production by promoting Rip2 phosphorylation. *Protein Cell* **8**, 55-66, doi:10.1007/s13238-016-0326-x (2017).
248 Brockmann, K. *et al.* Inflammatory profile in LRRK2-associated prodromal and clinical PD. *J Neuroinflammation* **13**, 122, doi:10.1186/s12974-016-0588-5 (2016).
249 Schork, N. J. Personalized medicine: Time for one-person trials. *Nature* **520**, 609-611, doi:10.1038/520609a (2015).
250 Ross, O. A. A prognostic view on the application of individualized genomics in Parkinson's disease. *Curr Genet Med Rep* **1**, 52-57 (2013).
251 Factor, S. & Weiner, W. *Parkinson's Disease: Diagnosis and Clinical Management*, 2007).
252 Barnum, C. J. & Tansey, M. G. Neuroinflammation and non-motor symptoms: the dark passenger of Parkinson's disease? *Current neurology and neuroscience reports* **12**, 350-358, doi:10.1007/s11910-012-0283-6 (2012).
253 Bower, J. H. *et al.* Head trauma preceding PD: a case-control study. *Neurology* **60**, 1610-1615 (2003).
254 Hatcher, J. M., Pennell, K. D. & Miller, G. W. Parkinson's disease and pesticides: a toxicological perspective. *Trends in pharmacological sciences* **29**, 322-329, doi:10.1016/j.tips.2008.03.007 (2008).
255 Taetzsch, T. & Block, M. L. Pesticides, microglial NOX2, and Parkinson's disease. *Journal of biochemical and molecular toxicology* **27**, 137-149, doi:10.1002/jbt.21464 (2013).
256 Kanthasamy, A. *et al.* Emerging neurotoxic mechanisms in environmental factors-induced neurodegeneration. *Neurotoxicology* **33**, 833-837, doi:10.1016/j.neuro.2012.01.011 (2012).
257 Rees, K. *et al.* Non-steroidal anti-inflammatory drugs as disease-modifying agents for Parkinson's disease: evidence from observational studies. *The Cochrane database of systematic reviews*, CD008454, doi:10.1002/14651858.CD008454.pub2 (2011).
258 Bower, J. H. & Ritz, B. Is the answer for Parkinson disease already in the medicine cabinet?: Unfortunately not. *Neurology* **76**, 854-855, doi:10.1212/WNL.0b013e31820f2e7a (2011).
259 Luckheeram, R. V., Zhou, R., Verma, A. D. & Xia, B. CD4(+)T cells: differentiation and functions. *Clinical & developmental immunology* **2012**, 925135, doi:10.1155/2012/925135 (2012).
260 Hamza, T. H. *et al.* Common genetic variation in the HLA region is associated with late-onset sporadic Parkinson's disease. *Nature genetics* **42**, 781-785, doi:10.1038/ng.642 (2010).
261 Guo, Y. *et al.* HLA rs3129882 variant in Chinese Han patients with late-onset sporadic Parkinson disease. *Neuroscience letters* **501**, 185-187, doi:10.1016/j.neulet.2011.05.245 (2011).

262 Ahmed, I. *et al.* Association between Parkinson's disease and the HLA-DRB1 locus. *Movement disorders : official journal of the Movement Disorder Society* **27**, 1104-1110, doi:10.1002/mds.25035 (2012).

263 Hill-Burns, E. M., Factor, S. A., Zabetian, C. P., Thomson, G. & Payami, H. Evidence for more than one Parkinson's disease-associated variant within the HLA region. *PloS one* **6**, e27109, doi:10.1371/journal.pone.0027109 (2011).

264 Wissemann, W. T. *et al.* Association of Parkinson's disease with structural and regulatory variants in the HLA region. *AJHG* **93**, 984-993 (2013).

265 Satake, W. *et al.* Genome-wide association study identifies common variants at four loci as genetic risk factors for Parkinson's disease. *Nature genetics* **41**, 1303-1307, doi:10.1038/ng.485 (2009).

266 International Parkinson Disease Genomics, C. *et al.* Imputation of sequence variants for identification of genetic risks for Parkinson's disease: a meta-analysis of genome-wide association studies. *Lancet* **377**, 641-649, doi:10.1016/S0140-6736(10)62345-8 (2011).

267 Sun, C. *et al.* HLA-DRB1 alleles are associated with the susceptibility to sporadic Parkinson's disease in Chinese Han population. *PloS one* **7**, e48594, doi:10.1371/journal.pone.0048594 (2012).

268 Latourelle, J. C., Dumitriu, A., Hadzi, T. C., Beach, T. G. & Myers, R. H. Evaluation of Parkinson disease risk variants as expression-QTLs. *PloS one* **7**, e46199, doi:10.1371/journal.pone.0046199 (2012).

269 Nalls, M. A. *et al.* Large-scale meta-analysis of genome-wide association data identifies six new risk loci for Parkinson's disease. *Nature genetics*, doi:10.1038/ng.3043 (2014).

270 Zhao, Y. *et al.* Association of HLA locus variant in Parkinson's disease. *Clinical genetics* **84**, 501-504, doi:10.1111/cge.12024 (2013).

271 Puschmann, A. *et al.* Human leukocyte antigen variation and Parkinson's disease. *Parkinsonism & related disorders* **17**, 376-378, doi:10.1016/j.parkreldis.2011.03.008 (2011).

272 Hill-Burns, E. M. *et al.* Identification of a novel Parkinson's disease locus via stratified genome-wide association study. *BMC genomics* **15**, 118, doi:10.1186/1471-2164-15-118 (2014).

273 Hughes, A. J., Daniel, S. E., Kilford, L. & Lees, A. J. Accuracy of clinical diagnosis of idiopathic Parkinson's disease: a clinico-pathological study of 100 cases. *Journal of neurology, neurosurgery, and psychiatry* **55**, 181-184 (1992).

274 Jacob, E. L., Gatto, N. M., Thompson, A., Bordelon, Y. & Ritz, B. Occurrence of depression and anxiety prior to Parkinson's disease. *Parkinsonism & related disorders* **16**, 576-581, doi:10.1016/j.parkreldis.2010.06.014 (2010).

275 Wang, A. *et al.* Parkinson's disease risk from ambient exposure to pesticides. *European journal of epidemiology* **26**, 547-555, doi:10.1007/s10654-011-9574-5 (2011).

276 Cockburn, M. *et al.* Prostate cancer and ambient pesticide exposure in agriculturally intensive areas in California. *American journal of epidemiology* **173**, 1280-1288, doi:10.1093/aje/kwr003 (2011).

277 Corsini, E., Sokooti, M., Galli, C. L., Moretto, A. & Colosio, C. Pesticide induced immunotoxicity in humans: a comprehensive review of the existing evidence. *Toxicology* **307**, 123-135, doi:10.1016/j.tox.2012.10.009 (2013).
278 Morrison, G. QUANTO 1.1: A computer program for power and sample size calculations for genetic-epidemiology studies. (2006).
279 Chen, H. *et al.* Nonsteroidal anti-inflammatory drugs and the risk of Parkinson disease. *Archives of neurology* **60**, 1059-1064, doi:10.1001/archneur.60.8.1059 (2003).
280 Hernan, M. A., Takkouche, B., Caamano-Isorna, F. & Gestal-Otero, J. J. A meta-analysis of coffee drinking, cigarette smoking, and the risk of Parkinson's disease. *Annals of neurology* **52**, 276-284, doi:10.1002/ana.10277 (2002).
281 Boss, J. M. Regulation of transcription of MHC class II genes. *Current opinion in immunology* **9**, 107-113 (1997).
282 Collins, T. *et al.* Immune interferon activates multiple class II major histocompatibility complex genes and the associated invariant chain gene in human endothelial cells and dermal fibroblasts. *Proceedings of the National Academy of Sciences of the United States of America* **81**, 4917-4921 (1984).
283 Choi, N. M., Majumder, P. & Boss, J. M. Regulation of major histocompatibility complex class II genes. *Current opinion in immunology* **23**, 81-87, doi:10.1016/j.coi.2010.09.007 (2011).
284 Sant, A. J., Chaves, F. A., Leddon, S. A. & Tung, J. The Control of the Specificity of CD4 T Cell Responses: Thresholds, Breakpoints, and Ceilings. *Frontiers in immunology* **4**, 340, doi:10.3389/fimmu.2013.00340 (2013).
285 Tao, X., Constant, S., Jorritsma, P. & Bottomly, K. Strength of TCR signal determines the costimulatory requirements for Th1 and Th2 CD4+ T cell differentiation. *Journal of immunology* **159**, 5956-5963 (1997).
286 Taneja, V. & David, C. S. Role of HLA class II genes in susceptibility/resistance to inflammatory arthritis: studies with humanized mice. *Immunological reviews* **233**, 62-78, doi:10.1111/j.0105-2896.2009.00858.x (2010).
287 Costa, C. *et al.* Cytokine patterns in greenhouse workers occupationally exposed to alpha-cypermethrin: an observational study. *Environmental toxicology and pharmacology* **36**, 796-800, doi:10.1016/j.etap.2013.07.004 (2013).
288 Righi, D. A., Xavier, F. G. & Palermo-Neto, J. Effects of type II pyrethroid cyhalothrin on rat innate immunity: a flow cytometric study. *International immunopharmacology* **9**, 148-152, doi:10.1016/j.intimp.2008.10.009 (2009).
289 Bloomquist, J. R., Barlow, R. L., Gillette, J. S., Li, W. & Kirby, M. L. Selective effects of insecticides on nigrostriatal dopaminergic nerve pathways. *Neurotoxicology* **23**, 537-544 (2002).
290 Cremer, J. E., Cunningham, V. J., Ray, D. E. & Sarna, G. S. Regional changes in brain glucose utilization in rats given a pyrethroid insecticide. *Brain research* **194**, 278-282 (1980).
291 Doherty, J. D., Morii, N., Hiromori, T. & Ohnishi, J. Pyrethroids and the striatal dopaminergic system in vivo. *Comparative biochemistry and physiology. C, Comparative pharmacology and toxicology* **91**, 371-375 (1988).
292 Esa, A. H., Warr, G. A. & Newcombe, D. S. Immunotoxicity of organophosphorus compounds. Modulation of cell-mediated immune responses

by inhibition of monocyte accessory functions. *Clinical immunology and immunopathology* **49**, 41-52 (1988).

Appendix I: Common Genetic Variant Association with Altered HLA Expression, Synergy with Pyrethroid Exposure, and Risk for Parkinson's Disease: An Observational and Case-Control Study

Previously published work[84].

Authors: G. T. Kannarkat, D. A. Cook, J-K. Lee, J. Chang, J. Chung, E. Sandy, K. C. Paul, B. Ritz, J. Bronstein, S. A. Factor, J. M. Boss, and M. G. Tansey

AI.1 Introduction

The etiology of Parkinson's disease (PD) remains largely unknown with less than 10% of cases attributable to an identifiable causative genetic mutation[250]. The clinical diagnosis of PD by its hallmark motor symptoms may be preceded by various non-motor symptoms, including depression, anosmia, constipation, and REM-sleep behavior abnormalities some of which have been postulated to be fueled by inflammatory processes[251,252].

Genetic polymorphisms in genes encoding glucocerebrosidase, α-synuclein, tau, and others have been reported to modify PD risk[250]. Environmental exposures, such as pesticide exposure and head trauma are associated with increased risk for developing PD[253,254]. Like other age-related diseases, current hypotheses suggest that genetic susceptibility must synergize with lifetime environmental exposures to initiate the development of PD pathology[255,256]. The major histocompatibility complex class II (MHC-II) that is responsible for antigen presentation to the adaptive immune system may be particularly important in linking genetic background to environmental exposures[231]. Inflammation has been implicated as a key driver of PD pathogenesis[99]. Post-mortem

examination of PD brains has revealed microglial activation and lymphocyte infiltration in areas of degeneration[103,230]. Increased expression of inflammatory cytokines, altered composition of peripheral immune cells, and the protective effects of chronic ibuprofen consumption further implicate inflammation in PD pathogenesis[230,257,258].

The MHC-II locus contains the most highly polymorphic genes in the human population and mediates antigen presentation to CD4+ T cells and induction of adaptive immunity[231,259]. MHC-II molecules present antigenic peptides on the surface of antigen-presenting cells (APCs), such as B cells, monocytes, macrophages, dendritic cells, and microglia[231,259]. The MHC-II locus encodes three different α/β heterodimeric isotypes (HLA-DR, -DQ, and -DP)[231]. Each isotype has the potential to present distinct antigenic subsets to CD4+ T cells and induce their differentiation in a specified manner[231]. Differentiated CD4+ T cells (Th1, Th2, Th17, etc.) promote specific inflammatory effector responses or as regulatory T cells (Tregs), suppress inflammation[259]. Given its key role in adaptive immunity, the MHC-II locus is an ideal candidate for linking the environment and genetic susceptibility to PD pathogenesis through inflammation.

Supporting a disease-promoting role for antigen presentation, multiple studies have identified associations between single nucleotide polymorphisms (SNPs) in the MHC-II region and risk for late-onset PD[260-269]. In several genome-wide association studies (GWAS), the *rs3192882* SNP has been associated with altered risk for PD[260,261,270,271]; yet ethnic background appears to influence the allele associated with increased risk. In the largest GWAS to look at this SNP, homozygous carriers of the high-risk *G* allele (21% of PD patients and 16% of CTRLs) were found to have a 1.7 fold increased relative risk of developing PD in people of European ancestry[260]. Additionally,

the *G* allele carried by 46% of PD patients and 40% of CTRLs was associated with increased levels of MHC-II as an expression-quantitative trait locus (eQTL) in subjects of European ancestry[264] and more strongly associated with risk for idiopathic PD rather than familial PD[272]. As an eQTL, this SNP could be associated with genetic or epigenetic regulatory elements that modify the expression of the MHC-II locus. ***These data led us to hypothesize that the rs3129882 GG genotype is associated with increased surface and mRNA expression and greater inducibility of the MHC-II locus in peripheral immune cells relative to the AA genotype.***

Given that the *rs3129882* SNP is located in the first intron of the monomorphic *HLA-DRA* gene and has not been associated with particular MHC-II haplotypes[264], it was somewhat surprising that a common genetic variant in an immune locus could influence the risk for a complex neurologic disorder. Clearly, the genetic association between the MHC-II locus and risk for PD is complex and may depend on a variety of factors such as ethnic background, environmental exposures, etc. As such, ***we hypothesized that this SNP would synergize with pesticide exposure, a known PD-relevant risk factor, to increase risk for PD and this risk might be further modifiable by ethnicity and race.*** Given the heterogeneity of findings in various GWAS for MHC-II and risk for PD, the *rs3129882* SNP warranted further exploration as a possible genetic marker in certain populations associated with complex genetic and/or epigenetic mechanisms that modulate risk for PD by affecting antigen presentation.

AI.2 Methods

AI.2a MHC-II Expression Cohort Subject Recruitment

PD patients and age-matched healthy CTRL subjects were recruited through the Clinical Research in Neurology (CRIN) IRB-approved research protocol at the Emory Movement Disorders Clinic and community outreach events sponsored by the American Parkinson's Disease Association, Wilkins Parkinson's Foundation, and Emory Udall Center of Excellence for Parkinson's Reasearch. Participants were excluded if they were younger than 50 years old, were older than 85 years old, or had neurologic, chronic infectious, or autoimmune comorbidities, and/or known familial PD mutations. For subjects not originally in the Emory cohort of the Hamza et al., 2010 study in which participants' first HLA-DRA intron was sequenced, the *rs3129882* Taqman SNP Genotyping Assay (Life Technologies) was used to genotype newly recruited subjects. Subjects homozygous at the *rs3129882* locus were asked to provide a blood sample (~50 mL). At the time of recruitment, a questionnaire was used to assess disease and inflammation/immune-relevant environmental exposures and comorbidities. Caffeine, NSAID, and nicotine intake was calculated as mg-years, dose-years, and mg-years, respectively. Levodopa equivalence dose was calculated based on parameters defined by the Parkinson's Disease Society of the United Kingdom.

AI.2b Peripheral Blood Mononuclear Cell (PBMC) Isolation, Sorting, and Stimulation

PBMCs were isolated from whole blood using Ficoll-Paque (GE Healthcare) density centrifugation. The upper plasma layer was frozen immediately at -80°C. B cells and monocytes were isolated by positive selection from total PBMCs using anti-CD19 and CD14 paramagnetic beads, respectively (Miltenyi Biotec). Remaining cell fraction was analyzed by flow cytometry for quality control of sorting. For stimulation,

monocytes were plated overnight with or without IFN-γ (PeproTech) in a 6-well plate at $5x10^5$ cells per well for flow cytometry or at $2x10^6$ cells per well for RNA isolation.

AI.2c RNA Isolation, cDNA synthesis, and RT-PCR

Cells were washed once in ice-cold phosphate-buffered saline and then lysed in 350 µL RLT buffer (Qiagen) supplemented with 1% β-mercaptoethanol (Sigma-Aldrich). Cell lysate was centrifuged through a Qiashredder (Qiagen) and then immediately frozen at -80°C. Later, RNA was fully isolated using RNAeasy Isolation Kit (Qiagen) and stored at -80°C. For cDNA synthesis, 0.5-2 µg of total mRNA was used per reaction in reverse transcription reactions using Superscript II (Life Technologies Corp) with oligo dT and random hexamer primers (Life Technologies Corp). The amount of SYBR-incorporated amplicons were measured for all real-time quantitative Bio-Rad iCycler instruments (Bio-Rad Laboratories) with an iQ optical module were used to measure the amount of SYBR incorporated amplicons for all real-time quantitative PCR reactions. DNA oligonucleotides (Integrated DNA Technologies) used for primers listed in **Table S4** were diluted to a final concentration of 100 nM for PCR reactions. All primers were tested by agarose gel electrophoresis to ensure that they formed single amplicon products of the correct size and optimized for Tm by temperature gradient real-time PCR followed by a melt curve analysis.

AI.2d Flow Cytometry Analysis

To stain for flow cytometry, $5x10^5$ cells per well were incubated in 1x FACS buffer (1% bovine serum albumin, 0.1% sodium azide, 1 mM EDTA) for 20 minutes at

4°C with anti-human HLA-DR:allophycocyanin/APC (1:20, BD Biosciences 559866), anti-human HLA-DQ FITC (1:20, BD Biosciences 347453), anti-human CD14:phycoerythrin/PE (1:100, Biolegend #301806) and anti-human CD19:peridinin chlorophyll/PerCP (1:100, Biolegend #302228). Cells were fixed with 1% paraformaldehyde (Electron Microscopy Services) for 30 minutes at 4°C. Cells were stored in 1x FACS Buffer at 4°C until run on FACS Calibur within 1 week of staining. Spherobeads (BD Biosciences) and OneComp Beads (ebiosciences) were used to set voltages and compensation settings between runs. Analysis of flow cytometry data was performed on FlowJo Software v10.0.6.

AI.2.e Mesoscale Discovery Multiplex ELISA

Plasma was obtained from the upper layer of Ficoll-Paque separation and stored at -80°C until sample analysis was performed. Plasma analyte levels were measured in duplicate using the Human Pro-inflammmatory Cytokine 7-plex, Human Chemokine V-PLEX, and Human CRP plates (Meso Scale Discovery). For measurement of CRP, samples were diluted 1:200. For all other assays, samples were measured undiluted.

AI.2.f Genevar Analysis

Genevar 3.3.0 software (Wellcome Trust Sanger Institute) was used to interrogate the HapMap3 cis-eQTL database. Association of levels of cis-eQTLs within 500 kilobasepairs of the *rs3129882* SNP with SNP genotype for all the ethnic groups included in the database was reported as Spearman's rank correlation (rho) with p-value.

AI.2g Pesticide Exposure Cohort and Epidemiological Methods

The PEG case-control study recruited incident PD cases and controls from three highly agricultural counties in Central California, Kern, Fresno, and Tulare, between January 2001 and December 2013. Population-based controls were recruited from the same tri-county study area and in the same age range as the cases using residential tax assessor's records. All subjects were required to have lived in California for at least 5 years and PD patients were examined at least once by our movement disorder specialists, multiple times, and met published criteria for idiopathic PD[273]. We described the details of case definitions[274] and subject recruitment[275] elsewhere. All procedures were approved by the University of California at Los Angeles (UCLA) Human Subjects Committee and informed consent was obtained from all participants**.**

In telephone interviews with patients and controls, we obtained detailed information on demographic characteristics, risk factors, and lifetime occupational and residential histories. We estimated ambient pesticide exposures resulting primarily from commercial applications to agricultural crops using a geographic information system (GIS) based computer model that links geocoded lifetime residential and occupations addresses of each participant to information on all commercial pesticide applications (date, location, and amount applied) from California State mandated pesticide use reports (CA-PUR) and land use data as published previously[276]. For each pesticide, we summed the pounds applied per year per acre within a 500-m radius buffer of an address since 1974 (year of CA-PUR mandate) and calculated study period average exposures for each subject and pesticide by summing the year-specific average exposures from 1974 to 10 years prior to the subject's index year (date of diagnosis for patients and interview for

controls), and divided the sum by the number of years in the relevant time period. We substituted years missing a geocoded location with the average value of all recorded years for each pesticide and person. We then dichotomized exposures based on the pesticide-specific median level in exposed controls (at or above). Participants could have received exposure at either residential or workplace addresses, or both.

The pesticide classes we examined were all previously identified as immunomodulatory[277]. Aside from paraquat, each of the pesticides fell into three different chemical classes: organophosphates, dithiocarbamates, and pyrethroids. After assessing exposure to individual pesticides, we counted the total number of pesticides in each group that each participant was exposed to at each location (residence/workplace address), and classified each participant as highly exposed (at or above the median number of pesticides in exposed controls) or receiving low/no exposure (none or below the median number of pesticides) based on the distribution for the total number of pesticides in exposed controls, except for the pyrethroids, where 75% of the exposed control population was only exposed to one pyrethroid pesticide, and we thus used the categories 'no' exposure versus exposure to one or more pyrethroid.

We used student's two-tailed t-test or a chi-square test to investigate differences in demographic factors between patients and controls. We assessed Hardy-Weinberg equilibrium for HLA *rs3129882* in control participants using a chi-square test and then evaluated association between the SNP and PD using logistic regression to calculate odds ratios (OR) and 95% confidence intervals (CI), assuming a recessive and additive genetic model as done in prior reports[260,271], and adjusted for potential confounders including age (continuous, at diagnosis for patients and interview for controls), sex, ever/never smoking

status (having smoked at least 1 cigarette per week for at least a year). To assess gene-environment interactions between HLA *rs3129882* and pesticide groups, we introduced a multiplicative interaction term into a logistic model assuming an additive genetic model and comparing only the *AA* and *GG* genotypes. Thus, we performed targeted analyses for specific chemicals (three different chemical classes and paraquat) selected *a priori* based on literature that suggest possible immune-modulatory effects of pesticides implicated in PD pathogenesis and for only one SNP. We used Quanto version 1.2.4[278] for power calculations and SAS 9.3 (SAS Institute Inc., Cary, NC) for all other analysis. In order to determine the *rs3129882* genotype of the PEG cohort, samples were coded to blind the researchers and the *rs3129882* Taqman SNP Genotyping Assay (Life Technologies) was used for genotyping.

AI.2h Statistical Analyses

A one-tailed Students' t-test was used to make comparisons between the high risk and low risk genotype groups in the immunophenotyping studies at Emory University. One-way and two-way analysis of variance followed by Holm-Sidak post-hoc tests were used when to compare the baseline characteristics of the study population and inducibility of the response to IFN-γ between the high risk and low risk, respectively, as indicated in figure legends. The Pearson coefficient was used to assess the correlation between two variables. Graphpad (Prism) and R (GNU project) software was used to perform statistical analyses. See Pesticide Exposure Cohort and Epidemiological Methods section above for detailed description of statistical methods used to interrogate the pesticide exposure cohort.

AI.2i Study approval

Written informed consent was received from participants prior to inclusion in the study. All participants provided written informed consent prior to inclusion in the research studies, and all procedures were approved *a priori* by the Institutional Review Board of Emory University in Atlanta, Georgia or of UCLA in Los Angeles, California.

AI.3 Results

AI.3a MHC-II Expression Study Population

To assess the effect of rs3129882 on MHC-II expression, 81 homozygous non-PD control (CTRL) and PD subjects were recruited into four groups: CTRL AA (n=25), CTRL GG (n=12), PD AA (n=15), and PD GG (n=29). This strategy allowed us to examine the effect of SNP genotype, as well as disease status, on MHC-II expression. The groups of this study population were balanced with respect to factors that modify PD risk[228,279,280], including age, smoking, non-steroidal anti-inflammatory drug (NSAID) use, caffeine intake, mean Unified Parkinson's Disease Rating Scale (UPDRS) motor score, levodopa equivalence dose, and duration of disease for the PD groups (**Table S1**).

AI.3b The rs3129882 GG genotype is associated with increased surface MHC-II expression

Given that the rs3129882 G SNP was associated with increased levels of MHC-II eQTL in subjects of European ancestry[264], we tested the hypothesis that in people of European ancestry, homozygosity for the G SNP would be associated with higher MHC-

II expression compared to homozygosity for the A SNP. Flow cytometry was used to measure the frequency of cells expressing both HLA-DR and –DQ (DR/DQ double-positive cells) on the cell surface of APCs. We focused our analyses on B cells and monocytes because they are the major APCs in the peripheral blood. Nearly all peripheral B cells and monocytes were HLA-DR positive (**Fig S1**). In our cohort, 80% of peripheral blood B cells were HLA-DR/DQ double-positive in all four groups of subjects (**Fig 1A**). Similarly, nearly all monocytes were HLA-DR positive but only 20-30% of peripheral blood monocytes were HLA-DR/DQ double-positive in all four groups of subjects (**Fig 1A**). Using flow cytometry, the average level of HLA-DR or HLA-DQ surface expression was also measured, reported as median fluorescence intensity (MFI). In both B cells and monocytes from the CTRL GG group, there was a significant two-fold increase in the MFI of HLA-DR compared to the CTRL AA group (**Fig 1B**). The MFI of HLA-DQ on B cells from GG individuals was also significantly increased in both CTRL and PD patients by 1.5- to 2-fold (**Fig 1C**). In this cohort, having the GG genotype was associated with increased MFI of HLA-DR on both B cells and monocytes and of HLA-DQ on B cells.

AI.3c The rs3129882 GG genotype is associated with increased IFN-γ inducibility of HLA-DQ expression

Given that MHC-II expression increases upon cellular activation[231,281], we also measured disease- and genotype-specific effects on induction of this locus using IFN-γ, a potent stimulator of MHC-II gene expression[281,282]. In response to IFN-γ, the frequency of monocytes that became HLA-DR/DQ double-positive cells was significantly higher in

the PD GG group relative to the PD AA group (**Fig 1D**). The level of induction of HLA-DR surface expression on monocytes was the same in all four groups of subjects (**Fig 1E**). In contrast, the HLA-DQ surface expression was significantly increased on IFN-γ stimulated monocytes from CTRL GG individuals compared to CTRL AA individuals (**Fig 1F**). In PD GG patients, HLA-DQ surface expression was significantly increased relative to PD AA patients at the highest dose of IFN-γ (**Fig 1F inset**). In summary, the rs3129882 GG genotype was associated with increased HLA-DQ expression on monocytes in response to IFN-γ.

AI.3d The rs3129882 GG genotype is associated with increased baseline expression and IFN-γ inducibility of MHC-II mRNA

Next, we interrogated transcriptional levels of MHC-II to determine possible mechanisms underlying the association of rs3129882 with altered surface MHC-II expression. To assess the extent to which APCs from AA versus GG individuals expressed differences in mRNA levels of the various MHC-II isotypes, we performed quantitative RT-PCR for the four MHC-II genes in closest proximity to rs3129882: HLA-DRA, HLA-DRB1, HLA-DQA1, and HLA-DQB1 that are common among all MHC-II haplotypes. In B cells from CTRL subjects, the high-risk genotype was significantly associated with increased mRNA levels of HLA-DRA, -DRB1, and -DQB1 (**Fig 2A**). In monocytes, the GG genotype was associated with increased HLA-DQB1 mRNA expression in both PD patients and CTRLs and with increased HLA-DRB1 mRNA expression in PD subjects (**Fig 2B**). In addition to these statistically significant 10- to 20-fold increases in mRNA expression, there were clear upward trends in expression of

HLA-DRB1 and -DQB1 mRNA in B cells from PD GG patients and HLA-DRB1 mRNA expression in monocytes from CTRL GG subjects.

Following IFN-γ stimulation, monocytes from PD GG patients displayed a >200-fold increase in mRNA levels of all measured MHC-II genes relative to PD AA patients and CTRLs of either genotype (**Fig 2C**). With the exception of significantly decreased inducibility of HLA-DQA mRNA in the CTRL GG group, the inducibility of the rest of the MHC-II genes was the same in PD AA patients and CTRLs of either genotype. In summary, the GG genotype was associated with significantly increased HLA-DRA, -DRB1, and -DQB1 mRNA expression in resting B cells independent of disease. In resting monocytes, the high-risk genotype was also associated with increased HLA-DRB1 and HLA-DQB1 mRNA expression independent of disease. Finally, monocytes treated with IFN-γ from the PD GG group displayed higher levels of all MHC-II mRNA.

AI.3e The rs3129882 high-risk genotype is associated with increased plasma CCL-3 (MIP-1α) levels in PD patients but not with altered frequencies of B cells and monocytes in the peripheral blood

In conjunction with cell-specific markers, differences in peripheral blood mononuclear cell (PBMC) composition and blood levels of cytokines/chemokines can indicate an active inflammatory process. Flow cytometry analysis of Ficoll-Paque separated PBMCs demonstrated no change in B cell or monocyte frequency between any of the study groups (**Fig S2A**). The levels of 17 selected immunomodulatory cytokines and chemokines were measured by multiplexed chemiluminescent immunoassays (**Fig S2B**). Individuals in the PD GG group displayed increased circulating plasma levels of

CCL-3 (also known as MIP-1α) greater than two-fold over the PD AA group. The levels of the other 16 cytokines and chemokines were not significantly different between the four groups (**Fig S2B**).

AI.3f Pyrethroid exposure and the high-risk rs3129882 genotype increases odds for PD

To determine whether there are interactions between pesticide exposure and rs3129882 in PD, 465 incident PD patients (diagnosed within 3 years of recruitment) and 497 population controls of European ancestry from the Parkinson's Environment and Gene (PEG) case-control study were examined. Basic demographic characteristics for the PEG study population can be found in Table S2. As expected, patients were more likely to be male and have a family history of PD, and less likely to have ever been smokers[81,251,280]. Our control population was in Hardy-Weinberg equilibrium for HLA rs3129882 (p= 0.18). Genotype alone did not significantly influence PD risk, assuming previously reported genetic models (additive model: OR=1.03, 95% CI=0.86, 1.24 for those with one risk allele (AG) and OR=1.07, 95% CI=0.74, 1.55 for those with two risk alleles (GG); recessive model: OR=0.83, 95% CI=0.59, 1.16; **Table 1**)[260,271]. We did not detect interactions with organophosphates, dithiocarbamates, or paraquat and rs3129882.

Investigating pyrethroid pesticides, in logistic regression models we estimated a positive interaction on a multiplicative scale when comparing groups homozygous at the SNP (AA versus GG; interaction p-value=0.02; **Table 2**), and when we used an additive genetic model to include heterozygous individuals (interaction p-value=0.007; **Table 2**). In both models, neither the genotype alone nor pyrethroid exposure alone significantly influenced PD risk, but in those jointly exposed to pyrethroids and having a GG genotype

we estimated significant increases in PD risk. For example, when comparing AA versus GG in those unexposed, we see a slight non-significant decrease in PD risk (OR=0.73, 95% CI=0.47, 1.14), and no effect when comparing pyrethroid exposure in those with the AA genotype (OR=1.04, 95% CI=0.65, 1.67), yet comparing those homozygous for the risk allele (GG) and exposed to pyrethroids to those with the AA genotype and unexposed, we see an increased risk of PD (OR=2.48, 95% CI=1.24, 4.97; **Table 2**).

Next, we assessed whether there were differences in disease characteristics of the AA vs GG individuals at baseline and during two follow up exams in a subset of the PEG population followed over time; mean years between baseline and exam 1 was 3.5 years (SEM=0.1) and exam 2 was 5.6 years (SEM=0.2). We did not see any significant differences in measures of disease-related clinical progression between AA and GG individuals at baseline or either follow-up time point (**Table S3**).

AI.3g Genetic variation associated with ethnicity can reverse allelic rs3129882 association of MHC-II expression changes

In order to contextualize the discrepancies among various GWAS with associations of the rs3129882 with risk for PD, we used the GeneVar software tool to interrogate the HapMap3 cis-eQTL database. The HapMap3 database is unique in that it consists of 726 lymphoblastoid cell lines developed from individuals of 8 different ethnic groups. We tested the hypothesis that association of SNP genotype with cis-eQTL level in the MHC-II locus would be affected by ethnicity. Indeed, we observed that in the individuals of the HapMap3 database, the allele that was associated with increased eQTL level depended on ethnicity (**Table 3**). For example, the G allele was associated with

increased levels of HLA-DRB1 eQTL in Utah Caucasians (rho=0.199, p=0.038) but with decreased levels in Han Chinese (rho=-0.281, p=0.0124) and Nigerian Yoruba (rho=-0.317, p=8.0E-4). Furthermore, HLA-DRB5 eQTL level was positively associated with the G allele in Utah Caucasians (rho=0.516, p=9.3E-9) but negatively associated with the G allele in most of the other ethnic groups.

AI.4 Discussion

The MHC-II locus and particularly the *rs3129882* SNP, has been implicated in modulating risk for PD[260,261,266]; and herein, we demonstrate that the *G* allele of this SNP, acting together with environmental pyrethroids exposure, increases the odds of developing PD and is associated with altered MHC-II expression in peripheral APCs. The association of the high risk genotype with altered MHC-II expression was revealed by: 1) increased surface protein expression of HLA-DR in monocytes; 2) greater inducibility of HLA-DQ surface protein expression in monocytes in response to IFN-γ; 3) increased mRNA expression of *HLA-DRA, -DRB1,* and *-DQB1* genes; and 4) greater inducibility of mRNA expression in PD patients' monocytes after IFN-γ stimulation. Notably, within our MHC-II expression study cohort more PD patients tended to be male and controls, who were often caregivers, tended to be women. Despite this unequal sex distribution, stratification of the data by sex did not account for statistical differences in MHC-II expression (data not shown). Taken together, the data indicate that in our cohort, *GG* homozygosity at the *rs3129882* SNP is associated with increased baseline and inducible MHC-II expression in APCs. This immune hyper-responsiveness may in turn be one reason why this SNP has been associated with altering risk for late-onset PD.

Specifically, the findings revealed that monocytes from individuals in our cohort with the *G* allele have more antigen-presenting capacity under resting conditions; and that within the context of PD, cytokine challenge increases mRNA expression of MHC-II genes approximately 200-fold. Surprisingly, plasma levels of cytokines were unchanged among all four groups except for increased MIP-1α in the PD GG group relative to the PD AA group, suggesting that immune risk for PD may be better predicted by cell-associated immune molecules rather than measurement of global fluid biomarkers. The pathologic significance of an isolated elevation in a single plasma chemokine is unclear. These novel findings directly implicate regulation of MHC-II expression and antigen presentation as important mechanisms underlying the reported association between late-onset PD and the MHC-II locus. This evidence supports a role for immunological processes and the synergy between these processes and environmental exposures such as pyrethroids in determining an individual's susceptibility to PD.

On the basis of the studies reported here, we speculate that the *rs3129882* SNP is a marker in some populations for a genetic and/or epigenetic mechanism(s) that control the expression of the MHC-II locus. A common mechanism in the MHC-II locus that promotes risk for PD may exist in many different human populations but may be marked by different disease-associated SNPs. Evidence for this is indicated by the divergent associations reported in GWAS in Han Chinese cohorts where the *A* allele is associated with increased PD risk while in European cohorts, the *G* allele is associated with increased risk[260,261,270,271]. The ethnicity-dependent directional changes in the HapMap3 database cis-eQTL associations in **Table 3** also point to the importance of taking into account ethnic differences when studying genetic variation at the MHC-II locus. Thus,

the association of various MHC-II SNPs with PD likely depends heavily on ethnic make-up and exposome.

The expression of genes at this locus is regulated by a complex interplay between transcription factors, chromatin architecture, DNA methylation sites, and histone remodeling [283]. In unstimulated cells from *GG* individuals in our cohort, mRNA expression of *HLA-DRA, DRB1,* and *DQB1* is increased, suggesting a mechanism that allows for basal increases in transcription of these genes (**Fig 2A, 2B**). The increase in the levels of β-subunit mRNAs is particularly interesting because the α-subunit mRNAs are typically much more abundant, making the level of β-subunit mRNAs an important limiting factor in production of mature MHC-II molecules. However, only in PD patients was the *rs3129882 G* allele associated with increased IFN-γ inducibility of mRNA expression of all the MHC-II genes. In CTRLs, the IFN-γ inducibility of *HLA-DQA* and *HLA-DRA* mRNA expression was significantly decreased (**Fig 2C**). This phenomenon suggests that in controls, a regulatory mechanism may exist to limit the level of mRNA expression of MHC-II, i.e. a "ceiling effect" upon APC activation. If this turns out to be the case, our data suggest this regulatory mechanism may be absent (or perhaps is lost as a result of the disease process itself) in individuals with a SNP in the MHC-II locus that hence increases risk of PD. Irrespective of the mechanism, enhanced transcription of MHC-II genes would be expected to increase surface expression of these molecules, resulting in functional consequences for engagement of the adaptive immune system.

Engagement of the adaptive immune system through MHC-II peptide presentation would allow for a specific, chronic inflammatory response mediated by CD4+ T cells[259]. Shifts in the overall levels of MHC-II and/or the relative levels of MHC-II isotypes could

impact normal immunologic processes in two main ways. First, antigenic peptide epitopes that promote pathogenesis leading to PD may be more likely to be presented to the adaptive immune system and dominate immune responses[284]. This could occur through skewed expression of HLA-DQ proteins. Second, the presentation of certain peptides on different MHC-II isotypes could alter the differentiation of CD4+ T cells into various subsets (i.e., Th1, Th2, Th17, or Tregs)[285]. Evidence for such phenomena can be demonstrated in human autoimmune disease and humanized rodent models of autoimmunity[286]. In this manner, antigen presentation via MHC-II on the surface of APCs to CD4+ T cells is a mechanism that could link the contribution of both genetic background and environmental exposure to susceptibility for developing PD.

In the context of risk for PD, two people who are exposed to the same insult are likely to respond very differently immunologically given their genetic and epigenetic background. Within the context of our findings, following exposure to an environmental agent such as pyrethroids or an event such as traumatic brain injury, we would predict that an individual with the *AA* genotype in our cohort (**Fig 3A**) might display an immune response that resolves completely in a few weeks. By contrast, an individual from our cohort with the *GG* genotype (**Fig 3B**) might display a heightened immune response that may not resolve quickly but may instead promote chronic neuroinflammation, thereby hastening degeneration of vulnerable neuronal populations. Indeed, an adaptive immune response that is propagated in response to highly specific antigens differentially presented by APCs from people with high-risk versus low-risk MHC-II alleles can explain the selective degeneration of vulnerable neuronal populations as is the case in PD.

In agreement with our understanding of risk for PD, environmental stimuli, such as pyrethroids, are likely to play a prominent role in synergizing with the differential immune responses associated with this SNP given that few HLA haplotype associations have been reported for PD risk and none segregate with this SNP[264]. Pyrethroid exposure has been associated in humans with acute alterations in immunoglobulin levels and T cell frequencies[287] and in animal models with altered APC function[288]. Related to Parkinson's disease, pyrethroids are associated with increased striatal dopamine uptake, increased striatal dopamine metabolism, and altered electroencephalographic activity in the SN in chronically exposed rodent models[289-291]. Other pesticides have been shown to directly impact antigen presentation and although this has not been reported for pyrethroids it is possible their effects on immune cells may explain the synergism with the MHC-II locus to increase risk for PD[292]. The identified combined risk conferred by the *rs3129882 G* allele and pyrethroids may be explained by complex interactions that impact both the nervous system and the immune system to initiate PD pathogenesis through voltage-gated sodium channels that are known targets of this class of pesticides. The follow-up of the PEG patients only cohort suggested no association between the *G* allele and disease severity/progression (**Table S3**). However, longer follow-up time may be necessary to reveal differences in disease progression that are not yet apparent in this cohort. It is important to note that subject recruitment occurred through a state-wide registry with 30 years of exposure data; and PD patients underwent a neurologic examination by movement disorder specialists. Our study is the first population-based analysis to explore and report pyrethroid-gene variant interactions; and thus, it requires replication in an

independent sample. Longitudinal studies of the MHC-II locus and PD would clarify the role of this locus in increasing risk.

The significance of our findings is three-fold. First, we provided direct evidence from human peripheral blood that implicates a mechanism for antigen presentation and the role of adaptive immunity in risk for PD. Functional studies that link GWAS hits to functional cellular changes are the next step in understanding how genetics, environment, and cellular responses synergize to increase risk for complex diseases. Second, our findings suggest that the level and quality of MHC-II expression could prove to be an effective immune marker for the prediction of disease susceptibility in addition to honing our understanding of disease pathogenesis. Third, our data suggest that cellular biomarkers may prove more useful than soluble molecules in plasma and CSF to identify individuals at risk for disease or for patient recruitment into neuroprotective trials testing immunomodulatory drugs.

AI.5 Figures

Target	Forward Primer (5'-3')	Reverse Primer (5'-3')
HLA-DRA	**GAGTTTGATGCTCCAAGCCCTCTCGC**	**CAGAGGCCCCCTGCGTTCTGCTGCA**
HLA-DRB1	**TGCTGAGCTCCCTACTGGCT**	**CGCGTACTCCTCTCGGTTATAG**
HLA-DQA	**CACCTTTTCTCTGGGACTTAAGC**	**TGAGGAATTAGGTAGCCGGGT**
HLA-DQB	**TATGCCTGCCCAGAATTCCC**	**CCATCAAGGCGGACCATGTGT**
18S rRNA	**GTAACCCGTTGAACCCCATT**	**CCATCCAATCGGTAGTAGCG**

Table AI.1. RT-PCR Primers. List of primers used for qRT-PCR to measure mRNA expression of MHC-II genes.

	CTRL AA	CTRL GG	PD AA	PD GG	All	p-value
N	25	12	15	29	81	
Age	65.5 ± 1.8	63.7 ± 1.8	67.4 ± 2.2	68.5 ± 1.5	66.6 ± 0.9	0.38
Sex	19F, 6M	11F, 1M	6F, 9M	9F, 20M	45F, 36M	0.003
Smoking (pack-yrs)	2.9 ± 1.9	7.5 ± 3.2	8.3 ± 4.6	12.2 ± 5.0	7.8 ± 2.1	0.43
Caffeine (mg-yrs)	6856 ± 1822	7959 ± 2068	5913 ± 1385	5907 ± 1341	6515 ± 806	0.49
NSAID use (dose-yrs)	1.95 ± 0.71	3.37 ± 1.3	4.34 ± 1.2	3.72 ± 1.0	3.30 ± 0.52	0.36
Number of Lifetime Head Injuries	0.22 ± 0.15	0.78 ± 0.36	0.47 ± 0.22	0.67 ± 0.26	0.50 ± 0.12	0.49
Age at Diagnosis			58.5 ± 3.0	59.5 ± 1.6	59.2 ± 1.5	0.40
Years with Disease			8.5 ± 2.0	9.0 ± 1.1	8.8 ± 0.95	0.78
Mean UPDRS Score			15.4 ± 2.9	16.8 ± 1.5	16.4 ± 1.4	0.41
Levodopa Equivalence Dose (mg)			222.5 ± 37.2	261.2 ± 45.5	244.4 ± 30.11	0.53

Table AI.2. Characteristics of MHC-II Expression Study Population. Data are expressed as the mean ± SEM for each of our four groups (CTRL AA, CTRL GG, PD AA, PD GG) and the entire study population. The table shows that our four groups are well balanced for the age, the self-reported environmental exposures, and clinician reported disease severity (UPDRS) measures. One-way ANOVA indicates no significance between groups at $p > 0.05$ for age, smoking, caffeine, NSAID use, number of lifetime head injuries, age at diagnosis, years with disease, mean UPDRS score, and

levodopa equivalence dose. Chi-square test indicates significant difference ($p = 0.003$) in proportion of males to females in groups but stratification of data by sex does not explain statistical differences in MHC-II expression (data not shown).

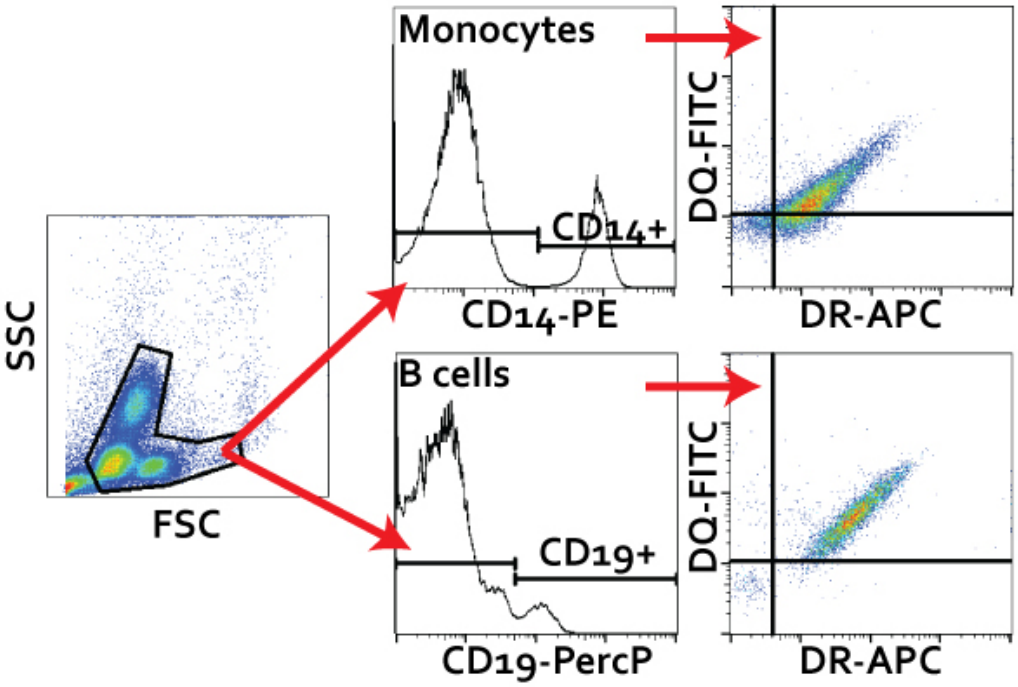

Figure AI.1. Gating Strategy for Flow Cytometry Analysis. Cells were stained for flow cytometry and analyzed on a FACS Calibur after standardization and compensation with Sphero beads, OneComp beads, and Raji and THP-1 cell lines. Gates were placed based on staining with isotype control antibodies. Analysis was performed and plots were generated using FlowJo software.

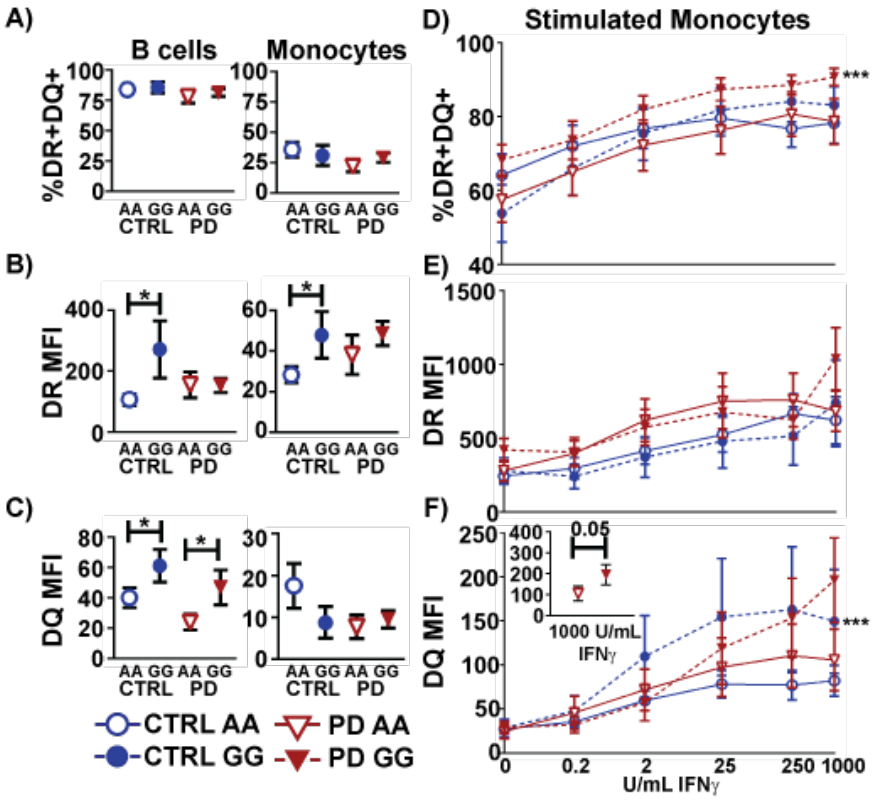

Figure AI.2. The high-risk rs3129882 GG genotype is associated with an increased level of MHC-II expression in B cells and monocytes and with increased inducibility of surface HLA-DQ expression. A) Frequency of HLA-DR/DQ double-positive, B) average level of HLA-DR expression, C) average level of HLA-DQ expression in B cells and monocytes was determined by flow cytometry staining of total PBMCs. One-tailed student's T-test between high risk and low risk allele groups was used to test for significance. * $p < 0.05$. HLA-DR MFI: CTRL AA vs CTRL GG B cells $t(33) = 2.28$ $p < 0.05$; Monocytes $t(34) = 2.14$ $p < 0.05$. HLA-DQ MFI CTRL AA vs CTRL GG B cells $t(28) = 1.76$, $p < 0.05$; PD AA vs PD GG $t(35) = 1.82$, $p < 0.05$. Surface MHC-II expression in paramagnetically, positively-sorted monocytes stimulated with various concentrations of IFN-γ was measured by flow cytometry staining to measure increase in D) frequency of HLA-DR/DQ double-positive cells, E) level of HLA-DR expression, and

F) level of HLA-DQ expression. Two-way ANOVA was performed to test for significance between GG and AA groups. *** $p < 0.001$. 2A) PD GG vs PD AA $F(1,190) = 11.97$ $p < 0.001$. 1F) CTRL GG vs CTRL AA $F(1, 163) = 10.39$ $p < 0.001$. Inset for DQ MFI (1F) panel shows sorted monocytes from PD patients stimulated with 1000 U/mL IFN-γ. One-tailed T-test was performed for significance. $t(31) = 1.52$; $p = 0.05$.

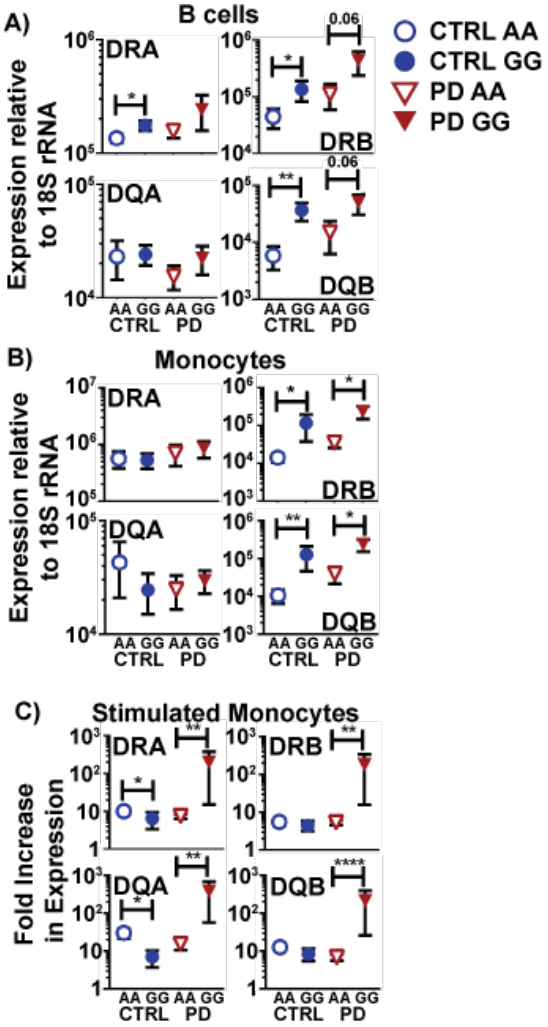

Figure AI.3. The high-risk rs3129882 GG genotype is associated with increased baseline expression and inducibility of MHC-II mRNA. RNA was isolated from

paramagnetically, positively sorted A) B cells and B) monocytes. MHC-II mRNA expression was quantified relative to 18s rRNA with RT-PCR.* $p < 0.05$, ** $p < 0.01$, **** $p < 0.0001$. B cell CTRL GG vs CTRL AA HLA-DRA $t(35) = 2.01$ $p < 0.05$; HLA-DRB1 $t(34) = 2.04$ $p < 0.05$; HLA-DQB1 $t(33) = 3.28$ $p < 0.01$. B cell PD GG vs PD AA HLA-DRB1 $t(25) = 1.59$ $p = 0.06$; HLA-DQB1 $t(33) = 1.64$ $p = 0.06$. Monocytes CTRL GG vs CTRL AA HLA-DRB1 $t(32) = 1.90$ $p < 0.05$; HLA-DQB1 $t(35) = 2.08$ $p < 0.01$; PD GG vs PD AA HLA-DRB1 $t(26) = 2.24$ $p < 0.05$; HLA-DQB1 $t(30) = 2.28$ $p < 0.05$ C) Fold change in MHC-II expression with or without 100 U/mL IFN-γ stimulation in paramagnetically, positively sorted monocytes was measured by RT-PCR after normalization to 18s rRNA levels. One-tailed T-test was performed as indicated. **** $p < 0.0001$ ** $p < 0.01$, * $p < 0.05$. CTRL AA vs GG HLA-DRA $t(33) = 1.77$ $p < 0.05$; HLA-DQA1 $t(13) = 1.80$ $p < 0.05$; PD AA vs PD GG HLA-DRA $t(36) = 1.76$ $p < 0.01$; HLA-DRB1 $t(29) = 1.65$ $p < 0.01$; HLA-DQA1 $t(24) = 1.82$ $p < 0.01$; HLA-DQB1 $t(30) = 2.53$ $p < 0.0001$.

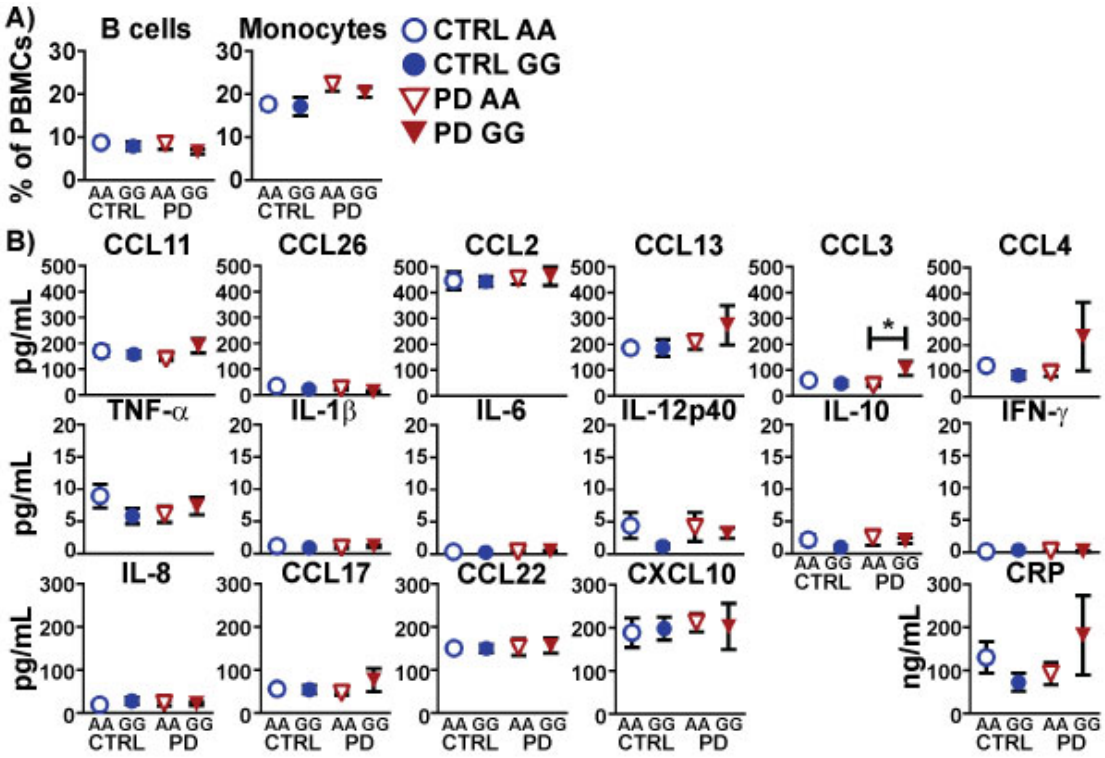

Figure AI.4. The rs3129882 high-risk genotype is associated with increased plasma CCL-3 levels in PD patients with the high-risk rs3129882 GG genotype but not with altered frequencies of B cells and monocytes in the peripheral blood. A) B cell and monocyte frequencies were determined by flow cytometry staining of total PBMCs. B) Mesoscale Discovery (MSD) Multi-Array immunoassay technology was used to measure plasma levels of the indicated cytokines and chemokines. Values are plotted as the mean ± SEM. Two-tailed student's T-test was used to test for significance between high risk versus low risk allele. * $p < 0.05$. CCL-3 PD GG vs PD AA $t(16) = 2.39$, $p < 0.05$.

Characteristic	Patients (n=465)	Controls (n=497)	P-Value[a]
Age[b], mean ± SEM	69.4 ± 0.46	67.4 ± 0.52	0.005
Age at PD onset, mean ± SEM	67.8 ± 0.53		
Male sex, n (%)	289 (0.52)	262 (0.48)	0.003
Family history of PD[c], n (%)	76 (0.16)	47 (0.09)	0.001
Ever cigarette smoker, n (%)	212 (0.46)	271 (0.54)	0.005
Years with Disease, mean ± SEM	2.49 ± 0.10		
UPDRS-III Score[d], mean ± SEM	21.0 ± 0.48		

[a]P-values based on comparison between cases and controls using with chi-square or t-test
[b]Age at PD diagnosis for patients and interview for controls
[c]First degree relative with PD; 3 patients missing PD family history
[d]17 patients missing UPDRS-III score

Table AI.3. General characteristics of PEG study population of European ancestry, n=962 (patients=465, controls=497). Data are expressed as the mean ± SEM for patients versus controls. The table shows that the PD patient group in the PEG study population is slightly older, more likely to have a family history of PD, has more males, and people with a history of cigarette smoking.

Genotype	Cases n (%)	Controls n (%)	Adjusted OR (95% CI)[a]	P-Value
AA	142 (0.31)	175 (0.35)	1.00 (ref)	--
AG	243 (0.52)	227 (0.46)	1.03 (0.86, 1.24)	0.72
GG	80 (0.17)	95 (0.19)	1.07 (0.74, 1.55)	
		AA vs GG:	0.95 (0.65, 1.38)	0.78
		AA/AG vs GG	0.83 (0.59, 1.16)	0.27
[a]Adjusted for age (continuous), sex, and smoking history.				

Table AI.4. HLA-DRA rs3129882 marginal effects in PEG population, n=962 (patients=465, controls=497). An additive model was used to assess the association

between the rs3129882 G allele and Parkinson's disease in the PEG population. Increased odds of developing PD was not associated with genotype alone in this population.

Ambient Pyrethroids[b]	***None***				***1+ pesticide***			
	Cases n (%)	**Controls n (%)**	**Adjusted OR[a] (95% CI)**	**p value**	**Cases n (%)**	**Controls n (%)**	**Adjusted OR[a] (95% CI)**	**p value**
Additive Genetic Model								
AA	95 (0.30)	117 (0.33)	1.00 (ref)		47 (0.32)	58 (0.42)	0.83 (0.53, 1.28)	0.42
AG	172 (0.54)	161 (0.45)	0.91 (0.73, 1.13)	0.38	71 (0.48)	66 (0.48)	1.25 (0.88, 1.78)	0.22
GG	50 (0.16)	81 (0.23)	0.82 (0.53, 1.27)		30 (0.20)	14 (0.10)	1.87 (1.08, 3.35)	0.03
							P=value for interaction:	*0.02*
AA vs GG								
AA	95 (0.66)	117 (0.59)	1.00 (ref)		47 (0.61)	58 (0.81)	1.04 (0.65, 1.67)	0.87
GG	50 (0.34)	81 (0.41)	0.73 (0.47, 1.14)	0.17	30 (0.39)	14 (0.19)	2.48 (1.24, 4.97)	0.01
							P=value for interaction:	*0.007*

[a]Adjusted for age (continuous), sex, and smoking history.

[b]Ambient pesticide exposure to any pyrethroids (at or above the median level seen in exposed controls) at both occupation and residence, from 1974 (year of CA-PUR implementation) to 10 yrs before diagnosis or interview. Pyrethroid group includes fenvalerate, permethrin, phenothrin, resmethrin, flucythrinate, cypermethrin, (S)-cypermethrin, tau-fluvalinate, fenpropathrin, lamda-cyhalothrin, bifenthrin, esfenvalerate, and tralomethrin; Cyfluthrin had no exposure in study population.

Table AI.5. Interaction, main, and joint effect estimates between HLA rs3129882 and pyrethroid exposure in PEG study population of European ancestry, using both an additive genetic model and AA vs GG; n=962 (patients=465, controls=497). Using both an additive genetic model and comparing only the homozygous groups, we assessed

the association between pyrethroid exposure and the risk rs3129882 genotype in the risk for PD. The table indicates the adjusted odds ratio and p-values for the main and joint effects and the p=value for interaction.

	Baseline with follow-up (n=88)		**Follow-up 1 (n=88)**		**Follow-up 2 (n=69)**	
	AA (n=53)	GG (n=35)	AA (n=53)	GG (n=35)	AA (n=41)	GG (n=28)
Age at PD diagnosis	65.3 ± 1.4	69.3 ± 1.6	--	--	--	--
Age at PD onset	63.7 ± 1.8	67.3 ± 2.1	--	--	--	--
PD Duration (years)	2.0 ± 0.2	1.6 ± 0.2	5.8 ± 0.4	5.1 ± 0.4	7.8 ± 0.5	7.2 ± 0.5
Follow-up (years)	--	--	3.8 ± 0.3	3.4 ± 0.3	5.8 ± 0.3	5.5 ± 0.4
Clinical features						
MMSE Score	28.6 ± 0.2	28.5 ± 0.3	28.3 ± 0.3	28.2 ± 0.4	28.0 ± 0.4	27.4 ± 0.6
GDS	3.1 ± 0.5	2.4 ± 0.4	3.7 ± 0.4	3.7 ± 0.6	3.3 ± 0.5	3.4 ± 0.5
UPDRS Score	17.7 ± 1.0	17.0 ± 1.4	24.7 ± 1.4	23.7 ± 1.9	29.8 ± 1.7	27.2 ± 2.3
Resting tremor	1.4 ± 0.2	1.3 ± 0.2	2.1 ± 0.3	2.0 ± 0.4	2.2 ± 0.5	2.0 ± 0.4
Bradykinesia	5.9 ± 3.5	5.5 ± 3.9	7.8 ± 0.6	7.9 ± 0.9	9.9 ± 0.7	9.1 ± 1.0
Rigidity	2.7 ± 0.2	2.5 ± 0.4	3.4 ± 0.3	3.0 ± 0.4	4.9 ± 0.5	4.7 ± 0.7
Postural reflex impairment	2.6 ± 0.2	2.8 ± 0.3	3.7 ± 0.4	3.7 ± 0.4	5.4 ± 0.6	4.9 ± 0.6
*p<0.05, based on genotype group comparisons using a t-test						

Table AI.6. Clinical characteristics of PEG PD patients of European ancestry, across follow-up exams by HLA rs3129882 genotype (AA vs GG). Data for clinical characteristics presented as mean +/- SEM. Follow-up exam 1 was a mean of 3.5 yrs after

baseline (SEM=0.1) and exam 2, 5.6 yrs after baseline (SEM=0.2). In this table, subjects homozygous for the rs3129882 SNP are compared in terms of clinical disease characteristics over time. There is no difference in the clinical characteristics between the groups at any time point.

HLA-DRB1	**rho**	**p-value**	***HLA-DRB5***	**rho**	**p-value**
Utah Caucasians	0.199	0.038	**Utah Caucasians**	0.516	9.30E-09
Han Chinese	-0.281	0.0124	**Han Chinese**	-0.038	0.7396
Gujarati Indians in Houston, TX, USA	-0.017	0.8774	**Gujarati Indians in Houston, TX, USA**	0.242	0.0283
Japanese in Tokyo, Japan	0.038	0.7364	**Japanese in Tokyo, Japan**	-0.131	0.2393
Luhya in Kenya	-0.347	0.0014	**Luhya in Kenya**	-0.315	0.0039
Mexicans in Los Angeles, CA, USA	0.052	0.7333	**Mexicans in Los Angeles, CA, USA**	0.193	0.2029
Masaii in Kenya	-0.338	5.20E-05	**Masaii in Kenya**	-0.037	0.666
Yoruba in Nigeria	-0.317	8.00E-04	**Yoruba in Nigeria**	-0.122	0.2079

Table AI.7. The direction of association of cis-eQTL level with the rs3129882 genotype depends on ethnicity. The level of HLA-DRB1 and HLA-DRB5 cis-eQTLs were significantly associated with rs3129882 genotype and were within 500 kilobasepairs of the rs3129882 SNP in the HapMap3 database. Association was reported as Spearman's rank correlation (rho) with p-value for all the ethnic groups within the database.

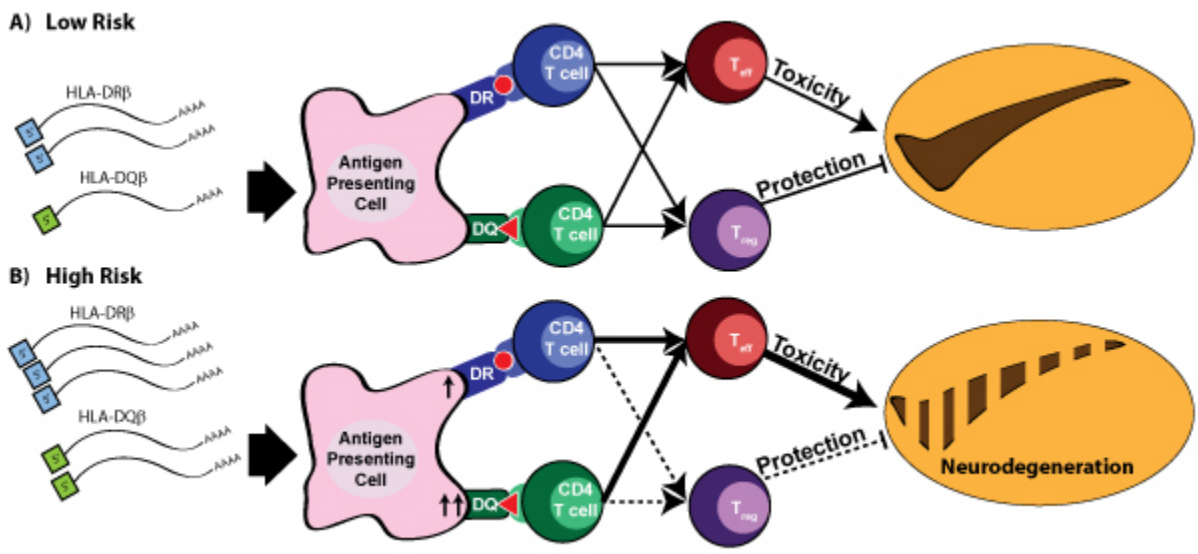

Figure AI.5. Model depicting the association of the rs3129882 SNP with altered MHC-II expression on APCs and the potential for skewing the adaptive immune response and the predicted effects on vulnerable neuronal populations affected in PD. Our data suggest that the rs3129882 SNP is linked to a genetic or epigenetic element that increases mRNA expression of MHC-II and ultimately surface expression of MHC-II. Increased surface expression of MHC-II can influence CD4+ T cell activation and differentiation leading to a heightened proinflammatory state that hastens neuronal dysfunction and death and predisposed individuals to PD. Two individuals exposed to the same environmental stimulus, one with the low risk SNP (A) and the other with the high risk SNP (B), are likely to respond differently immunologically because of underlying genetic and epigenetic mechanism(s) that influence MHC-II expression.

Appendix II: Other Unpublished Data

The following figures represent data generated from ongoing projects in the lab and information requested by committee members during committee meetings.

AII.1 Immunophenotyping of Human G2019S LRRK2 Subjects*

Human subjects with and without PD and with and without the G2019S LRRK2 mutation were recruited and immunophenotyped using methods similar to those discussed in chapter 2. At the time of writing the make-up of the study population is described in **Table AII.1**. Subjects were immunophenotyped using flow cytometry and the antibodies described in **Table AII.2**.

Due to technical error during the setup of the flow cytometer, many of the samples collected yielded unusable data. Despite this, some information on the frequencies of the immune cells subsets in PD subjects was collected (**Fig AII.1**). The number of samples evaluated is currently too low to make any conclusions, but sample collection is ongoing.

AII.2 LRRK2 expression by *rs3129882* genotype

These data are from the same study and represent the cohort from chapter 2. In addition to LRRK2 mutations, the subjects were genotyped for the *rs3129882* SNP. LRRK2 MFI from both monocytes and T cells was divided into three groups representing the AA, GG, or AG genotype. In the $CD14^+$ monocyte population, LRRK2 expression was increased in healthy control AA subjects compared to GG; however, in PD subjects LRRK2 expression was increased in AG subjects compared to AA (**Fig AII.2**). In $CD3^+$ T cells, PD subjects had increased LRRK2 expression in GG subjects compared to AA.

In both monocytes and T cells, PD subjects with the GG SNP also had increased LRRK2 expression. While the sample size for each genotype is underpowered for publication, these preliminary data suggest that further investigation into this line of study is warranted.

AII.3 Figures

	G2019S	
	Carrier	Non-Carrier
HC	1	4
PD	3	12

Table AII.1. Study population recruitment. Participants are defined by their mutation carrier and disease statues.

Fluorochrome	Isotype	Dilution	Teff	Dilution
Live/Dead: UV	1:2000			
Fc Block	1:20			
FITC	REA	-	CD45RO	50
PE	Ms IgG1	800	FoxP3	100
PerCP-Cy5.5	Ms IgG1	200	CD4	100
PE-TR	Ms IgG2a	28	CCR7	20
PE-Vio770	REA	-	CD3	200
APC	Ms IgG2b	40	CCR6	50
APC H7	Ms IgG1	200	CD8	100
BV421	Ms IgG1	50	CD25	50
BV510	Ms IgG1	100	CCR4	100
BV650	Ms IgG1	400	CD127	100
AF700	Rb	10	LRRK2	50
BV711	Ms IgG1	17	CXCR3	20

Table AII.2. Antibody markers and fluorophore conjugations used for immunophenotyping.

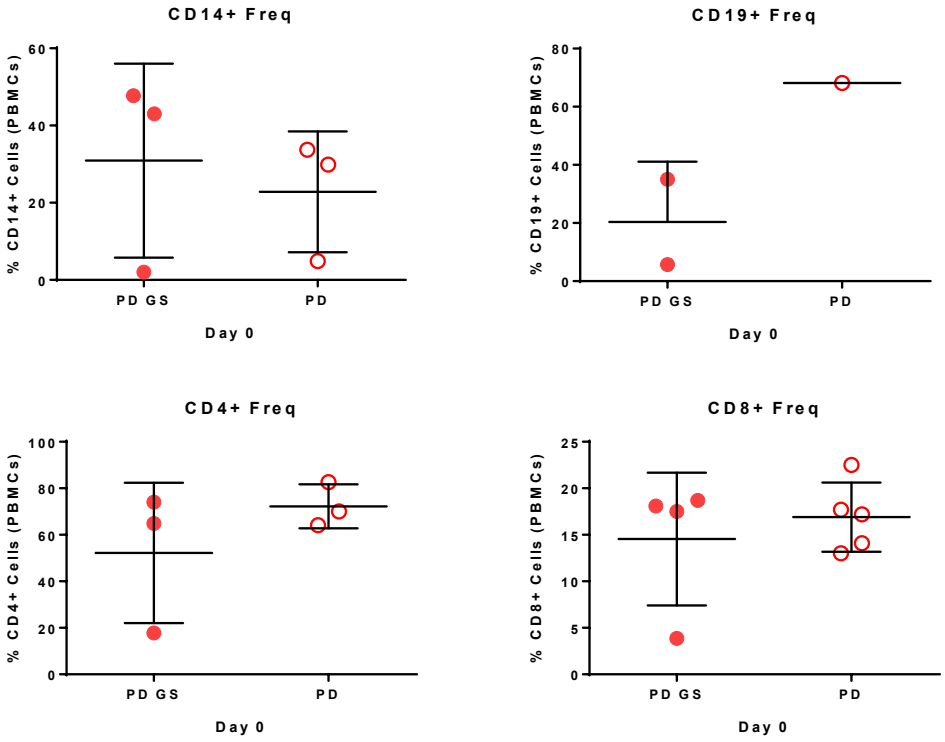

Figure AII.1. Immune cell frequencies of PD subjects with and without the G2019S LRRK2 mutation.

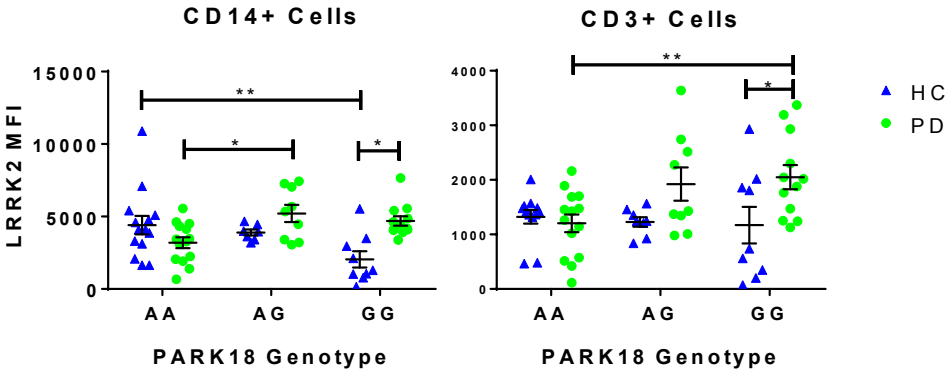

Figure AII.2. LRRK2 expression levels are altered depending on rs3129882 genotype and disease status.